Università degli Studi di Cagliari

PhD Degree in Industrial Engineering
Cycle XXXI

MULTIVARIABLE MODELLING AND CONTROL OF CONTINUOUS PROCESSES

Wastewater treatment plants and complex fluids production as case studies

Scientific Disciplinary Sector
ING-IND/26

PhD Student	Roberto Mei
Coordinator of the PhD Programme	Prof. Francesco Aymerich
Supervisor	Prof. Massimiliano Grosso

Final exam. Academic Year 2017–2018
Thesis defence: January-February 2019 Session

This work has been made possible by the European Union's Horizon 2020 research and innovation programme (grant agreement N°636942).

To my grandfathers

Acknowledgements

I want to be thankful to my supervisor, Prof. Massimiliano Grosso, for giving me this opportunity, for guiding me through this not-so-easy path and for all the teachings.

A big thank you to Prof. Stefania Tronci, for all the help and the teachings and to Prof. Roberto Baratti for all his observations and advices.

Thank you to Francesc Corominas from P&G, for the collaboration and the help regarding the experimental side of this work.

Thank you to Erwin Giling and Paul Van Neer from TNO, for the discussions regarding the calibration of the ultrasound sensor.

Thank you to Federico Orefice, Carla Vinci and Marina Gherazzu for their experimental work and for sharing proposals and ideas.

I would also like to thank my colleagues Claudio, Elisa and Simona, for their support and friendship during these years.

An infinite thank you goes to Marta, for all the support. Especially in the hardest moments of this period of my life.

Thank you to my parents, for the moral and economic support that gave me the opportunity to arrive here, and to my brother.

Finally, a special thank you to all my friends.

Contents

Abstract

In this thesis, the multivariable modelling and control of continuous processes is discussed. Two main lines of research were followed: the multivariable system identification for processes subjected to disturbances and the multivariable modelling and control of a continuous production of complex fluids.

For the first topic, wastewater treatment plants were used as case study. The goal of the work was to develop a method to implement multivariable variations of the manipulated inputs chosen for the identification phase, in order to obtain as much information as possible on the system in the shortest time. Signals for manipulated inputs were randomly generated according to the Generalized Binary Noise approach and inputs combinations were selected on the basis of the D-Optimal Design criterion. The Benchmark Simulation Model No. 1 was used as process simulator. Non-linear autoregressive neural networks were implemented to evaluate transfer functions of linear models. The procedure allowed to obtain good results as regards the estimation of gain constants of such models.

For the second topic, the production of non-Newtonian water-free detergents was considered as case study, with the goal to develop control strategies for such process. Rheological characterization of the product was addressed by means of rheometers and a viscometer. The Carreau model was chosen for the description of the rheological behaviour. The process was first modelled relating the parameters of the Carreau model with the mass flow rate of one ingredient. A single-input single-output feedback Proportional-Integral controller was designed with the purpose to control a point on the viscosity curve of the product. The main outcome was that a viscosity curve was controllable with such control configuration, but the selection of the right controlled variable needs particular care. A second modelling attempt was made exploiting a multi-input multi-output control configuration.

A process simulator based on a non-linear neural network was built. A double feedback controller was implemented with the objective to control two separate points of the viscosity curve using two manipulated variables. A Model Predictive Control was designed with the purpose to control more than two points on the viscosity curve using the same manipulated variables. The second controller returned faster responses in terms of dynamics with respect to the double feedback controller. Finally, the possibility to control the detergent production process by using an on-line ultrasound rheological sensor was explored. A data-driven approach was applied by means of Partial Least Squares technique and neural networks, in order to obtain a model capable to relate ultrasound variables with off-line rheological measurements of viscosities of the product. Fittings of experimental data by the neural network were better than those obtained with the Partial Least Squares model. A "smart operator" action was implemented as a control system, by means of a second neural network model. Thus, the control system was based on two data-driven models based on neural networks. Simulated tests of this control algorithm returned satisfactory results, proving the possibility of a real-time control of the viscosity curve of a complex fluid during its continuous production.

CHAPTER 1

Introduction

In this chapter the motivations behind the work done during the Ph.D. are explained and an overview of the thesis is proposed. Then a system identification problem for systems subjected to disturbances is introduced. Next, the modelling and control of non-Newtonian fluids production process is presented, followed by a description of the state of the art control for complex fluids production. Afterwards, a brief introduction to rheology is given. Finally, contributions to the literature derived from this work are mentioned.

1.1 Motivations and overview of the thesis

The work done during the Ph.D. and this thesis concern about the multivariable system identification, modelling and control of chemical processes. Two main lines of research were tackled: the multivariable system identification for processes subjected to disturbances and the multivariable modelling and control of a continuous production process of complex fluids.

With this regard, it is important to underline that system identification is the basis for the development of any control systems. Indeed, the control of the studied production process of complex fluids required the identification of the proper input-output relations of the system. The process was affected by non constant disturbances. This motivated to study the issue of the system identification even by resorting to other dynamic systems. For such purposes, techniques aimed to properly address

system identification were firstly investigated on a complex case consisting of a wastewater treatment plant. This choice was justify by the fact that this type of plants, subjected to persistent and variable disturbances, are well-known and studied in the scientific literature and because a process simulator was already available. The objective was to develop identification techniques on this process and then extend them to other sectors and to the complex fluids production process.

The first part of the work dealt with the system identification for systems subjected to disturbances and wastewater treatment plants were used as case study. In this type of systems a wastewater is treated through physical, biological and chemical processes to obtain a clear water. The efficiency of this kind of plants can definitely improve by using advanced controllers (Hreiz, Latifi, and Roche [1]). On the other hand, the system identification phase, that is strictly necessary for the control design, is quite difficult because of the numerous unmeasurable disturbances entering the system. Hence the need to study and improve the techniques for the identification phase is required.

Further details are reported in Paragraph 1.2 and a full treatment about the work is reported in Chapter 2.

The other part of the work was carried out as a part of the CONSENS (Integrated Control and Sensing for Sustainable Operation of Flexible Intensified Processes) European project funded by the European Union through the Horizon 2020 Framework Programme for Research and Innovation ([2], [3] and [4]). The project, which took place for three years since 2015 to 2018, had as goal the improvement of continuous production processes of high value products. Three case studies were part of the project and University of Cagliari (UNICA) was involved in the third one with the task of developing innovative techniques to monitor and control a continuous production process of a water-free detergent. Other two partners worked on the same case study: consumer goods multinational producer Procter & Gamble, who provided materials and experimental set-ups, and TNO, a Dutch research institute who worked on an innovative rheological sensor.

During the project, the development of the on-line rheological sensor by TNO proceeded in parallel with the study and the design of possible control strategies for this kind of processes performed

by UNICA. Because of the temporary unavailability of the sensor, developed controllers where tested through simulations.

Further details are reported in Paragraphs 1.3, 1.3.2 and 1.3.1. Then, Chapter 3 deals with the process description, the experimental tests and the modelling of the process. Next, in Chapter 4, a punctual control system applicable to the water-free detergent production is described. In Chapter 5 a multivariable control system is designed for controlling the process. In Chapter 6 the on-line rheological sensor was finally implemented for process control.

1.2 Multivariable modelling of a process subjected to disturbances

Nowadays process control is a crucial part of all industrial plants in order to ensure observance of safety and environmental regulatory and to achieve the required results in terms of specifications and quality. However, the development of advanced control systems needs for mathematical models describing the processes involved. These models can be obtained either through a first principles approach or through black-box identification. The latter case requires a huge number of experimental trials during which the normal functioning of the plant is interrupted. The costs related to this experimental tests can be significant, because usually the time needed is high. For example, in recent literature (Darby and Nikolaou [5]) is reported that for designing a special kind of advanced controllers like Model Predictive Controls, half the time of the whole project is needed for plant tests and subsequent identification phase. The need of time is caused by the way in which the system identification is performed: in fact, the classical approach is based on appropriate variations of each manipulated input one at the time (and by the following analysis of the responses of the system). When dealing with large industrial systems, where several inputs and outputs are present, the identification phase can last a lot. A multivariable system identification, meaning a simultaneous variations of manipulated inputs, can help to cut down the amount of time needed for this phase and, as a result, reduces costs.

When system identification is performed on system subjected to disturbances, it becomes more difficult. In fact disturbances are un-manipulated and usually un-measured inputs which enter the system and influence the behaviour of outputs without the possibility to separate in an immediate way the contribute on the outputs given by them from the one given by manipulated inputs.

In the first part of this work, the possibility to carry out a multivariable system identification in presence of disturbance has been addressed using as case study wastewater treatment plants. For this purpose, a simulation environment for wastewater treatment plants composed of five biological reactors and one settler was used. Special attention was given to the manipulated inputs variation program in order to minimize the time needed for the identification phase. Then, simulations have been executed and the results were analysed to obtain process models suitable for controllers.

1.3 Multivariable modelling and control of a non-Newtonian fluid continuous production process

As introduced in Paragraph 1.1, the CONSENS European project had the objective to improve continuous production processes of high quality and high value products through flexibility and intensification. Considering the whole European industry, the main expected impacts of intensification in continuous processes are:

- financial savings;
- reduction of CO_2 emissions;
- reduction of usage of non-renewable raw materials;
- improvements on the development of new products.

The advantages of continuous production processes with respect to batch processes are various including a better uniformity for the final products and an important reduction of consumption of both energy and raw materials, with a consequent positive impact on costs both for producers and consumers. However, to

perform an effective control on a continuous process, fast sensors and well designed closed loop controllers are strictly necessary. Furthermore, it is important to have a clear understanding of the process and to develop models of it.

To deal with the third case study, a good understanding of rheology and of complex fluids production industry is necessary.

1.3.1 A brief introduction to rheology

In the previous paragraphs the concept of complex fluids was introduced. For the purpose of better understanding the meaning of complex fluids, a brief introduction to rheology is necessary.

Rheology studies the deformations of the matter (solids and fluids) when it is subjected to stress. It plays a key role in many areas including food industry, biology, construction, personal care products, hygiene products, sludge treatment, and so on.

When introducing rheology, the basic concepts are represented by ideal solids and ideal fluids (Macosko [6]).

We talk about **ideal solids** when the matter reacts to a shear stress in an elastic way with a reversible deformation. This behaviour is mathematically described by Equation 1.1 where τ is the shear stress, L is the longitudinal length of the deformation, l is the initial length of the solid and G is the shear modulus which represents the resistance to deformation. The larger G is, the smaller the deformation for the same shear stress is. The deformation is reversible: when the stress is removed, the deformation is cancelled.

$$\tau = G \cdot \frac{dL}{dl} \tag{1.1}$$

G depends mainly on the chemical-physical nature of the material. For example, for a gum-like material the shear modulus is approximately equal to 0.01 GPa, while for steel is about 200 GPa.

Ideal fluids react to a shear stress in a viscous way (they flow) with an irreversible deformation. The behaviour is described by Equation 1.2. τ is the shear stress. $\frac{d\varphi}{d\rho}$ is the velocity gradient (also called shear rate and indicated with $\dot{\gamma}$). φ is the velocity profile. ρ is the perpendicular direction with respect to the flow. μ is the dynamic viscosity which represents the resistance to flowing.

The larger μ is, the smaller the flow of the fluid for the same shear stress is. The deformation is irreversible: the energy transmitted with the shear stress is dissipated by the flowing and a part is lost as heat.

$$\tau = \mu \cdot \frac{d\varphi}{d\rho} = \mu \cdot \dot{\gamma} \tag{1.2}$$

Viscosity can depend on several factors:

- chemical-physical nature of the material;
- pressure;
- temperature;
- shear rate;
- time.

When dealing with non-ideal materials, it is common to encounter substances with a mixed behaviour both of ideal solids and ideal fluids. These compounds are called **viscoelastic** materials and they show both viscous and elastic characteristics. A simplified model, the Maxwell model, describes viscoelastic materials summing the two contributions of the elastic and the viscous deformations (Equation 1.3). However, the mathematical description for this kind of materials is usually more complicated and this goes beyond the scope of this work.

$$\dot{\gamma} = \frac{\dot{\tau}}{G} + \frac{\tau}{\mu} \tag{1.3}$$

For all fluids, the shear stress can depend on multiple factors. On the basis of these dependencies, fluids can be classified in different ways. Typical classifications take into account the dependence between shear stress and shear rate and between shear stress and time. These classifications are treated in the following sub-paragraphs.

Fluids with a shear rate-dependent shear stress

A simplified, though effective, way to characterize the complex nature of fluids is to describe the dependence of the shear stress on the shear rate. Fluids can be classified in two main categories on the basis of this dependency:

- **linear dependency**: Newtonian fluids;

- **non-linear dependency**: non-Newtonian fluids.

In **Newtonian fluids** (Figure 1.1) the dependence between shear stress and the shear rate is linear and the viscosity is constant as shear rate varies. Typical examples of Newtonian fluids are water, air, milk, honey, blood plasma ([7]). They are mathematically described by Equation 1.4, and, as it can be seen, they show a ideal fluid behaviour. When talking about *complex fluids* one refers to fluids with a behaviour different from Newtonian fluids.

$$\tau = \mu \cdot \dot{\gamma} \tag{1.4}$$

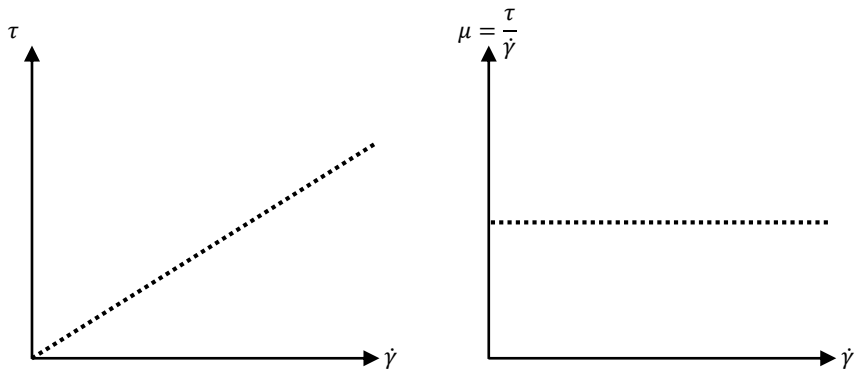

Figure 1.1: Example of viscosity curve for Newtonian fluids

For **non-Newtonian** fluids, the dependence between shear stress and the shear rate is non-linear and the apparent viscosity varies with the shear rate. They are mathematically described by Equation 1.5 where μ_a is the apparent viscosity.

$$\tau = \mu_a(\dot{\gamma}) \cdot \dot{\gamma} \tag{1.5}$$

On the basis of the dependence of viscosity on shear rate, non-Newtonian fluids are further classified in (see also Figure 1.2):

- **shear thinning** fluids: the apparent viscosity decreases when shear rate increases therefore the resistance to flow is larger for low values of $\dot{\gamma}$. This is due to the microscopical structure of the material: products who seem homogeneous are in fact composed of particles with irregular shapes, or they consist of solutions of long chain molecules polymers, or they are drops of liquid dispersed in another liquid.

- **shear thickening** fluids: the apparent viscosity increases when shear rate increases, therefore the resistance to flow is larger for high values of $\dot{\gamma}$. As an example, this behaviour is typical for high concentrated suspension of a solid material in a liquid. At rest, intra particles forces are dominating. When the stress increases, particles bend together.

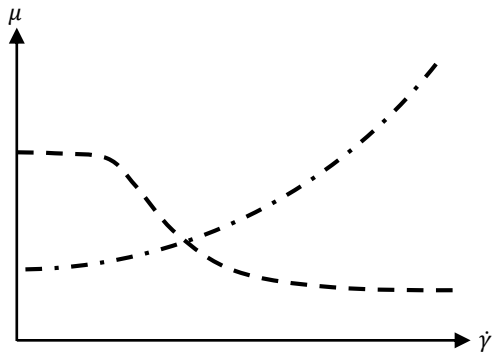

Figure 1.2: Examples of viscosity curves for non-Newtonian fluids: shear thinning fluids (dashed line) and shear thickening fluids (dash-dot line)

Fluids with a time-dependent shear stress

The dependence of the shear stress on the time classifies fluids in:

- thixotropic fluids;
- rheopectic fluids.

When **thixotropic** fluids are subjected to a shear stress, their viscosity decreases with time. For a constant shear rate, it needs a finite time to achieve the so called equilibrium viscosity (which is lower than the initial one). This behaviour is also shown in Figure 1.3.

Rheopectic fluids show a behaviour (Figure 1.4) which is opposite to thixotropic fluids (and for this they are also called anti-thixotropic fluids.) Their viscosity increases with time and the equilibrium viscosity reached with a constant shear rate in a finite time is larger than the initial one.

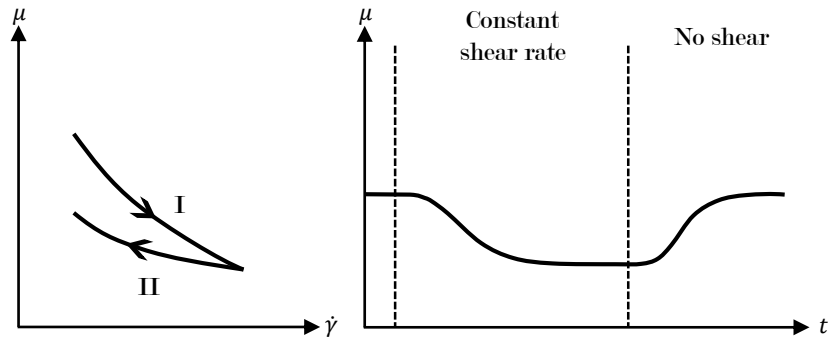

Figure 1.3: Viscosity curves for thixotropic fluids

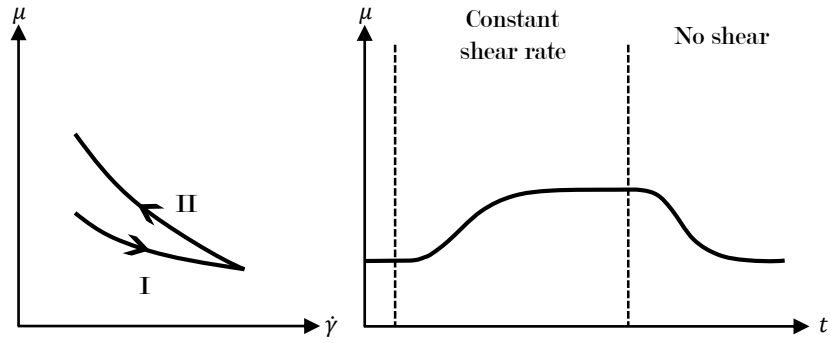

Figure 1.4: Viscosity curves for rheopectic fluids

Rheometry

With the term *rheometry* one refers to all the techniques used to measure rheological properties of a material. Measuring instruments are basically divided in:

- viscometers;
- rheometers.

Viscometers are usually used to measure the viscosity of fluids at precise conditions of the flow. Famous examples of such instruments are falling sphere viscometers and U-tube viscometers. Rheometers are used for more complete measurements of the rheology of fluids and they can also explore the viscosity of fluids when forces applied and flow conditions vary.

Another convenient classification for rheometers divides them in two groups: drag flows rheometers, in which shear is generated

between a fixed surface and a moving surface, and pressure-driven flows, in which shear is generated by a pressure difference (Macosko [6]). Drag flows rheometers mainly consist of sliding plates and rotational geometry rheometers. In the first type, the fluid is positioned between two plates and one of them slides to generate the shear. In the second type, the fluid is positioned between two concentric elements and one of them rotates to generate the shear. Typical geometries for rotational rheometers are concentric cylinders, cone and plate and parallel plates (Figure 1.5).

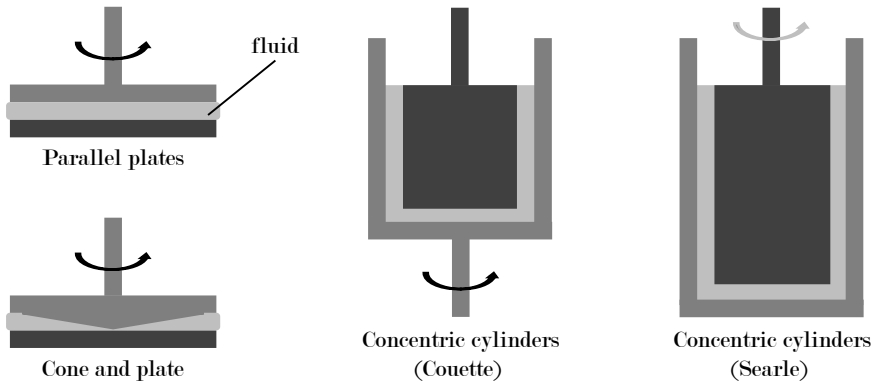

Figure 1.5: Typical geometries for rotational rheometers

Rotational rheometers basically consist of an electric motor which generates a torque on the shaft, which in turn is responsible for the rotation of the mobile element. This kind of rheometers can provide a controlled stress input (and measure the shear rate, mainly on the rotor axis) or a controlled shear rate (and measure the shear stress, on the rotor axis or through the non-rotating element). The first ones are called *controlled stress* rheometers (or CS-rheometers), the second ones *controlled rate* rheometers (or CR-rheometers) (Schramm [7]).

Rheometers may be equipped with devices for an accurate control of temperature, and many accessories are available in order to test different kinds of materials and investigate different kinds of properties.

1.3.2 State of the art process control in complex fluids production

In the previous paragraph, complex fluids have been defined as fluids which behave differently with respect to Newtonian fluids, that is with a viscosity which varies with the shear rate.

Industrial continuous production processes of complex fluids still suffer of problems related to the monitoring and control quality of products. Rheological properties and parameters, such as shear rate dependent viscosity, which deeply affect the quality of products are measured and verified only when the production is finished. This is typically done with random checks and off-line measurements. This can lead to production batches out of specifications, especially when used ingredients are not the same as in the original formulation. If this happens, products could be no more suitable for commercialization or their use in successive phases of the production chain. Because of that, it may be necessary to throw large quantities of products, with important economic losses.

The main reason behind the difficulty to apply a rigorous quality control during production is the absence of sensors able to provide real-time information about the various rheological properties of the complex fluids during the production. Thus, up to our knowledge, a real-time process monitoring is not possible. Furthermore, it is difficult to perform a proper system identification, which is necessary to obtain optimal information to describe relations between inputs (both manipulated inputs and disturbances) and the rheological behaviour of the process. In the industry there are just few applications of on-line viscometers. But such sensors are able to measure only a point value of viscosity corresponding to a certain shear rate value. Thus, basically there are no feasible solutions for non-Newtonian fluids. In addition, traditional measurement methods, like off-line rotational rheometers, cannot be used for automatic control because they are not capable to provide real time measurements.

In recent years many studies have been accomplished in order to investigate the problem and try to design and develop sensors able to measure rheological properties of non-Newtonian fluids in real-time and non invasive techniques represent a line of research

very promising.

For example, Kotzé et al. ([8], [9] and [10]) worked on a methodology based on ultrasonic velocity profiling (UVP) with which an instantaneous velocity profile of a fluid containing particles is measured across the ultrasonic beam axis. This technique combines the ultrasonic velocity profiling with the measurement of pressure difference. In addition it is non invasive, that is it does not interfere with the flow. It could be used to monitor concentrated and opaque suspensions. Results obtained with concentrated cement pastes showed that UVP is a promising technique for the characterization of the flow of viscous fluids.

Meacci et al. [11] worked on an industrial system for on-line analysis of various opaque and non-Newtonian fluids. They named this system Flow-Viz and it uses ultrasounds to estimate the velocity profile of the flow moving along a pipe.

Yoshida et al. [12] presented a sensor based on ultrasonic spinning rheometry (USR) which is expected to provide various rheological information. The sensor was tested for thixotropic fluids, shear thinning fluids, and multiphase fluids.

All these promising results about novel sensors for on-line rheological measurements foster the developing of control strategies based on the rheological characteristics of products. In fact when such technologies will become mature and available on the market, a real-time control of viscosity curve could be implemented in production plants, in order to control the rheological properties of the product during production.

1.4 Contributions

The topics discussed in this thesis were also used as contributions for the following journal papers and conference participations.

Roberto Mei, Massimiliano Grosso, Roberto Baratti and Stefania Tronci. "On-line control of the rheological properties for a continuous production of a non-Newtonian fluid". Poster presented at the *EuroPACT 2017 - 4 rd European Conference on Process Analytics and Control Technology*, Potsdam, Germany, May 10-12, 2017.

Roberto Mei, Massimiliano Grosso, Stefania Tronci, Roberto Baratti and Francesc Corominas. "Real-Time Control of Viscosity Curve for a Continuous Production Process of a Non-Newtonian Fluid". In: *Chemical Engineering Transactions*, 57 (2017), pp. 1099-1104. DOI: 10.3303/cet1757184.

Roberto Mei, Massimiliano Grosso, Francesc Corominas, Roberto Baratti and Stefania Tronci. "Multivariable Real-Time Control of Viscosity Curve for a Continuous Production Process of a Non-Newtonian Fluid". In: *Processes*, 6(2, 2018), 12. DOI: 10.3390/pr6020012.

Alessandra Taris, **Roberto Mei**, Massimiliano Grosso, Stefania Tronci, Francesc Corominas, Erwin Giling and Paul Van Neer. "Data driven calibration of in line ultrasound rheological sensors". *AERC 2018 - 12 th Annual European Rheology Conference*, Sorrento, Italy, April 17-20, 2018.

Roberto Mei, Massimiliano Grosso, Federico Desotgiu and Stefania Tronci. "System identification for a system subjected to persistent disturbances". In: *Computer Aided Chemical Engineering*, 43 (2018), pp. 1183-1188. DOI: 10.1016/B978-0-444-64235-6.50206-0.

Part I

Multivariable modelling of a process subjected to disturbances

CHAPTER 2

System identification for a system subjected to disturbances

In this chapter the problem of system identification in systems subjected to disturbances is presented. The particular case of wastewater treatment plants is then introduced, followed by a full description of the used simulation environment. Eventually, a strategy for manipulated inputs generation is proposed. The results of simulations are then presented and a multivariable identification by processing the obtained data through non-linear neural networks is performed. Finally, results obtained by system identifications are presented.

2.1 Case study: wastewater treatment plants

As introduced in Paragraphs 1.1 and 1.2, system identification is a crucial aspect for modern industries in order to obtain reliable empirical input-output models which are suitable to their usage in the design of advanced control systems. The economic and time efforts related to this phase are generally significant and this makes necessary to improve it and optimize it as much as possible.

In this regard, the work presented in this Chapter aims to address the possibility to perform a multivariable system identification in systems subjected to continuous disturbances, with the goal to reduce the amount of time needed for the identification phase. This work demonstrated to give useful insights for the

development of the proper system identification for the complex fluids production process. The problem was firstly studied and analysed on a complex case, well-known and described in the literature and with an available process simulator. At this purpose, civil wastewater treatment plants were used as case study since they represent a perfect case of multi-input multi-output systems with continuous variable disturbances.

Civil WasteWater Treatment Plants (WWTPs) are plants in which a wastewater coming from urban sewer is treated through chemical, biological and physical processes in order to obtain a clear water. This effluent, which must contain low levels of water pollutants according to local regulations, can be re-introduced in the environment to close the water cycle previously interrupted by human activities (Tchobanoglous et al. [13]).

In the first half of the 20^{th} century wastewater treatment systems like trickling filters have been gradually replaced by more efficient activated sludge processes (Vismara and Butelli [14]).

Such WWTPs are generally composed by various units to accomplish different functions, as listed below:

- screening, to separate coarse refuses from wastewater;
- separation of sands and oils;
- sedimentation, to separate suspended solids from water;
- biological reactions, to remove biological pollutants, mainly ammonia and nitrate nitrogen from the wastewater; these reactions take place in activated sludge reactors which can be of two types:
  - anoxic/anaerobic biological reactors;
  - aerobic biological reactors;
- secondary sedimentation, to separate biological sludges from water;
- disinfection, to kill pathogen micro-organisms.

Furthermore, an equalization tank is usually present in the plant to equalize, as much as possible, the flow rate of the processed water and avoid peaks of contaminants in the system.

The sludges coming from primary and secondary sedimentation are then processed through sludge digestion, in order to stabilize them. The obtained material can be sent to disposal or, if suitable, can be used as fertilizer or even to produce biogas and then energy.

To study the best methodology to perform a system identification in such plants, it was chosen to proceed using a simulation environment with the idea to develop techniques for the identification applicable, in the future, to a real plant.

2.2 Benchmark Simulation Model no. 1

The Benchmark Simulation Model no. 1 (hereafter referred as BSM1) is a simulation environment for activated sludge WWTPs currently developed by International Water Association (IWA) through IWA Task Group on Benchmarking of Control Strategies for WWTPs (on Benchmarking of Control Stategies for WWTPs [15]). This study group continues works done in the past by Working Groups of COST Action 682 and 624 (Alex et al. [16]).

The Benchmark provides all the tools to simulate a typical activated sludge WWTP defining the plant layout, simulation models and influent loads.

The plant is composed of five activated sludge reactors connected in series. The first two are anoxic environments while the following three are aerobic reactors. This configuration combines nitrification and denitrification reactions, as often happens in reality. The reactors are followed by a settler. The wastewater enters in the first reactor along with two recycle streams, go through all the reactors and arrives to the settler. Here, treated water is separated from the sludge and then sent to disinfection. In Figure 2.1 a schematic representation of the plant layout is reported.

The benchmark is based mainly on two mathematical models: the Activated Sludge Model No.1 (Henze et al. [17]), or ASM1, as regards the biological part of the plant and the Takàcs model (Takács, Patry, and Nolasco [18]) as regards the settler.

The ASM1 describes the biological activities taking place in the plant by using eight processes:

- aerobic growth of heterotrophs;
- anoxic growth of heterotrophs;
- aerobic growth of autotrophs;
- decay of heterotrophs;
- decay of autotrophs;

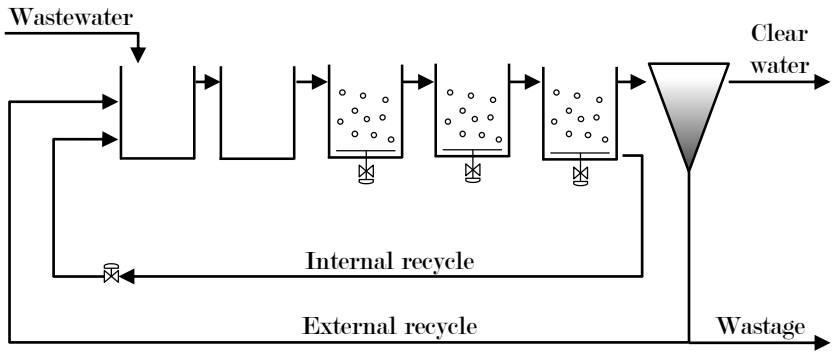

Figure 2.1: Plant layout of the BSM1

- ammonification of soluble organic nitrogen;
- hydrolysis of entrapped organics;
- hydrolysis of entrapped organic nitrogen.

For further details about the BSM1, one can refer to the manual of the Benchmark ([15]). The influent data used in this work are provided by the Benchmark study group (data can be downloaded from their website [19]) and they were originally proposed by Vanhooren et al. [20]. They consist of a long-term time series of 16 variables describing typical dynamic variations for a wastewater inlet flow covering a total time of 609 days, with samples every 15 minutes. These influent data represent the disturbances entering the system and they are treated as unmeasurable inputs.

For the control of oxygen concentration in the biological reactors, PI controllers have been designed to act on the transfer rate of oxygen in each aerated reactor. The plant configuration was modified with respect to the Benchmark to have also the reactor 2 oxygenated. Constant flow rate values for both external recycle and wastage flow were set, respectively equal to 18446 and 385 m^3/d.

2.3 System identification

2.3.1 Introduction to identification techniques

In order to design process control in industrial systems, models of the process are needed. When first principles modelling is not applicable due to the complexity and the uncertainties of the system, black box modelling is used. In this case, the system is excited by input variations and the obtained input-output responses are then analysed (Ogunnaike and Ray [21]).

Basic techniques for system identification consist of varying singularly each manipulable input according to step functions or sine wave functions.

2.3.2 Goal of the system identification

The system identification performed here focused only on the biological part of the plant (activate sludge reactors and their outputs), whereas the sedimentation phase has not been modelled.

This was an attempt to improve the identification strategy implemented by Foscoliano et al. [22] and it was partially based on the work by Darby and Nikolaou [5]. As previously introduced, in that work ([22]) the authors designed linear model predictive controllers in order to control the concentration of nitrate and ammonia nitrogen in activate sludge reactors simulated through the BSM1. The controlled variables of a particular configuration of this study were nitrate nitrogen concentration in reactor 2 and ammonia nitrogen concentration in reactor 5. Oxygen concentrations in reactor 2, 3, 4 and 5 and the flow rate of internal recycle were chosen as manipulated variables. Therefore, the system identification carried out before the control designing phase was performed in order to establish the relationships between the two controlled variables (considered as outputs) and the five manipulated variables (considered as inputs). The approach for the identification was to vary each manipulated variable one at the time, according to step functions. This procedure took a total time of more than 100 days.

The main goal of the work described in this part of the thesis was to address a new approach, which will be demonstrated to

allow a reduction of the time required for the identification. In particular the attention focused on multivariable system identification, which provides for simultaneously variations of all inputs to obtain as much information as possible on the system in the shortest time.

2.3.3 Multivariable system identification

A system like the one in hand is a multi-input and multi-output (MIMO) system composed of $g = 2$ outputs and $h = 5$ inputs. Mathematically, it can be described by Equation 2.1 ([5]), where $\boldsymbol{y}(t)$ is the vector containing the outputs values at the time t, $\boldsymbol{u}(t)$ is the vector containing the manipulated input values at the time t. $\boldsymbol{K}$ is the matrix of the gains and $\boldsymbol{e_N}(t)$ is the vector of measurements noise (assumed uncorrelated and distributed according to a Gaussian distribution of mean equal to zero and variance equal to σ^2).

$$\boldsymbol{y}(t) = \boldsymbol{K} \cdot \boldsymbol{u}(t) + \boldsymbol{e_N}(t) \tag{2.1}$$

Assuming $\boldsymbol{Y}$ and $\boldsymbol{U}$ as two matrices containing, respectively, all the values of the g outputs and of the h inputs for each sampling time, if the number of samples for outputs and inputs is equal to N, the matrices $\boldsymbol{Y}$ and $\boldsymbol{U}$ can be written as reported in Equation 2.2 and Equation 2.3. In these Equations, y_g, with g which varies from 1 to 2, are the time vectors representing the evolutions of the two outputs, nitrate nitrogen concentration in reactor 2 and ammonia nitrogen concentration in reactor 5, respectively. u_h, with h which varies from 1 to 5, are the vectors representing the time evolutions of the five manipulated inputs. They are oxygen concentrations in reactor 2, 3, 4 and 5 and the flow of internal recycle, respectively.

$$\boldsymbol{Y} = \begin{bmatrix} y_1(1) & \cdots & y_g(1) \\ \vdots & \ddots & \vdots \\ y_1(N) & \cdots & y_g(N) \end{bmatrix} \tag{2.2}$$

$$\boldsymbol{U} = \begin{bmatrix} u_1(1) & \cdots & u_h(1) \\ \vdots & \ddots & \vdots \\ u_1(N) & \cdots & u_h(N) \end{bmatrix} \tag{2.3}$$

If outputs and inputs are known, it is possible to estimate the gains matrix $\boldsymbol{K}$. For example, applying the least squares method it is possible to define $\hat{\boldsymbol{K}}$, estimator of $\boldsymbol{K}$, as reported in Equation 2.4, defining also the information matrix $\boldsymbol{X}$, as reported in Equation 2.5.

$$\hat{\boldsymbol{K}}^T = (\boldsymbol{U}^T\boldsymbol{U})^{-1}\boldsymbol{U}^T\boldsymbol{Y} = (\boldsymbol{X})^{-1}\boldsymbol{U}^T\boldsymbol{Y} \tag{2.4}$$

$$\boldsymbol{X} = \boldsymbol{U}^T\boldsymbol{U} \tag{2.5}$$

It is clear from Equation 2.4 that the estimation of the gains matrix, which is the purpose of a system identification, and its accuracy can be improved by a proper selection of the inputs. This will lead to maximize the information on the system obtained by experiments. This can be accomplished through Design of Experiments (Goodwin and Payne [23]). A particular class of DoE is composed by Optimal Design and for the case in hand, the D-optimal design was chosen. This is a design method based on the maximization of the determinant of the information matrix $\boldsymbol{X}$ ([24]). As indicated by [23], if N is large, it is possible to approximate the covariance matrix of inputs C_m with the average information matrix, calculated as reported in Equation 2.6.

$$C_m = \frac{\boldsymbol{X}}{N} \tag{2.6}$$

Thus, maximizing the determinant of the C_m is equivalent to maximize the determinant of the information matrix $\boldsymbol{X}$. If the determinant of C_m is maximized (in case of dealing with standardized variables this implies that its value is close to 1), this means that the determinant of the information matrix is maximized and that the chosen inputs are uncorrelated. Therefore, the found combination of inputs is suitable for identification.

Acting on the system with inputs generated to satisfy the conditions such that the determinant of the information matrix $\boldsymbol{X}$ is maximized, leads to estimate the gains matrix $\boldsymbol{K}$ in a most accurate way.

2.3.4 Generalized Binary Noise

For the choice of the variations program of each manipulated input, it was chosen to rely on the Generalized Binary Noise (GBN) approach described by Tulleken [25].

Conventional Binary Noise (BN) is a system identification technique in which inputs are excited with binary noise signals, meaning that inputs are subjected to positive and negative amplitude variations around their stationary values. The inputs can assume only two fixed values, an upper level variation and a lower level variation. Thus, variables vary only according to step functions. When applying the BN, the probability that a variable assumes, at each switching time, the value opposite to the previous one is fixed and equal to 50%. In the GBN approach, this probability can be between 0 and 1.

It is demonstrated that the GBN approach ensures obtaining input-output data that allow accurate identification results. This is mainly due to the fact that, in the BN technique, the frequency spectrum of the switchings is more or less flat, while in the GBN approach, the spectrum can be manipulated, giving more importance to the lower and middle frequencies.

2.3.5 Inputs generation

In order to apply what discussed so far, inputs used for identification were generated through the following iterative procedure:

- a combination of inputs was randomly and independently generated. For each manipulated input, a binary signal was generated according to the GBN technique:
  - inputs can vary only according to step functions;
  - inputs can assume only their minimal or maximum value, as reported in Table 2.1;
  - the probability has a value different from 0.5.
- then the determinant of C_m is evaluated:
  - if the value of the determinant is almost 1 (in this case a value equal or larger than 0.95 was considered fair) then the determinant of the information matrix considered

is maximized and the corresponding combination of inputs is suitable for identification;
– if the value of the determinant is far from 1 (lower than 0.95, in this case), the procedure starts over.

Inputs	Units	Min	Max
Oxygen in reactor 2	mgO_2/L	0.25	0.75
Oxygen in reactor 3	mgO_2/L	1.50	2.50
Oxygen in reactor 4	mgO_2/L	1.75	2.25
Oxygen in reactor 5	mgO_2/L	1.25	1.75
Internal recycle	m^3/d	49804.2	60871.8

Table 2.1: Minimal and maximum values for manipulated inputs

Due to uncertainty regarding the characteristic times of the system, it was important to avoid variations with a too much high frequency but also to avoid waste of time in steps that last too long. To explore these aspects, three parameters were set: the total time, representing the duration of the test (that is, the time required for the system identification in the actual plant); the step time, representing the smallest duration of a step; the switching frequency, which is the probability of a switch at the end of the step. A total of seven experimental set-ups were designed and tested, where these parameters were mixed-up, as reported in Table 2.2.

Set-up number	Total time [d]	Step time [d]
1	60	1
2	60	2
3	60	0.5
4	30	1
5	30	0.5
6	90	1
7	90	2

Table 2.2: Parameters for the experimental set-ups

For all the experiments, the switching frequency was assumed equal to 0.2. This choice was based on the fact that a value of switching frequency between 0 and 0.5 can excite, with more emphasis, the lower frequencies. This improves the system identification (Tulleken [25]). In Figure 2.2, a generated manipulated input relative to oxygen concentration in reactor 3 is shown as example. The corresponding frequency spectrum is also reported. As can be seen, the lower frequency were favoured, with the range of frequencies between 0 and 15 d^{-1} resulting as the most excited.

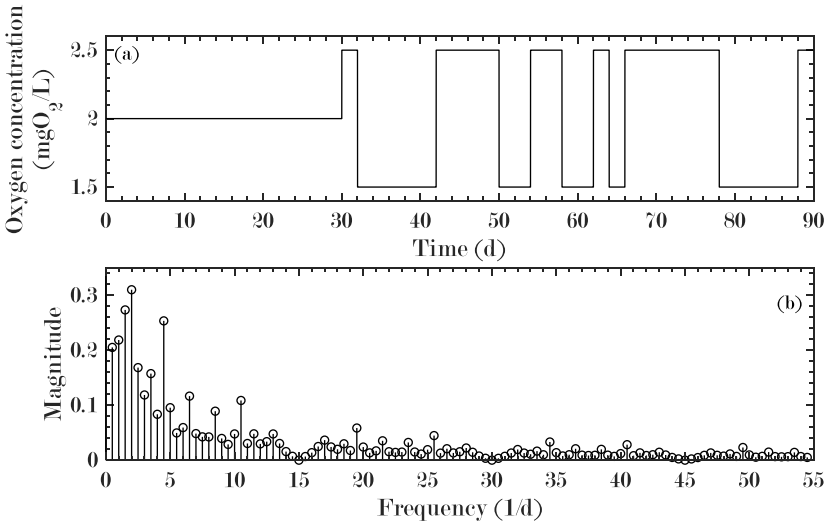

Figure 2.2: Scheme of an input function and its spectrum

2.4 Results

In order to simulate the responses of a real plant when the multivariable system identification is performed in reality, the BSM1 was stressed with manipulated inputs generated as explained in Paragraph 2.3.2 and, simultaneously, with an inlet flow representing the wastewater entering the system. This flow is described by 16 different time varying parameters, to mimic typical dynamic variations for a civil wastewater flow.

For its resolution, the system was initialized for a simulated time of 15 days with a constant inlet flow and constant values

for the five manipulated inputs. For further 15 days, the variable inlet flow was used. Finally, for a period of time depending on the tested set-up, simulations were performed using the variable inlet flow and variable manipulated inputs. This last period of time is the parameter of interest because it represents the time needed if the multivariable identification is performed in a real plant. The first two periods of time were needed in the simulations just for the initialization of the solving algorithms.

Among all the set-ups tested, the set-up number 2 was the one who returned the better outcomes. In fact, set-ups providing for a total time of 120 days gave not good results whereas set-ups with a total time of 30 days were considered not enough informative. In the following, obtained results from set-up number 2 are discussed.

Figure 2.3 reports the disturbances as applied to the simulation for set-up number 2.

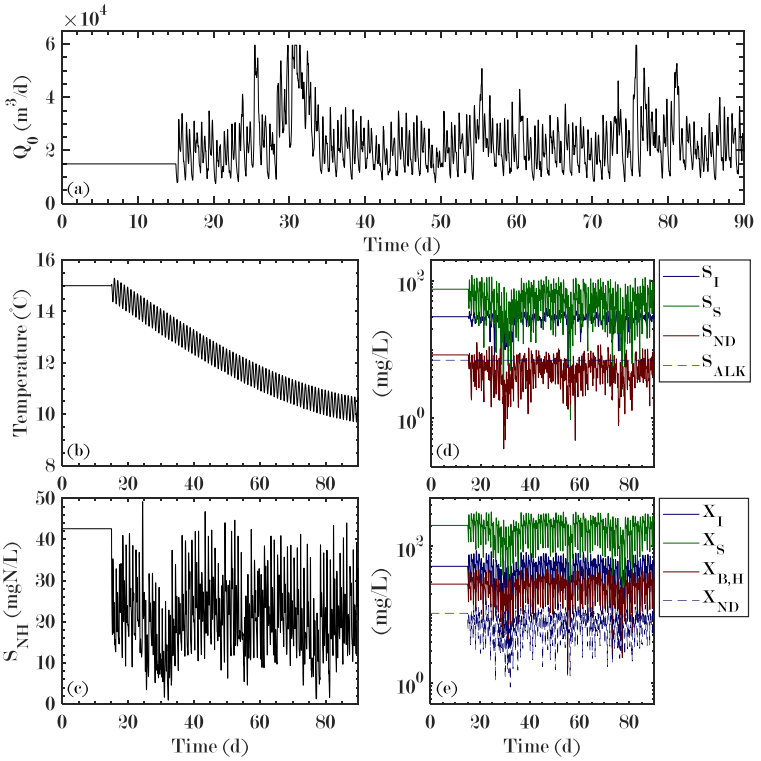

Figure 2.3: Evolution of disturbances

Variables are: inlet flow rate (a), temperature (b), inlet am-

monia concentration (c), parameters describing soluble matter (d) and other parameters describing particulate (e). As can be seen variations are significant. The temperature is an example of variable which varies during the day but also during seasons.

In Figure 2.4 manipulated inputs are reported. Oxygen concentrations ($SP - SO_x$, where x indicates the reactor number) show fluctuations due to the fact that they are controlled variables, and of course the controllers are affected by the fluctuations entering the system with the disturbances. The flow of the internal recycle (Q_a) looks not affected by noise because in this case it was simulated as a fixed value without a control system. Actually it should show fluctuations as well.

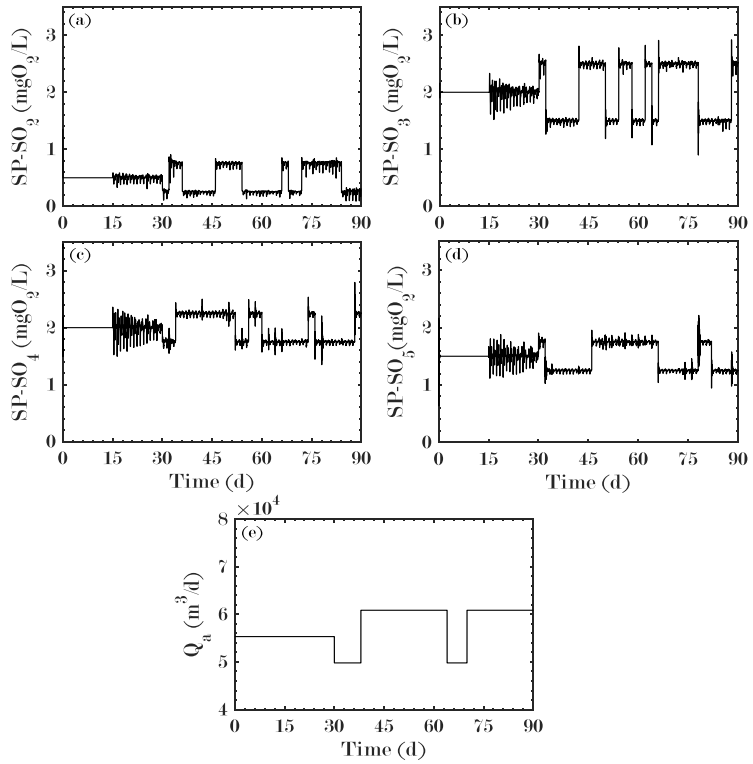

Figure 2.4: Evolution of manipulated inputs

In Figure 2.5 the results regarding the two outputs ($SNO-R2$ for nitrate nitrogen concentration in reactor 2 and $SNH - R5$ for ammonia nitrogen concentration in reactor 5), which will be controlled variables, are reported. Both outputs show highly

non-linear responses.

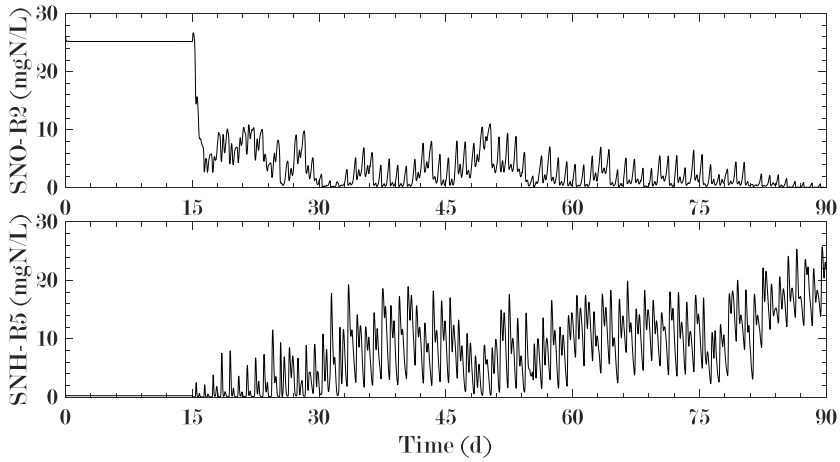

Figure 2.5: Evolution of the two outputs

2.5 Multivariable identification results

As showed in Figure 2.5, the process shows highly non-linear responses for both nitrate nitrogen concentration in reactor 2 and ammonia nitrogen concentration in reactor 5.

Similar results would be obtained if input variations were performed in a real plant. The procedures discussed from now on are applicable in the same way with data coming from real plants.

First, because linear controllers will be finally applied on the process, system identification by means of linear models was tested but it ended up with negative outcomes. Because of that, system identification using non-linear models was performed. At this purpose, non-linear autoregressive with exogenous inputs (NARX) neural networks were chosen. These neural networks were composed of two layers of neurons (a hidden layer and an output layer), with one input signal and one feedback signal entering the hidden layer (Figure 2.6) with a certain delay. To perform the identification, 10 NARX neural networks were trained and validated, one for each time series input-output pair using the simulated input and the corresponding output and with a sampling time of 15 minutes (Figure 2.7).

In order to evaluate the goodness of a trained neural network,

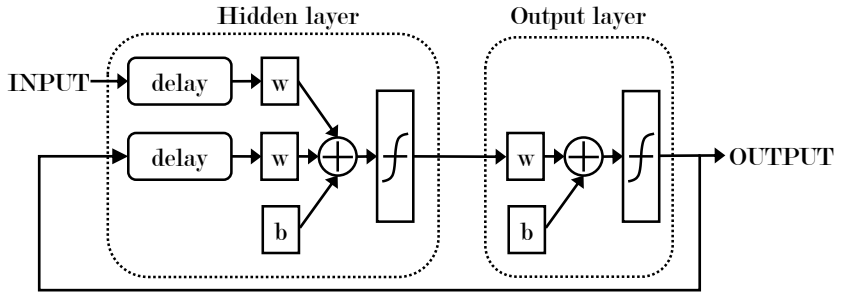

Figure 2.6: NARX neural network structure

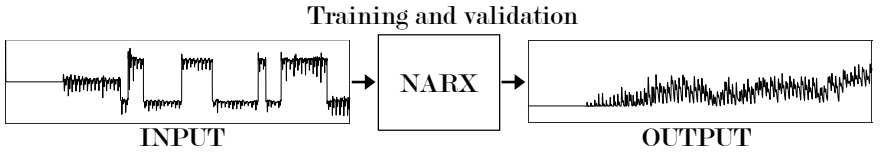

Figure 2.7: Flowsheet of NARX neural networks training

each of them was considered suited to describe the process if it was able to satisfy three conditions:

- the sign of the estimated gain constants must be coherent with the physics of the process;
- the magnitude of the responses for positive input variations (starting from nominal conditions) must be comparable to the magnitude of the responses for negative input variations, taking in to account the non-linearity of the process;
- the order of magnitude of the found gain constants must be consistent with the process in ideal situation of constant inlet flow conditions.

At this point, transfer functions of linear models were evaluated using the trained neural networks. In the case under study, the identification was performed before the implementation of linear control systems. Due to this fact, linear models describing the input-output relationship are needed.

To this purpose, each trained and validated neural network was stressed with positive and negative step variations of the corresponding input (Figure 2.8). Obtained responses were non-linear. Despite that, two transfer functions of a first order plus

dead time (FOPDT) model were evaluated for each input-output pair. One for the positive input variation, and one for the negative one. Couples of parameters obtained for each input-output pair were then used to calculate mean values.

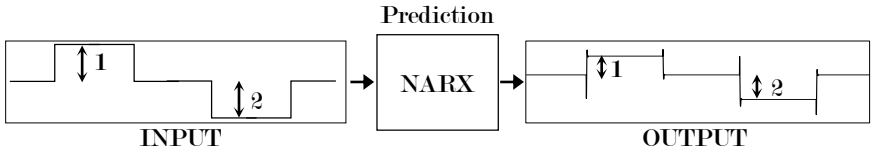

Figure 2.8: Flowsheet for the evaluation of a transfer function of a linear model

The evaluation of gain constants returned reliable values, but this procedure did not allow to obtain realistic values for time constants. This is probably due to fact that the complexity of the input signals is not trivial, to the dynamics of the states of the system and to the fact that all the disturbances entering the system have different periodicity. Further and more refined studies are needed to address the evaluation of time constants in a proper way. As regards the results concerning gain constants, values obtained with set-up 2 are reported in Table 2.3 and Table 2.4 compared to the one obtain by Foscoliano et al. [22] where single step identification was used.

SNO-R2		
Manipulated input	**Multivariable identification Set-up 2 (60 d)**	**Single step identification 105 d**
Oxygen in reactor 2	0.360	0.647
Oxygen in reactor 3	0.273	0.200
Oxygen in reactor 4	0.673	0.608
Oxygen in reactor 5	0.196	0.365
Internal recycle	$0.25 \cdot 10^{-4}$	$0.28 \cdot 10^{-4}$

Table 2.3: Comparison between gain constants for nitrate nitrogen concentration in reactor 2 obtained trough multivariable identification and single step identification [output per unit of input]

SNH-R2		
Manipulated input	**Multivariable identification Set-up 2 (60 d)**	**Single step identification 105 d**
Oxygen in reactor 2	-1.208	-1.178
Oxygen in reactor 3	-0.142	-0.780
Oxygen in reactor 4	-0.860	-0.776
Oxygen in reactor 5	-1.277	-0.195
Internal recycle	$0.19 \cdot 10^{-4}$	$0.13 \cdot 10^{-4}$

Table 2.4: Comparison between gain constants for ammonia nitrogen concentration in reactor 5 obtained trough multivariable identification and single step identification [output per unit of input]

As can be seen, the sign of constant gains can be considered correct for each multivariable identification. Even the absolute values were generally correct, but in some cases there was one order of magnitude of difference with respect to the values obtained with the identification performed singularly. Most important, these results were obtained with a system identification phase that lasted 60 days, almost half the time needed in the cited work.

2.6 Conclusions

Multivariable system identification in a process continuously stressed by varying disturbances has been studied as a strategy to speed up the procedure of system identification with respect to classical approach like single step identification. In literature there are no cases of such complex system identifications with non constant disturbances. The Benchmark Simulation Model no. 1 was used as simulator. The optimal design of experiments was used to program simultaneously variations of manipulated inputs. Non-linear autoregressive with exogenous inputs neural networks were implemented to evaluate transfer functions of linear models. This choice is coherent with the literature, since it is basically a black-box modelling that can be applied to any non-linearity. The procedure allowed to obtain good results as regards the estima-

tion of gain constants of such models. Both sign and magnitude were generally correct. However, further work is necessary to obtain more reliable results for time constants, which were not estimated correctly. The reason could lie in the complexity of the input signals and in the dynamics of the states of the system. A possible improvement for the estimation of time constants could be to analyse the disturbances entering the system in case their measurements are available in the plant.

Part II

Multivariable modelling and control of a continuous production process of complex fluids

CHAPTER 3

Rheological characterization of the product

In this chapter water-free detergents and issues related to their production are presented. Next the production process and the pilot plant used for experimental tests are described. Then, the results obtained through off-line experimental tests are presented. Afterwards, the on-line behaviour of the system is analysed. Finally some attempts of modelling the system are discussed. A more detailed discussion is postponed to the following chapters.

3.1 Water-free detergents

Since invention of washing machines and their massive introduction in consumer houses, laundry detergents have assumed increasing importance and the research by production companies is constant. Typically, laundry detergents are composed of several ingredients necessary for the cleaning procedure. Some of these ingredients are, for example:

- surfactants, for lowering surface tension;
- disinfectants, to deactivate pathogen micro-organisms;
- scents, to ensure a pleasant smell to laundry;
- rheological modifiers, to stabilize rheological properties;
- anti corrosive substances, to protect washing machines mechanisms.

In traditional detergents, all these elements are generally dispersed in a water solution. Water-free detergents instead, are composed of single concentrated doses in form of pouches which contain

all the compounds needed for the cleaning process but no water, which is added in the process by the final consumer.

In fact, the presence of water in traditional detergents shows some draw backs. First of all, when products are transported from the factory to retailers, a big part of the load is effectively water. This means that transportation costs are larger. But there are also consequences on the environment, due to bigger consumption of fuel that leads also to an increased production of CO_2. Thus, behind the production of water-free products for household hygiene there are economical and environmental reasons. In fact, one of the objective of water-free detergents is to reduce the mass to transport. Furthermore, another problem of traditional detergents is represented by capability to use the right dosage. In many cases the quantities used by final consumers are excessive and this causes wastes and, as a consequence, possible water pollution mainly by phosphorus compounds. For all these reasons, the need of single doses (in form of pouches) of water-free detergents arises. This ensures lower costs of transportation, lower air pollution, right detergent dosage, lower water pollution and better cleaned laundry.

But, while detergents diluted in water have a Newtonian rheological behaviour, water-free detergents may show a complex rheological behaviour, with an apparent viscosity drastically varying during the process. This have consequence both during the production and the consumption phases. During production, issues may arise due to the fact that, during manufacturing, shear rate conditions may be really high. If the product has a too much high viscosity, the nozzles injecting the product in the pouches can get stuck and the production must be suspended, with significant time and economic losses. Also, if the viscosity of the final product is not correct, the cleaning process can fail because of a product which is not uniformly spread in the laundry. And this is cause of badly cleaned laundry and therefore unsatisfied consumers.

For all these reasons is necessary to monitor and control in real time the continuous production process of this kind of products to ensure the required achievements in terms of quality of the product.

3.2 Process and pilot plant description

To the purpose of study the process of the continuous production of water-free detergents, experimental tests were carried out in a pilot plant, located at the facilities of the Brussels Innovation Center (BIC) in Belgium, by Procter & Gamble, partner of the CONSENS project.

The pilot plant consisted basically of a series of tank containing the ingredients for the production and a main pipe. Each ingredient was pumped from the tank to the main pipe through secondary lines and with a certain mass flow rate. Each injection point in the main pipe was separated from the others. The different ingredients moved along the pipe because of a pressure differential and they were mixed up by means of static mixers positioned between inlets.

The ingredients used in this phase to simulate the production were four and they were representative of a very simplified formulation of this type of product. They were:

- a base (hereafter refereed as *ingredient A*);
- a solvent (*ingredient B*);
- perfumes (*ingredient C*);
- a rheological modifier (*ingredient D*).

The precise nature of the compounds cannot be disclosed for confidentiality reasons. This does not affect the purpose of this work since what it was studied and developed here was the methodology to monitor and control processes like the one treated.

Along the pipe different sensors of pressure, flow rate, and temperature were placed. Their presence and position, as well as the length of the pipes, depended on the specific design tested, which varied during the study. Additionally, in some cases, on-line viscometers were used to measure the on-line viscosity of the product.

The product was finally collected in a tank where samples are taken for the off-line rheological measurements performed with a rheometer.

A simplified scheme of the pilot plant is reported in Figure 3.1. The design of the plant is repaired by Patent N. US 2013/0225468 A1. For further details see Corominas, Beelen, and Akalay [26].

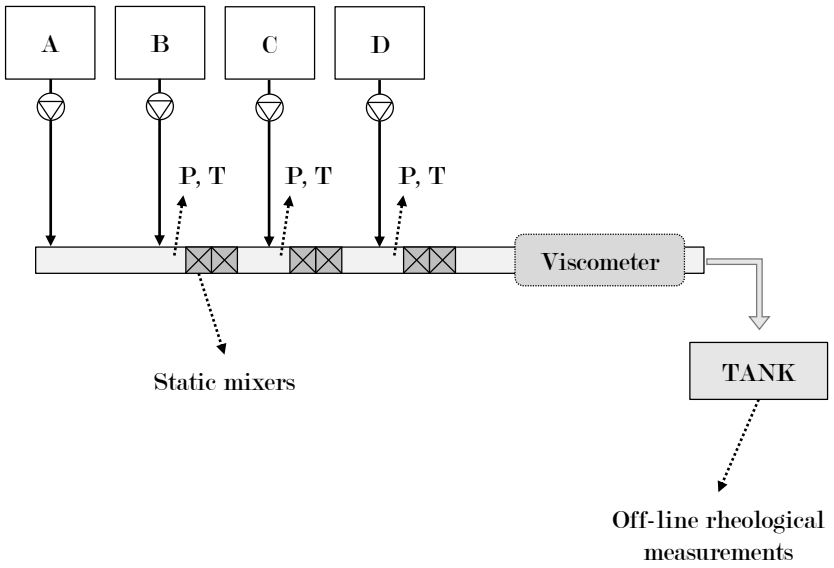

Figure 3.1: Simplified scheme of the pilot plant

3.2.1 Experimental campaigns

Various typologies of tests have been conducted in order to analyse the rheological and dynamic behaviour of the product when different combinations of ingredients were used and also understanding the impact of each ingredient on the rheology of the detergent. Particular attention was given to ingredients B and D influences on viscosity. In all the trials the system was initialized with a start up phase which led the process to nominal condition in terms of mass flow rates. When stationary conditions were reached, positive and negative step variations were applied to the mass flow rates of ingredients in order to perform on-line system identification and to study the effects on rheology.

Off-line rheological analyses were conducted, at the BIC by Procter & Gamble, using an AR 2000 rotational rheometer by TA Instruments ([27]), equipped with a 40 mm parallel plate and a Peltier plate, and an Anton Paar HTR 301 automated rheometer ([28]), equipped with a 40 mm cone and plate measuring system, a Peltier hood and a Peltier chamber. Measurements were cross-validated, at University of Cagliari, with an Anton Paar MCR 102 rotational rheometer ([29]), equipped with 25 mm and 50 mm parallel plates and a Peltier plate.

In some of these tests, an Endress-Hauser Proline Promass 83I Coriolis flow-meter was used, positioned in the main pipe, after the last static mixer. For further details about the viscometer, one can refer to the technical documents present on the producer website ([30]). This measurement instrument is capable to provide measurements of flow, density and temperature but also an on-line viscosity measurement. The measuring principle for viscosity is the Coriolis effect, applied by inducing an oscillation into the measuring pipe (in which the fluid flows) trough an oscillating mass. This generates a shear force which is used to calculate viscosity. But the on-line viscosity value returned by the Promass is a measurement that can be related to a point estimation of the viscosity. This means that this type of instrument is suitable for Newtonian fluids, but not for non-Newtonian fluids, because it is not capable to describe changes of the apparent viscosity with the shear rate. Despite that, this viscometer can surely provide effective information regarding the dynamic of the system.

An ultrasound rheological sensor prototype was also used in some cases. Further details about this sensor are reported in Chapter 6.

Table 3.1 reports a summary of performed experimental tests and corresponding used sensors and instruments. A first set of samples, produced with positive and negative variations of mass flow rate of ingredients B and D, was analysed through off-line rheological measurements by means of the AR 2000 rheometer and cross-validated with the MCR 102 rheometer. The Promass 83I viscometer was also installed in the pilot plant, thus dynamic information were available. With the same samples, temperature variations analyses were performed by means of the MCR 102 rheometer. More details regarding these experiments are reported in the following paragraphs and in Chapters 4 and 5.

A second set of samples, again produced with positive and negative variations of mass flow rate of ingredients B and D, were analysed through off-line rheological measurements by means of the HTR rheometer. In this case, the pilot plant was equipped with the ultrasound rheological sensor. More details are reported in Chapter 6.

	ΔP sensors	T sensors	On-line viscosity (Promass 83I)	Off-line rheological measurements (AR 2000)	Off-line rheological measurements (MCR 102)	Off-line rheological measurements (HTR)	Ultrasound sensor prototype
Run I	×	×	×	×	×		
Run II	×	×				×	×

Table 3.1: Summary of experimental campaigns

3.3 Rheological behaviour of the product

3.3.1 Off-line rheological behaviour

Performed analyses consisted mainly of measurements of viscosity when shear rate varied. First, the temperature of the Peltier plate of the rheometer was set, then the sample was placed on it, and the measurement plate was lowered to the defined gap. A *pre-shear* treatment was carried out in order to stress samples with a constant shear rate value (typically, 0.01 s^{-1} or 0.1 s^{-1}) for a time that depended on the specific test. This phase at constant shear rate was important to remove possible history effects on the product. In fact, as explained in Paragraph 1.3.1, many materials have rheological properties which depend on their previous history. The pre-shear phase helps to cancel these effects. This needs to be performed for each measurements and it contributes also to make the various experimental tests comparable. Furthermore, the pre-shear phase is crucial to mitigate temperature gradient, especially when measurements are performed at a temperature which is different from the temperature of the product. When the pre-shear phase was concluded, a variation of shear rate according

to a logarithmic ramp was performed, starting from the pre-shear value and arriving typically to a shear rate value equal to 1200 s^{-1}.

Many of these experimental trials have been conducted in this way, testing hundreds of samples taken at many different conditions. From the results of these test, the off-line rheological behaviour of the product turned out to be as non-Newtonian shear-thinning fluids, with a viscosity that decreases when shear rate increases. In Figure 3.2 an example of such experimental viscosity curve for a sample of product, obtained in Run I, is reported. As can be seen, the fluid clearly shows a shear-thinning fluid behaviour. It appears to be a power law relationship between viscosity and shear rate for intermediate values of shear rate. Furthermore, viscosity decreases according to a plateau for high values of shear rate.

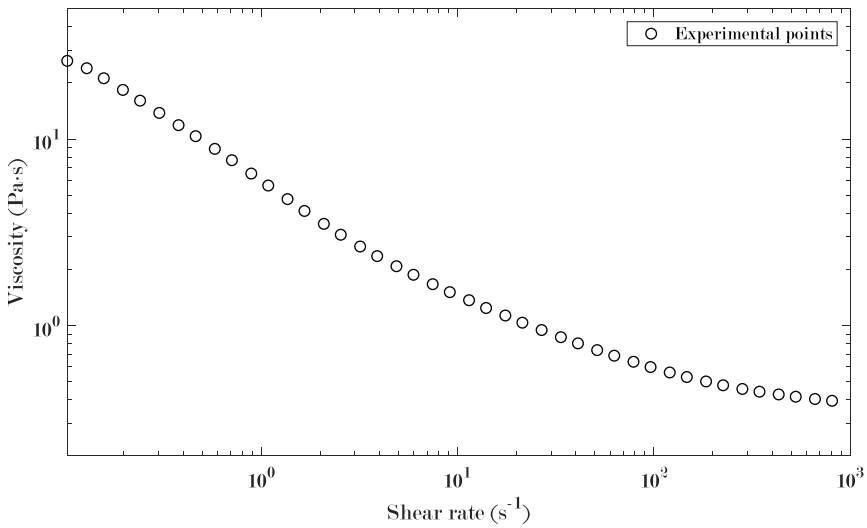

Figure 3.2: Example of an experimental viscosity curve of the studied product

For these reasons, in order to describe the dependence of viscosity on the shear rate, a Carreau model was chosen (Bird and Carreau [31] and Carreau, MacDonald, and Bird [32]). This model describes a shear-thinning fluid which shows constant value of viscosities (μ) for low and for high values of shear rate ($\dot{\gamma}$), and a variable viscosity according to a power law for intermediate values of shear rate. The model is reported in Equation 3.1, where

μ_0 is the viscosity for shear rate equal to 0, μ_∞ is the viscosity for high values of shear rate, the reciprocal of λ represents the shear rate value in correspondence of which the behaviour change from Newtonian to power law and finally $\nu = 1 + arctan(\alpha)$ where α is the slope of the power law. In Figure 3.3 a schematic representation of the Carreau model is reported.

$$\mu = \mu_\infty + \frac{\mu_0 - \mu_\infty}{[1 + (\lambda \cdot \dot{\gamma})^2]^{\frac{\nu}{2}}} \tag{3.1}$$

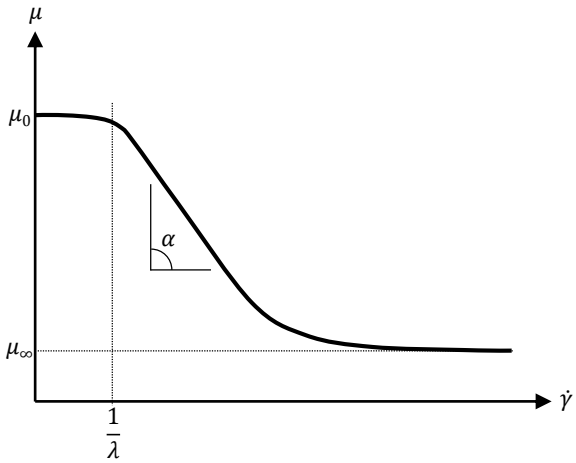

Figure 3.3: Description of the Carreau model

The chosen model was able to capture the viscosity curves of the product under investigation. In Figure 3.4 is reported, as example, a non-linear regression performed with the Carreau model over the example curve of Figure 3.2. With such regression, the four parameters of the Carreau model were estimated. However, the Newtonian zone at low shear rate was not appreciable in this curve because the experimental test started at 0.1 s^{-1}. This might cause an inaccurate estimation of η_0 and λ parameters. This made tests done starting from a shear rate equal to 0.01 s^{-1} probably more reliable in terms of good estimation of these two parameters. However, measurements at very low shear rate could be strongly affected by measurement errors.

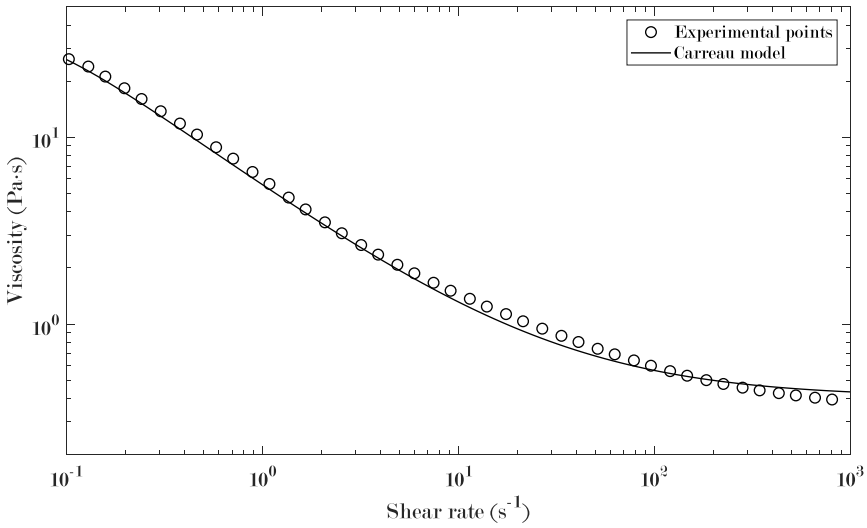

Figure 3.4: Example of a non-linear regression with Carreau model overlying experimental points

3.3.2 On-line rheological behaviour

Figure 3.5 reports the on-line information returned by some sensors present in a typical trial when positive and negative variations of mass flow rate of ingredient D were applied. The same is reported in Figure 3.6 as regards ingredient B. These data were obtained in Run I. As can be seen by these results, the on-line viscosity, measured by the Promass 83I viscometer, appears to be negatively correlated to the amount of ingredient B and to the amount of ingredient D: when increasing ingredients D or B mass flow rates, on-line viscosity decreases, and vice versa. Also, non-linear responses are appreciable. Indeed, amplitudes of responses for positive variations of mass flow rates are different from amplitudes of responses for negative variations of mass flow rates. Regarding dynamics, the effects of ingredient B on viscosity appears to be more rapid and almost immediate with a negligible time constant. This is not true for ingredient D, which surely shows a not negligible time constant, with seemingly first-order like dynamics. For what concerns delay times, they are mainly related to the length of pipes, and it is appropriate to consider them as adjustable parameters according to the used configuration.

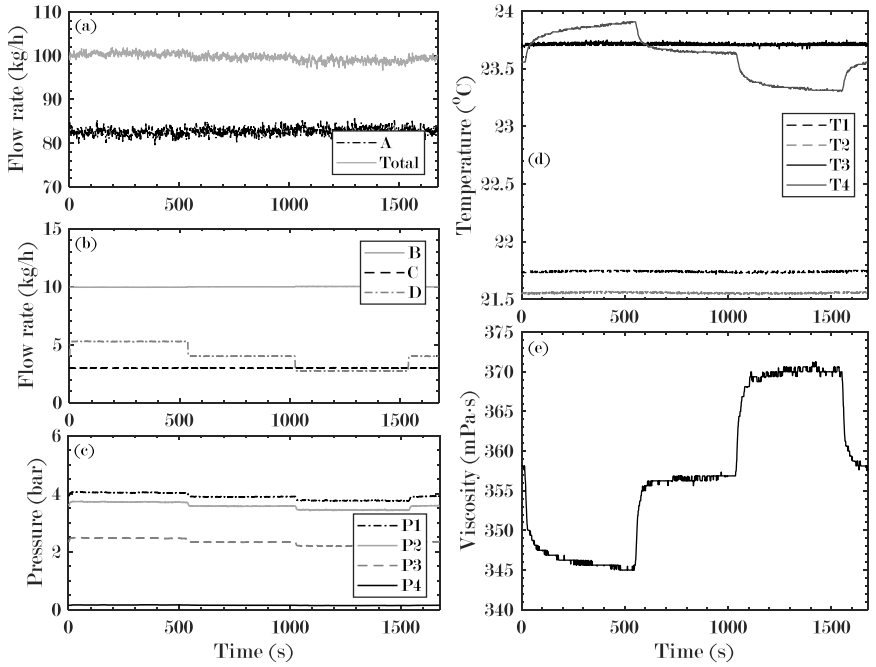

Figure 3.5: On-line data obtained for variations of ingredient D

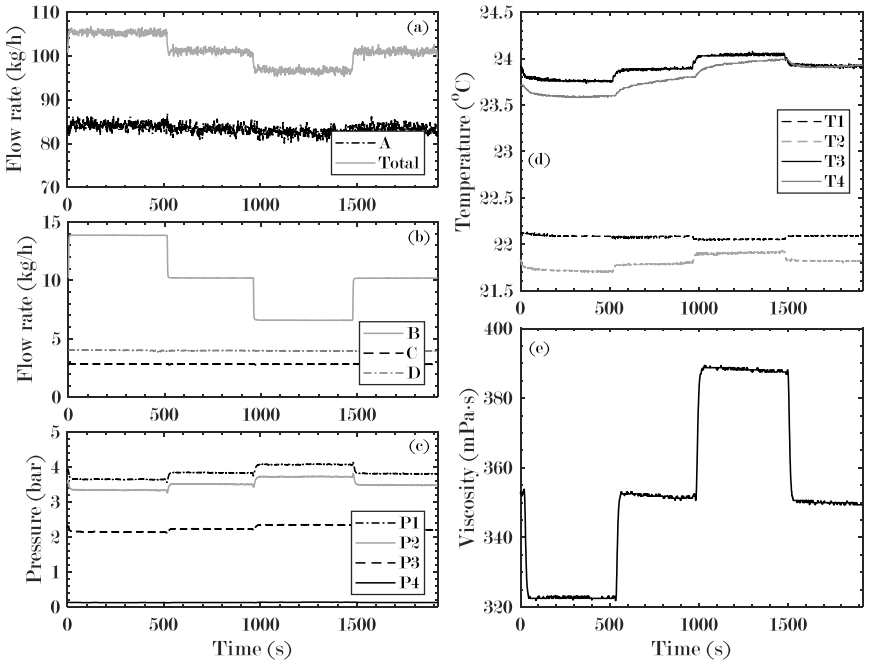

Figure 3.6: On-line data obtained for variations of ingredient B

As previously said, these tests were not informative on the whole rheology of the product. The results were mostly useful to obtain details regarding the characteristic times of the process. It was assumed that characteristic times found in this way were valid for viscosities in the entire range of shear rate values investigated. In order to estimate them, system identifications with different kind of transfer function models were tested. On-line viscosity was used as output and mass flow rate of ingredient B and ingredient D are used as inputs. The best results were returned by first order plus dead time (FOPDT) models. Because of the non-linear responses of the system, constant gains will not be considered here, and their analysis and estimations are addressed in next chapters. As regards the identification of characteristic times, in Figure 3.7 is reported an example of on-line viscosity response following mass flow variations of ingredient D and the corresponding obtained FOPDT model.

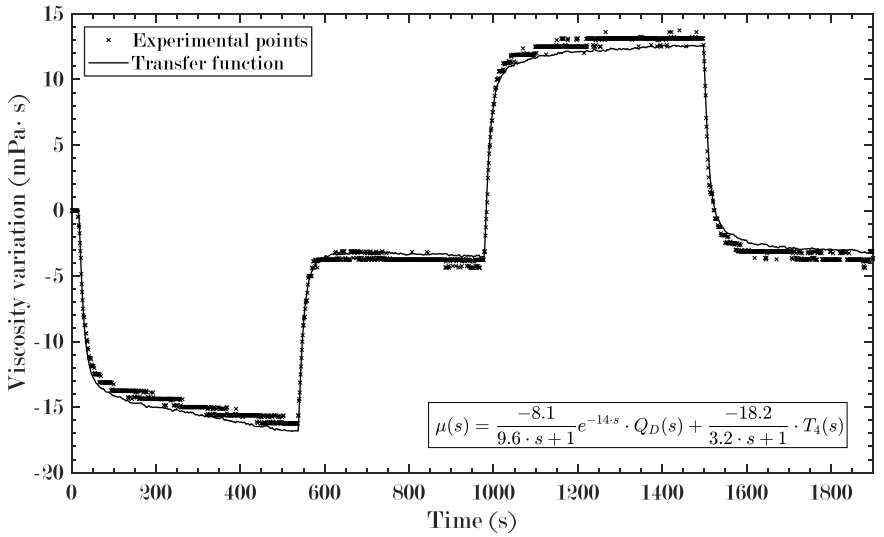

Figure 3.7: Transfer function fitting measured on-line viscosity

Because of the different actual temperatures of the ingredients (mainly due to the different specific heats and the different storage temperatures), it is necessary to filter out the effects of the temperature on the measured viscosity. To do that, even a term for the dependence between on-line viscosity and temperature measured in correspondence of the viscometer was added to the

model as measurable disturbance. As can be seen, the matching of the model is quite good and similar results have been obtained for different conditions and for both ingredients. Using this strategy, time constants and dead times have been calculated to describe the dependency between the on-line viscosity and ingredient B and D for different conditions. Numerical details are discussed in next chapters and they are reported in Paragraphs 4.2 and 5.2 for the corresponding cases.

3.3.3 Effects of ingredients on rheology

The results returned by the Promass 83I viscometer, described previously in Paragraph 3.3.2, suggest that on-line viscosity is negatively correlated to the amount of ingredient B and to the amount of ingredient D, meaning that when the amounts of these ingredients in the mixture increase, the on-line viscosity value decreases and vice versa. But these experiments can not be considered informative on the whole rheology of the product, since the on-line viscometer is only capable to perform a point estimation of the viscosity. Thus, data obtained by the Promass were considered useful only to estimate delay times and time constants of the system.

Real rheological effects of ingredients on the product rheology can be investigated analysing outcomes returned by the more reliable off-line rheological measurements. These measurements showed that when the amount of ingredient D in the blend increases, viscosities at low shear rates increase while viscosities at high shear rates decrease. The opposite happens when the flow rate of ingredient D decreases. The viscosity curve experiences some sort of rotation with a pivot at intermediate shear rate. The inversion point occurs in a range of shear rate between, more or less, 500 s^{-1} and 650 s^{-1}. This described behaviour of the off-line viscosity is showed in Figure 3.8 for ingredient D variations. As can been seen, for the same variation of flow rate of ingredient D, both in positive and negative directions, the effects on viscosity are extremely non-linear.

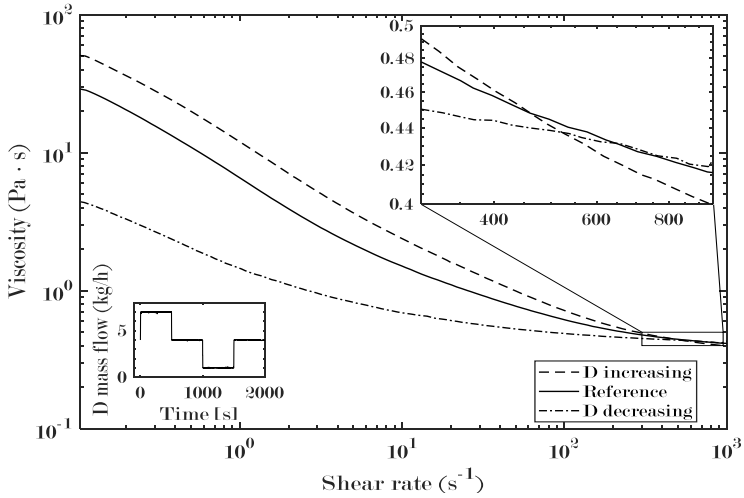

Figure 3.8: Impact of ingredient D on viscosity curve

As regards ingredient B, the behaviour is less complex. In fact, there is a sort of simple dilution effect: when the amount of ingredient B in the recipe increases, viscosities increase and vice versa. Even in this case, the response is non-linear.

In Chapter 4, a more detailed modelling of the process is addressed with the purpose to design single-input single-output control system, while in Chapter 5 the process is modelled by means of a neural network to design a multi-input multi-output controller.

CHAPTER 4

SISO control system

In this Chapter the development of a one-point control system for the control of a viscosity curve is addressed. A stationary model is built from off-line rheological measurements of viscosity against shear rate. A dynamic part is then added to the model by exploiting on-line viscosity measurements. A PI control system is then designed and tuned. Afterwards, analysis of different configurations of the control system are carried out in order to study the performances of the controller. Finally, results are presented.

4.1 Introduction

As introduced in Paragraph 1.3.2, industrial continuous production processes of complex fluids can not rely in reliable real-time control systems of the rheological properties due to the lack in the current market of instruments capable to provide reliable on-line rheological information for non-Newtonian fluids. Research in this field is active, first results are promising and some solutions are emerging. In this Chapter, a preliminary analysis of control problems for these kinds of processes is addressed and a control strategy applicable in the future, when such measurements instruments will become available, is developed.

As explained in Paragraph 3.1, when dealing with the production of complex fluids like water-free detergents, viscosity values measured at low and high shear rate are both very important production parameters and they need to be carefully checked and verified in order to ensure that the production proceeds without any inconveniences and to obtain a product which respects speci-

fications. In future implementations of control systems applied to cases like this one, a specific range of values of viscosity against shear rate may be indicated as specification, as reported for example in Figure 4.1, where the target range is represented by the dark area bounded by the dotted lines. A controller should be capable to maintain the entire viscosity curve of the product (solid line curve in the Figure), measured on-line during production, inside the desired range of viscosities, acting on manipulated inputs. The viscosity curve could go out of specifications for different reasons. For example, if suppliers provide raw materials with changes in recipes or if changes in process parameters occur. Such inconveniences could lead to out-of-specifications viscosity curves that could lie totally or partially (dashed line curves in Figure 4.1) outside the target range.

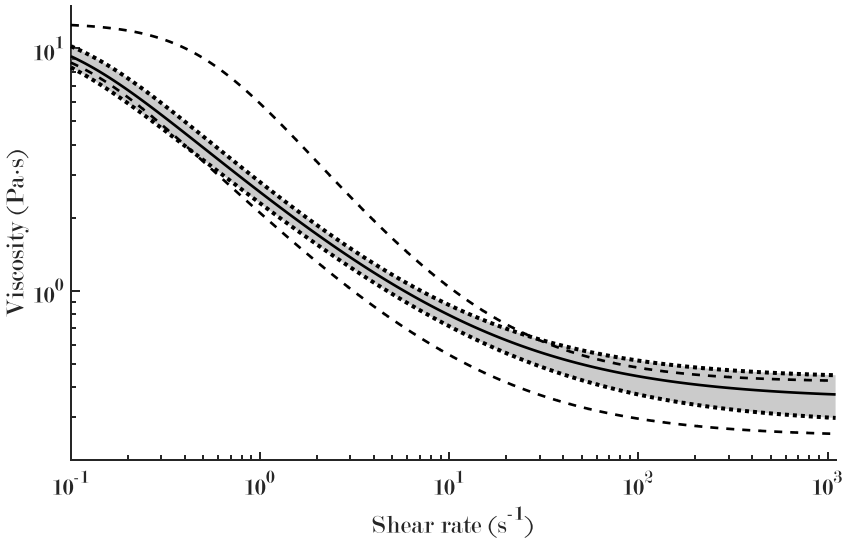

Figure 4.1: Target range of viscosity (darker area bounded by dotted lines) represented together with an example of an in-control viscosity curve (solid line) and examples of out-of-control viscosity curves (dashed lines)

The main objective of the strategy implemented and discussed in this Chapter was to maintain an entire viscosity curve close to a target curve as much as possible as a disturbance moved away the system from nominal conditions. In the treated case the disturbance consisted in a change of temperature of the product during production. It was assumed that only one manipulated variable

was available. In particular, the mass flow rate of ingredient D was chosen as manipulated input.

Due to the lack of available real-time rheological sensors, the control system has been designed simulating the production process of the detergent. A model was built from off-line rheological data and with dynamic information obtained by the Promass 83I viscometer. This model relates viscosities of the final product to the quantity of a specific ingredient used during the production.

4.2 Process modelling and system identification

The water-free detergent is a shear-thinning non-Newtonian fluid and for its mathematical description, the Carreau model was chosen (see Chapter 3). In order to build a model capable to simulate the process, it was decided to relate the viscosity curve of the final product to the quantity of ingredients. To this purpose, empirical relationships between the four parameters of the Carreau model and the amount of ingredient D used during production were studied.

First, a reference recipe has been defined with the mass flow rates of ingredients reported in Table 4.1. Then, different batches of product have been produced in the pilot plant: the reference recipe and recipes where the amount of ingredient D was increased by 19.25%, 31.75%, 42.50% and 73.75% and decreased by 21%, 31.75%, 42.5% and 73.75%, for a total of 9 different combinations of ingredients. Changes in ingredient D during production were accomplished according to step variations of the flow rate. Time

Ingredient	**Flow rate [kg/h]**
A	83
B	10
C	3
D	4

Table 4.1: Amount of ingredients in the reference recipe

was given to ensure that the new stationary state was reached. Samples of the nine different products were taken from the end of the main pipe of the plant.

4.2.1 Stationary model

Off-line measurements of viscosity against shear rate have been carried out. Measurements have been accomplished according to the following program:

- pre-shear phase with a constant shear rate value of 0.05 s^{-1} for 3 minutes;
- variable shear rate phase with variations of shear rate according to a logarithmic ramp from 0.05 s^{-1} to 1200 s^{-1} in 3 minutes and with 32 experimental points for decades;
- temperature equal to 20°C.

Figure 4.2 shows results of these measurements: viscosity curves are reported for each of the nine different batches. The curve relative to the reference recipe (dashed line) is reported together with curves representing recipes with an increasing amount of ingredient D (solid lines) and with curves representing recipes with a lower amount of ingredient D (dashed-dotted lines).

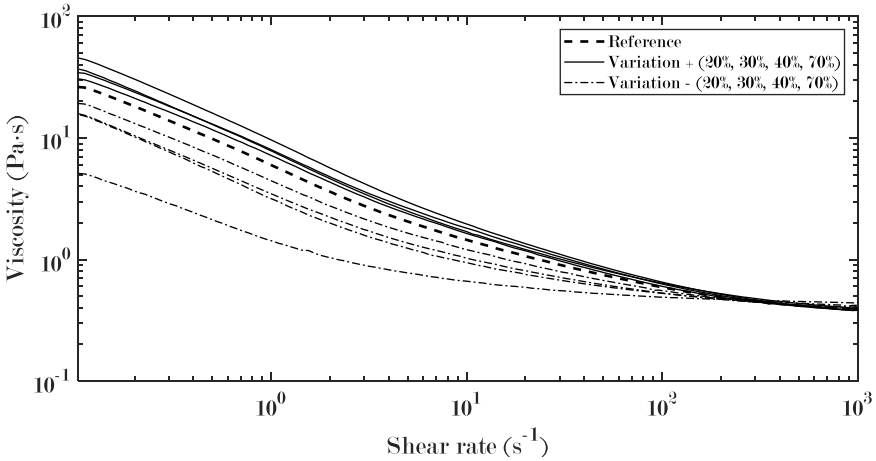

Figure 4.2: Experimental viscosity curves for batches of product with different amounts of ingredient D

As can be seen, Q_D variations have more influence in the left part of viscosity curves, in correspondence to low values of shear

rate. The influence decreases when the shear rate increases. For low values of shear rate, viscosity increases when Q_D increases. For high values of shear rate (more or less above 400 s^{-1}), the behaviour is opposite, with the viscosity that decreases when Q_D increases.

With the purpose to obtain an estimation of the four parameters of the Carreau model (μ_0, μ_∞, λ and n, as illustrated in Paragraph 3.3.1) for each experimental curve, non-linear regression of the model have been performed. For the parameters estimation, iterative least squares technique was used. Results are reported in Table 4.2, where Q_D is the mass flow rate of ingredient D.

The parameter μ_0 increases with the amount of ingredient D. Instead, the parameter μ_∞ decreases its value as ingredient D increases. These results correspond with the general characterization of the fluid. The two parameters λ and ν do not seem to depend on the amount of ingredient D.

At this point, linear regressions have been performed in order to better understand if significant dependences between each of these four parameters and the amount of ingredient D were present. Table 4.3 reports the R^2 statistic and the $p - value$ of the F-statistic for the four regressions. As regards μ_0 and μ_∞, R^2

$Q_D[kg/h]$	Δ	μ_0	μ_∞	λ	ν
1.05	-73.75%	7.5019	0.4622	13.1799	0.7591
2.30	-42.50%	26.5819	0.4601	16.038	0.8103
2.73	-31.75%	28.9572	0.4303	19.5065	0.7488
3.16	-21.00%	29.9716	0.4187	14.5125	0.7423
4	-	39.0804	0.413	12.9359	0.7563
4.77	+19.25%	44.9615	0.3603	12.9979	0.7341
5.27	+31.75%	51.7496	0.361	13.5853	0.7327
5.70	+42.50%	61.6792	0.3917	16.2601	0.7593
6.95	+73.75%	71.98	0.3563	14.6509	0.7637

Table 4.2: Parameters of the Carreau model obtained from non-linear regressions of the viscosity curves representing recipes with different amounts of ingredient D

values are close to one while $p-values$ are lower than the typical significance level (0.05). For λ and ν, R^2 values are close to zero and $p-values$ are greater than 0.05.

	μ_0	μ_∞	λ	ν
R^2	0.9819	0.8353	0.0153	0.0823
$p-value$	0.0000	0.0006	0.7512	0.4542

Table 4.3: R^2 and $p-value$ statistics for the four regression of Carreau model parameters

Because of these reasons, for μ_0 and μ_∞ linear models have been chosen. On the other hand, one can conjecture that λ and ν do not depend on the ingredient D flow rate and they can be considered as constant. Figure 4.3 shows the evolution of the four parameters with the variation of flow rate of ingredient D and the corresponding models.

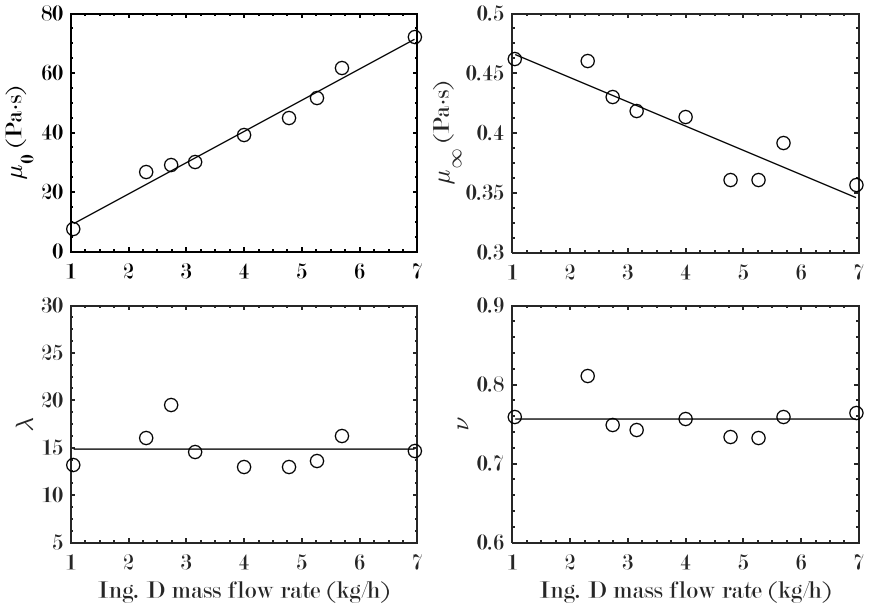

Figure 4.3: Relationships between the four parameters of Carreau model and amount of ingredient D

Equations 4.1-4.4 report the definitive models that were adopted to relate the dependence of the parameters on Q_D.

$$\mu_0(Q_D) = 10.5052 \cdot Q_D - 1.6653 \tag{4.1}$$

$$\mu_\infty(Q_D) = -0.0203 \cdot Q_D + 0.487 \tag{4.2}$$

$$\lambda = 14.8519 \tag{4.3}$$

$$\nu = 0.7563 \tag{4.4}$$

Eventually, the empirical model describing the dependence between viscosity and ingredient D is reported in Equation 4.5. Figure 4.4 reports the performance of the built model when compared to the experimental curves.

$$\mu(\dot{\gamma}, Q_D) = \mu_\infty(Q_D) + \frac{\mu_0(Q_D) - \mu_\infty(Q_D)}{[1 + (\lambda \cdot \dot{\gamma})^2]^{\frac{\nu}{2}}} \tag{4.5}$$

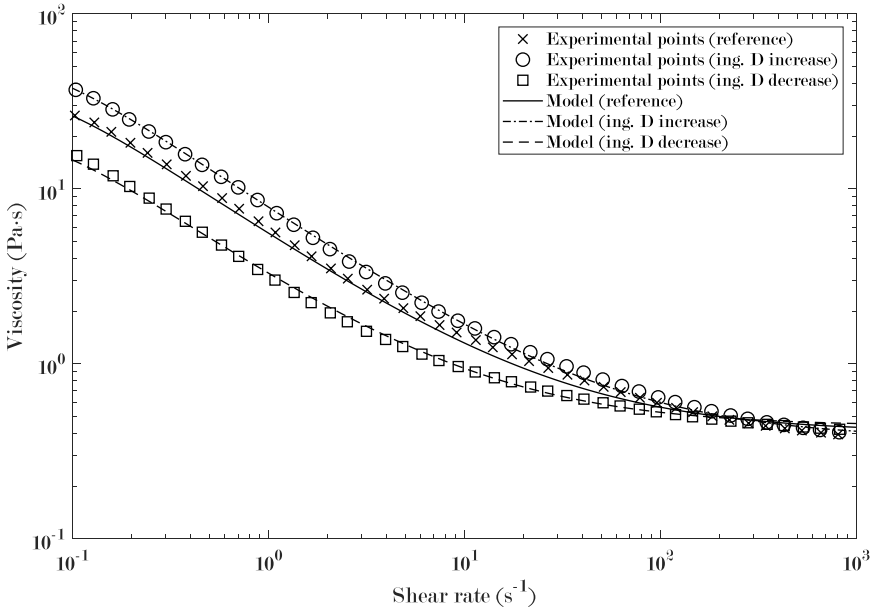

Figure 4.4: Performance of the model

4.2.2 Dynamic model

A dynamic part was then added to the stationary model in Equation 4.5, exploiting a dynamic characterization of the process by means of the data collected with the on-line viscometer Promass 83I. On-line viscosities recorded by the Promass during step variations of ingredient D were used to perform a system identification. This was due to the fact that it was the only on-line reliable measurement available for characteristic time. Behaviours of on-line viscosities, similar to the one reported in Figure 3.5 sub-plot e, were approximated according to first order plus dead time models. Results regarding gain constants were discarded, while results obtained for dead times and time constants were used to calculate two mean values of these parameters. For the dead time a value of 16.5 seconds was calculated, while for the time constant, 16.63 seconds was obtained. These values, obtained with the on-line viscometer, were assumed as a reasonable estimation of the characteristics times of the entire range of shear rate of interest.

Thus, the final dynamic model describing the dependence of the viscosity from the shear rate and the amount of ingredient D present in the mixture was a FOPDT model composed of a stationary part with the purpose to calculate constant gains, and a dynamic part accounting for the characteristic times of the process. The model is eventually reported in Equation 4.6, where k_p is the gain constant, τ_p is the time constant and t_d is the dead time. Figure 4.5 reports a scheme of the model.

$$\frac{\Delta\mu(\dot{\gamma})}{\Delta Q_D} = \frac{k_p(\dot{\gamma}, Q_D)}{\tau_p s + 1} e^{-t_d s} \tag{4.6}$$

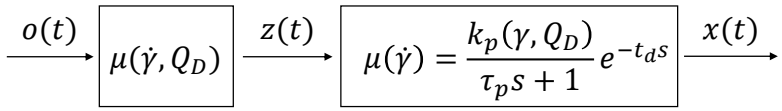

Figure 4.5: Block diagram of the applied model

This model was validated with the following procedure. Starting from nominal condition of production (amounts of ingredients as the reference recipe), a step variation of 20% of the flow rate of

ingredient D was given. During this, samples of the product were collected during the transient phase. With these samples, off-line measurements of viscosity against shear rate were accomplished. Results of these experiments were compared to the performance of the model. The outcome was quite satisfactory. Figure 4.6 shows the evolution of the model, reported along with experimental points.

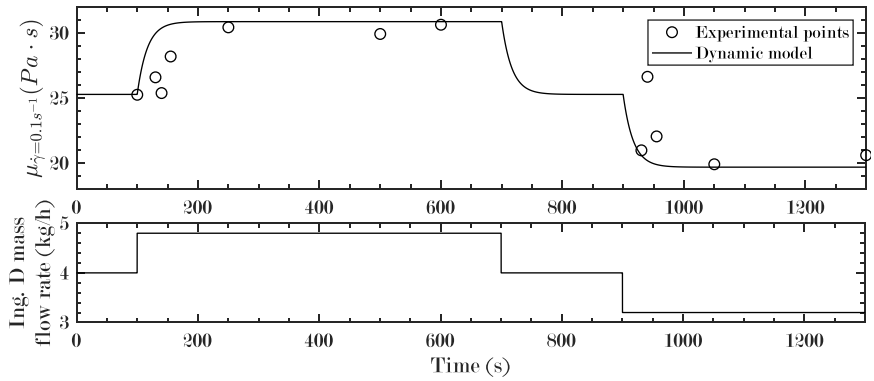

Figure 4.6: Validation of the dynamic model

Finally, the dependence of the viscosity on the temperature was taken into account and modelled. Off-line measurements of viscosity were accomplished according to the program previously illustrated but with different temperatures (from 15°C to 30°C, one for sample and with an interval of 2.5°C). Then, viscosities at $\dot{\gamma}$=0.1 s^{-1}, 1 s^{-1}, 10 s^{-1}, 100 s^{-1} and 1000 s^{-1} were extracted from these data. Dependences of these viscosities with respect to the temperature were evaluated. Results are reported in Figure 4.7. As can been seen, for each value of shear rate explored, viscosity decreases with the increasing of temperature. Viscosity data at $\dot{\gamma}$=0.1 s^{-1} are quite scattered. The scattering decreases when the shear rate increases. To describe the viscosity-temperature dependence, an exponential functionality was assumed (see Equation 4.7).

$$\mu = e^{d_1 + d_2 T} \tag{4.7}$$

Values of d_1 and d_2 are reported in Table 4.4, together with respective Mean Square Error (MSE) values.

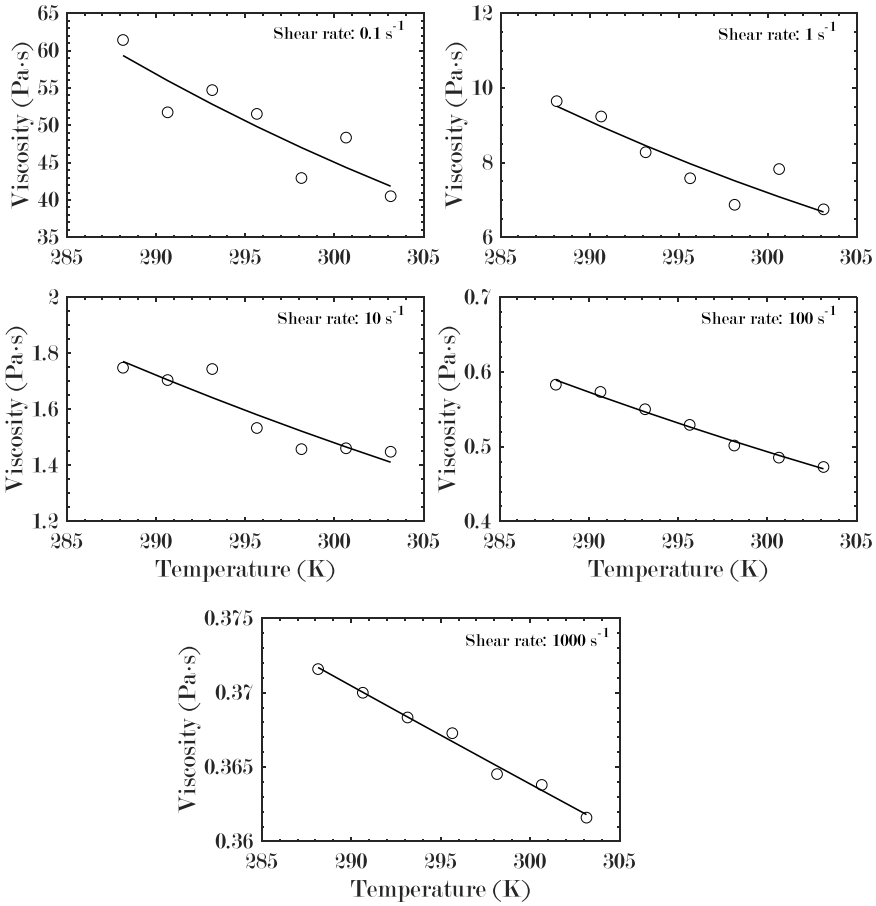

Figure 4.7: Viscosity dependence from temperature

	d_1	d_2	MSE
$\mu_{0.1s^{-1}}$	10.7946	-0.0233	12.6442
$\mu_{1s^{-1}}$	9.0462	-0.0236	0.2488
$\mu_{10s^{-1}}$	4.9336	-0.0151	0.0037
$\mu_{100s^{-1}}$	3.7975	-0.0150	$0.27532 \cdot 10^{-4}$
$\mu_{1000s^{-1}}$	-0.4715	-0.0018	$0.15988 \cdot 10^{-6}$

Table 4.4: Parameters for the dependence of viscosity on temperature

4.3 Control design and results

The goal of the control system was to keep the viscosity curve of the product near a target viscosity curve as much as possible when disturbances entering the process moved away the curve from nominal conditions (see Figure 4.1). The biggest challenge was to do that by using only one manipulated input (in this case, ingredient D flow rate), because possible controllable outputs were in principle infinite. The choice of the controlled output became then crucial. In practice, a shear rate value has to be selected, where the corresponding viscosity has to be controlled. The controller should be able to mitigate the effects of perturbations for viscosities at any shear rate value. If these condition can be respected, a single input - single output (SISO) controller was implementable.

Because the analysis of viscosity curves of the product shows that variations of ingredient D affect mostly the viscosities corresponding to low shear rate values, this part of the viscosity curve was probably most suitable to be controlled. A PI feedback controller (see Ogunnaike and Ray [21] for more details) was designed to act on the flow rate of ingredient D, when a step variation of temperature enters the process as a disturbance and perturbs the system. Different controllable points on the viscosity curve have been chosen as controlled outputs and tested. The performances of the controller in the different implementations have been evaluated by the Mean Square Error (MSE, Equation 4.8) and the load on the manipulated input (Equation 4.9). n_d indicates the total number of points in which the viscosity curve is discretized while the index i is the i-th of these points. n_d is equal to 100 and i varies from 10^{-1} to 10^{3}. The points are logarithmically spaced. $\mu(\dot{\gamma}_i)_{target}$ and $\mu(\dot{\gamma}_i)$ are respectively the i-th viscosity of the target curve and the i-th viscosity of the actual curve.

$$MSE = \frac{1}{n_d} \sum_{i=1}^{n_d} [\mu(\dot{\gamma}_i)_{target} - \mu(\dot{\gamma}_i)]^2 \tag{4.8}$$

$$load = \frac{max(\Delta Q_D)}{\Delta T} \tag{4.9}$$

During simulations the dynamics of sensors and actuators were

neglected. Results are reported in Table 4.5.

$\dot{\gamma}[s^{-1}]$	Load	MSE
0.1	0.1234	0.25218
0.17	0.1515	0.12882
0.25	0.1763	0.15174
0.5	0.2198	0.48892
1	0.2478	0.90507
5	0.2364	0.71567
10	0.2170	0.4559
100	0.2292	0.6121

Table 4.5: Values of load and MSE for different controlled points

As can be seen, the minimum distance between the controlled curve and the target curve was obtained when the system was controlled at 0.17 s^{-1}, with a low load on the manipulated variable. It should be remarked that this value was the best one for this case under study but it may be different when treating other processes and other non-Newtonian fluids.

Figure 4.8 shows a summary of the controlled system with the control applied at $\dot{\gamma}$=0.17 s^{-1}, together with the evolution of the system when there was no control system acting and the evolution of the system when the controlled point was set to be at $\dot{\gamma}$=500 s^{-1}. In sub-plot *a* the disturbance in terms of temperature variations is reported, with a temperature increase of 5°C occurring at t=100 s. In response of that (sub-plot *b*), the control at $\dot{\gamma}$=0.17 s^{-1} increases the amount of ingredient D to counteract the effect of temperature (dashed line, IV), while the control at $\dot{\gamma}$=500 s^{-1} behaves in opposite way, decreasing the quantity of the manipulated variable (dotted-dashed line, II).

The effects of these actions can be seen in sub-plots *c* and *d* where the viscosities at $\dot{\gamma}$=0.17 s^{-1} and $\dot{\gamma}$=500 s^{-1} are, respectively, reported. For both cases, controllers act well for their respective controlled outputs but move away the curve from the target curve (solid line, I) for the other case, more than in the case of uncontrolled viscosity (dotted line, III). Notice that the effects on the overall curve are different: a change in ingredient D amount has more significant effects for viscosities at low shear rate values.

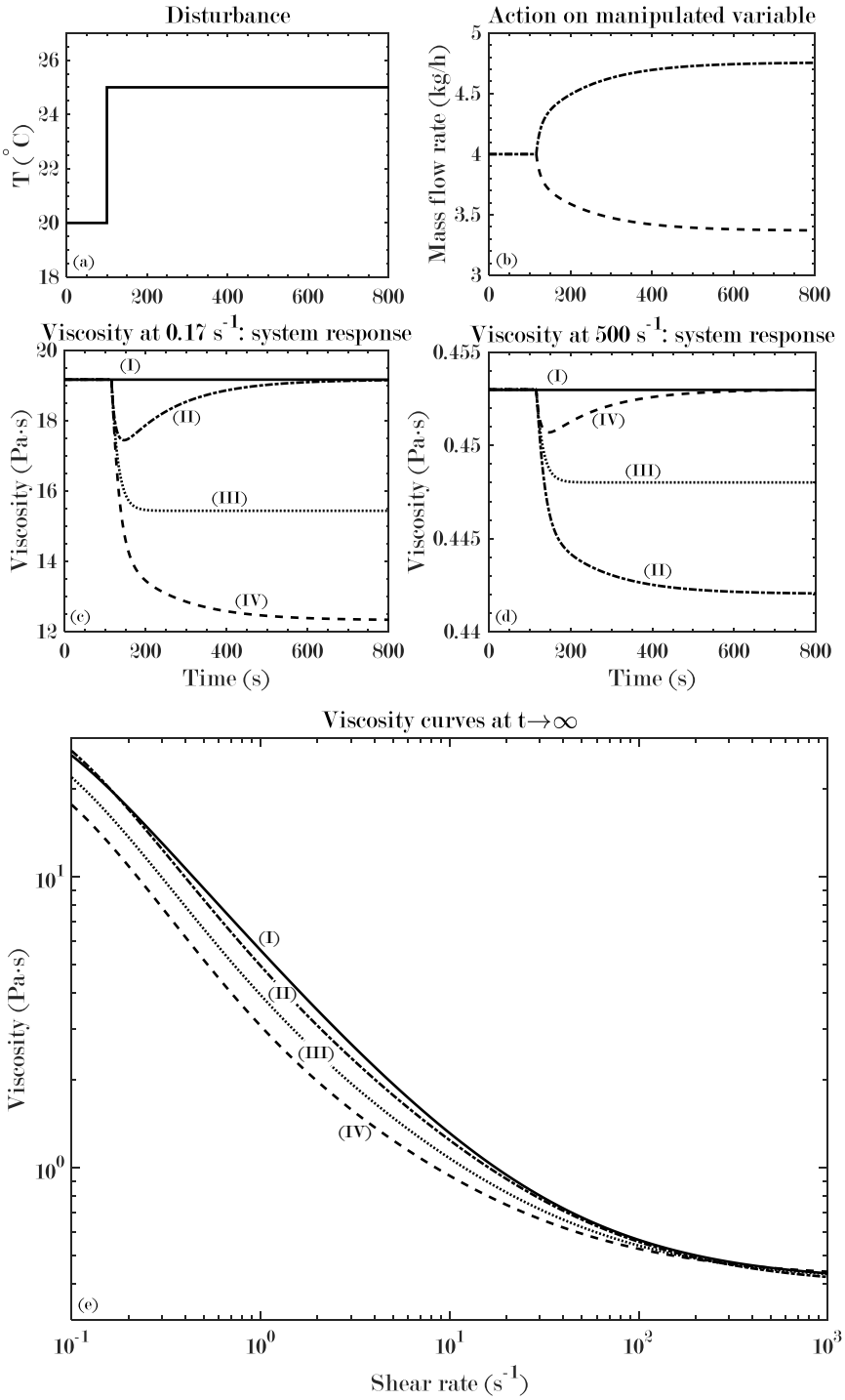

Figure 4.8: Summary of the controlled system for the different control actions

Consequently, the control applied at $\dot{\gamma}$=500 s^{-1} does not give satisfactory results as regards the whole viscosity curve, but rather it gives opposite results. This is easily seen in sub-plot *e* where the controlled curve with the control applied at $\dot{\gamma}$=500 s^{-1} is more distant from the target curve than in the case that there was no control (dotted line, III).

All these considerations show clearly that the choice of the most suitable point to control is a crucial part of designing a SISO control system in systems like the one treated here. A poor choice could even bring the system in the opposite direction with respect to the desired one.

4.4 Conclusions

In this Chapter a possible strategy to face real-time control of viscosity curves during the continuous production process of non-Newtonian fluids was presented.

The production process of water-free detergents was used as case study. Data were collected from a pilot plant where the production was accomplished by mixing four different ingredients.

A simulation model was built with the purpose to mimic the evolution of the process when production was running, with the purpose to study and develop control strategies. This model relates the viscosity curve of the final product to the amount of a specific ingredient used as manipulated input. A dynamic characterization was included in the model. The dependence between the viscosity and the temperature was also considered. With this simple model, issues related to the control of the viscosity curve during production have been studied.

A one-point control of the viscosity curve of a non-Newtonian fluid was implemented with the goal to maintain the viscosity curve as close as possible to the target curve. Analysis were performed in order to understand how the choice of different shear rates where viscosity is evaluated affected the curve. In particular the controller was designed to act when a disturbance perturbed the system. In this case the disturbance was represented by a step variation of temperature.

The obtained outcomes showed that in similar cases an analysis

of the best point suited for the control is needed. This is especially true when having only one manipulated input at disposal. An understanding of the effects of this variable on the viscosity curve is necessary. In cases like the one here presented, a poor selection of the controlled point on the viscosity curve could lead to undesired results, with the controlled curve moving away from the target curve.

In the future these control strategies may be easily implemented for similar processes when on-line rheological sensors will become available and reliable. However, although a one-point control is possible for this particular case, it should be not applicable for other kinds of processes.

CHAPTER 5

MIMO control systems

In this Chapter the possibility to implement a multivariable control system in continuous production process of water-free detergents is addressed. First, a process simulator is built by exploiting non-linear neural networks. Then, different multivariable control systems are implemented with the purpose to control different selected outputs on the viscosity curve. Results are finally presented.

5.1 Introduction

In Chapter 4, a one-point control of the viscosity curve for a continuous production process of water-free detergents has been designed and tested with the purpose to maintain the viscosity curve of the product as close as possible to the target curve, when the system was perturbed by disturbances. Results showed that, at least for the case at hand, it was possible to use only one point on the viscosity curve as controlled output. It was also found that a poor choice of this output may be counterproductive., bringing the system to an opposite direction with respect to the wanted one. Furthermore, a SISO control system, as the one designed, was not adequate if specifications are more severe and require to control, with high precision, viscosities both at low and high shear rate values. For all these reasons, different approaches are needed.

At this purpose, a multi-input multi-output (MIMO) control approach can surely ensure a more efficient way to control such a process. For example, a double feedback control system may be applied to control, separately, two different points on the viscosity curve using two different ingredients mass flow rates. Another

solution could be the use of a Model Predictive Control (MPC) (Ogunnaike and Ray [21]), which can handle non-square system. In this way two manipulated variables can be used to control more than two points of the viscosity curve. A MPC is also effective when dealing with systems with high time delay like the one addressed.

To design and test multivariable control systems, a process simulator was built exploiting a data-driven based approach. The simulator was based on off-line rheological measurements of viscosity against shear rate and on the dynamic characterization cited in Paragraph 3.3.2. Then, two control configurations have been implemented and analysed: a double feedback control system and a MPC control algorithm, both for set-point tracking and disturbance rejection and with two manipulated variables at disposal.

5.2 Process simulator

The role of the process simulator was to provide dynamic viscosity responses, taking as inputs the amounts of ingredients. The simulator was designed to mimic a process including a rheological sensor.

A first principle description of the system was not considered due to the high complexity of the system. Because of that, efforts focused on data-driven modelling. As in the previously described implementation of a control system (see Chapter 4), on-line complete information about rheological properties of the product were not available due to the lack of reliable sensors. Thus, off-line rheological measurements, obtained with rheometers, were used to build a static model. Dynamics were later added exploiting data gathered by the Promass viscometer, as previously done.

To relate off-line viscosities measurements at different values of shear rate with the amounts of ingredients, a non-linear neural network was designed and trained. Figure 5.1 reports the structure of it. The four inputs entering the neural network are the amounts of ingredients in terms of mass fractions. The four outputs were chosen on the basis of the work carried out for the SISO control system and they are the viscosities at 0.1 s^{-1}, 1 s^{-1},

10 s^{-1} and 1100 s^{-1}. After some attempts, it was chosen to rely on a single hidden layer consisting of six neurons and an output layer consisting of four neurons. One hidden layer was considered sufficient. For both the hidden and output layers, a sigmoidal activation function was used.

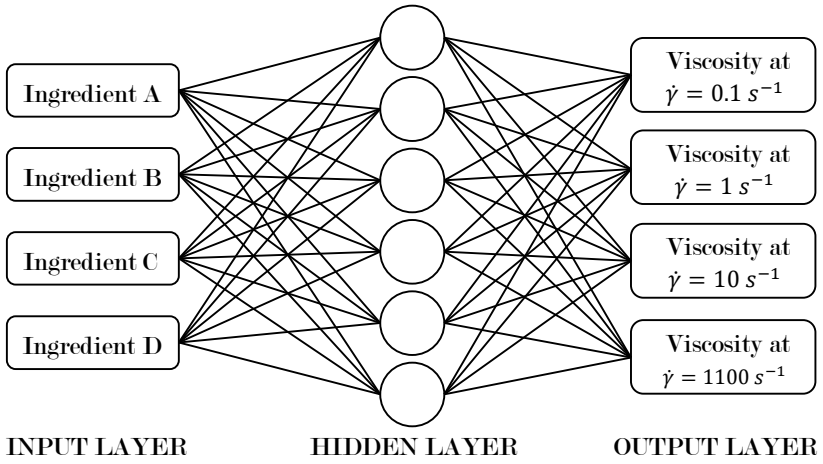

Figure 5.1: Structure of the designed and trained neural network

Experimental tests were carried out varying the amounts of ingredients, exploring 27 different conditions shown in Figure 5.2, with ranges of ingredients mass fractions as reported in Table 5.1. A total of 171 viscosity curves (viscosity against shear rate) were collected. The neural network was trained according to the Levenberg–Marquardt algorithm and using 70% of data for training, 15% for validation and 15% for test.

The performances of the neural network were evaluated by means of the parameters R^2 (Equation 5.1) and Mean Absolute Deviation (MAD, Equation 5.2). In these equations, μ_i is the measured viscosity, $\bar{\mu}$ is the mean viscosity, N is the number of

	A	**B**	**C**	**D**
Min	0.730	0.072	0.000	0.012
Max	0.880	0.250	0.039	0.066

Table 5.1: Minimum and maximum values for ingredient mass fractions

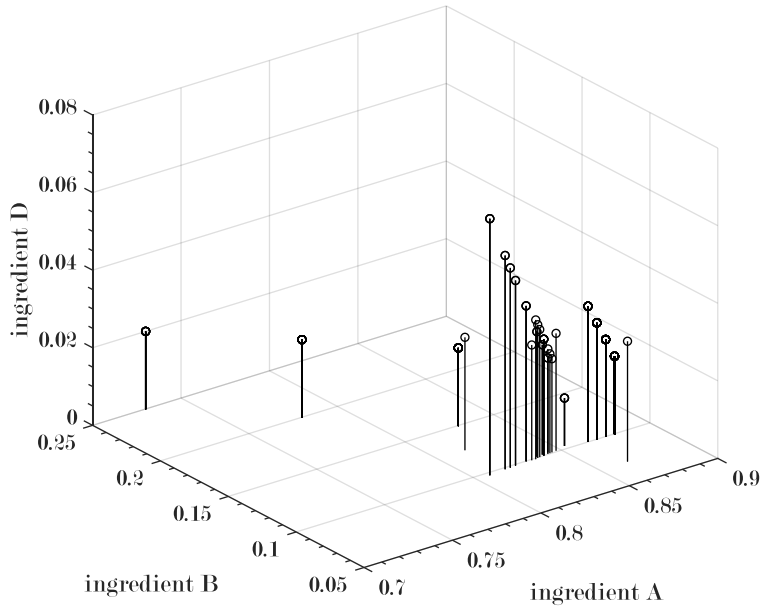

Figure 5.2: The 27 different combinations of ingredients investigated. Ingredient C mass fraction can be calculated by subtraction

experimental points and $\hat{\mu}_i$ is the estimated viscosity.

$$R^2 = 1 - \frac{\sum_{i=1}^{N}(\mu_i - \hat{\mu}_i)^2}{\sum_{i=1}^{N}(\mu_i - \bar{\mu})^2} \tag{5.1}$$

$$MAD = \frac{1}{N}\sum_{i=1}^{N}\left|\frac{\mu_i - \hat{\mu}_i}{\mu_i}\right| \tag{5.2}$$

The trained neural network was capable to predict viscosities with satisfying results (Table 5.2). R^2 coefficients are relatively high, indicating a good prediction. Only at 1100 s^{-1} the R^2 is relatively low (0.937), probably due to the fact that viscosity variations in this range of shear rate are small in terms of absolute values. As regarding MADs, values are always lower than 10%.

Figure 5.3 reports measured viscosities against predicted viscosities. The circles represent data used for training and validation, while diamonds are data used for test. Predictions are satisfying. However, at 1100 s^{-1} there are some uncertainties in the prediction.

$\dot{\gamma}(s^{-1})$	R^2	$MAD(\%)$
0.1	0.97597	8.6
1	0.96732	7.0
10	0.98126	4.0
1100	0.93699	3.7

Table 5.2: Performances of the neural network

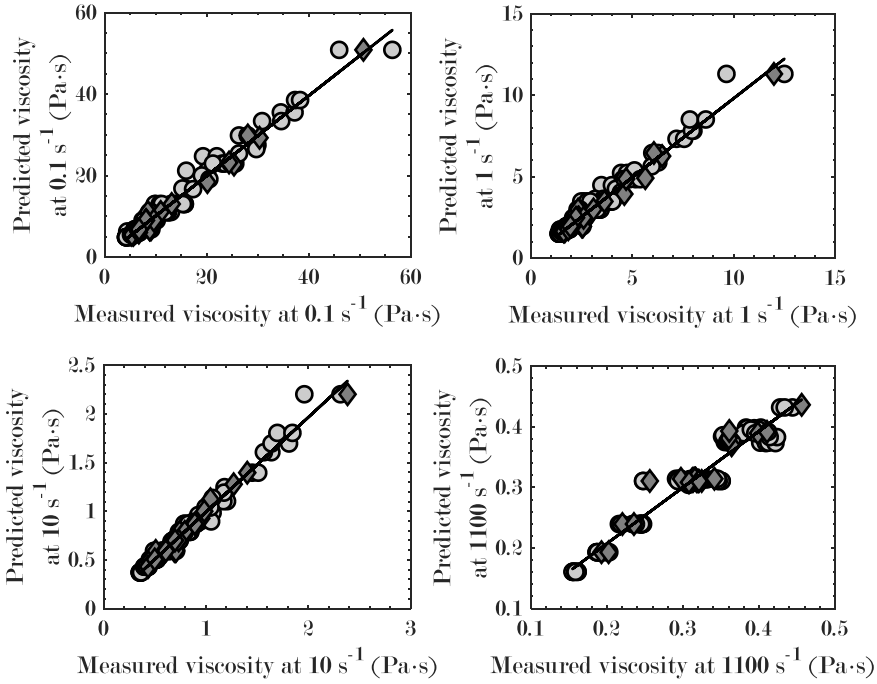

Figure 5.3: Measured viscosities against predicted viscosities

Figure 5.4 reports standard residuals against predicted viscosities. Residuals r_i are defined as reported in Equation 5.3, where i indicates the i-th observation, v_i is the measured value and $\hat{v}_i$ is the predicted value. They represent the part of the observation that the model is unable to describe. They should behave as random numbers.

$$r_i = v_i - \hat{v}_i \tag{5.3}$$

It is common to use the definition of *standard residuals* r_i^{std}, as

reported in Equation 5.4 where MSE is the mean square error.

$$r_i^{std} = \frac{r_i}{\sqrt{MSE}} \tag{5.4}$$

As shown in Figure 5.4, calculated standard residuals do not show a deterministic structure, confirming that the model seems to correctly describe the observations.

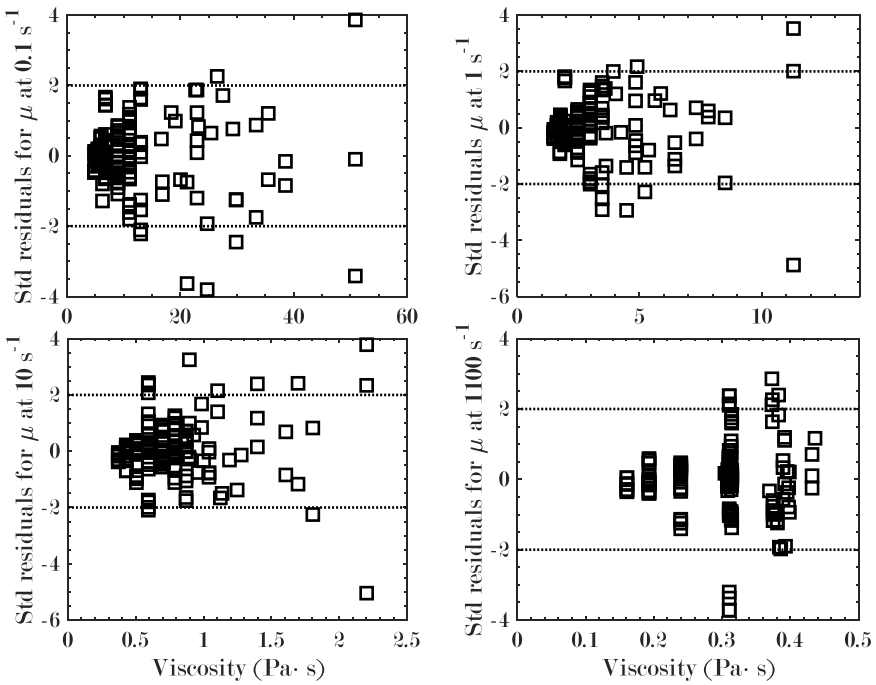

Figure 5.4: Standard residuals for the four predicted viscosities

The built neural network describes stationary relationships between viscosities and amount of ingredients. A continuous-time description of the process was obtained by exploiting Hammerstein models (Daniel-Berhe and Unbehauen [33]), which are models that describe dynamic processes using non-linear blocks coupled together with a linear block (Figure 5.5). The trained neural network was included in the Hammerstein-like model as a non-linear memory gain (first block) (Tronci et al. [34] and Tronci and Baratti [35]), then a simple linear dynamic is added (second block).

The obtained model can be described by Equation 5.5, where x represents the n-dimensional state vector, o represents the m-dimensional inputs vector, A_M is a constant matrix and f_{NN} is the memoryless model consisting of the neural network.

$$\dot{x}(t) = A_M x(t) + f_{NN}(o) \tag{5.5}$$

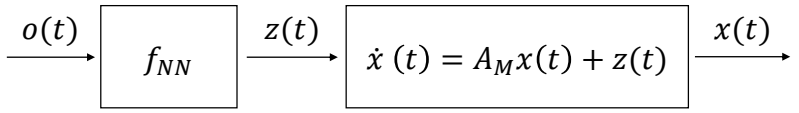

Figure 5.5: Block diagram of the applied Hammerstein model

As previously accomplished, dynamic data were obtained with Promass viscometer. Due to the fact that a first order plus dead time model seems to be sufficient to describe the dynamic behaviour of the system (Figure 5.6), mean values for the time delay and the time constant were calculated with data coming from different plant configuration and assumed valid for the entire range of explored shear rate. The time delay was set equal to 8 s and the time constant was set equal to 20 s.

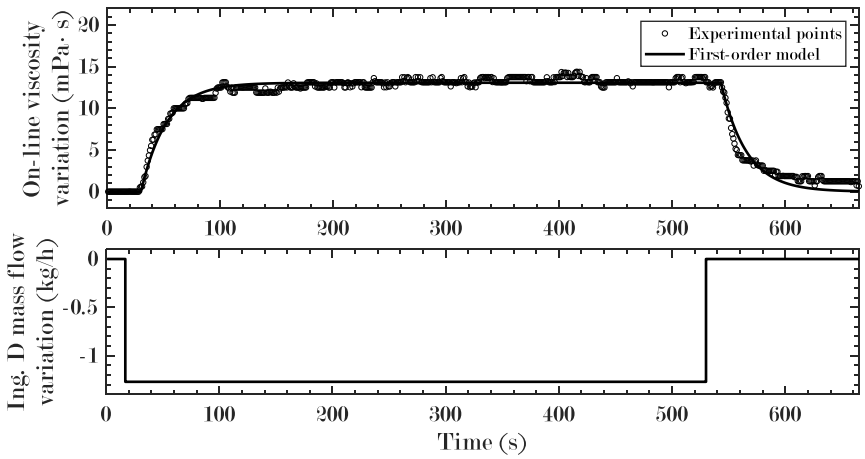

Figure 5.6: First order plus delay model (solid line) compared to experimental points (circles) of on-line viscosity for a step variation of mass flow ingredient D

Equation 5.6 reports the model of the process simulator, where μ_i are the calculated viscosity at each control loop, μ_i^{NN} are the

viscosity calculated with the neural network, μ_i^P are the calculated viscosity at the previous control loop, t_d is the time delay of the process, τ_p is time constant of the process, i is the i-th viscosity.

$$\mu_i = (\mu_i^{NN} - \mu_i^P) \cdot H(t - t_d) \cdot (1 - e^{-\frac{t-t_d}{\tau_p}}) + \mu_i^P \tag{5.6}$$

5.3 Double feedback control

A double feedback control system was designed and tested exploiting two separate feedback controllers implemented with proportional and integral actions (hereafter referred as PI controllers). The control system will act as a double SISO with two manipulated variables and two controlled variables.

The configuration was the following: the process simulator provides some points of the rheological curve corresponding to the actual situation of the process. Random noise was then added to this curve in order to simulate the measurement noise. Then two points of the curve, one at low shear rate (0.1 s^{-1}) and the other at high shear rate (1100 s^{-1}), are extracted and sent separately to the PI controllers for comparison with targets.

The separation was possible because a Relative Gain Array (RGA) analysis (Bristol [36]) showed decoupled variables. The differences between targets and measured values represent the errors of the system and the two controllers act separately on the two manipulated variables. In more detail, one PI controller receives the error at low shear rate and acts on the mass flow of the ingredient D while the other PI controller receives the error at high shear rate and acts on the mass flow of the ingredient B. This choice was due to the fact that ingredient B affected the whole rheological curve, with negative gain constants describing the relationship between ingredient B flow rate and viscosities at the different values of shear rate investigated. On the other hand, ingredient D had much more influence on the rheological curve in the low shear rate region and lower influence on high shear rate region. Furthermore, positive gain constants described the relationship between ingredient D flow rate and viscosities in correspondence of low shear rate values, negative gain constants described the relationship between ingredient D flow rate and

viscosities in correspondence of high shear rate values. A schematic representation of the control loop is reported in Figure 5.7.

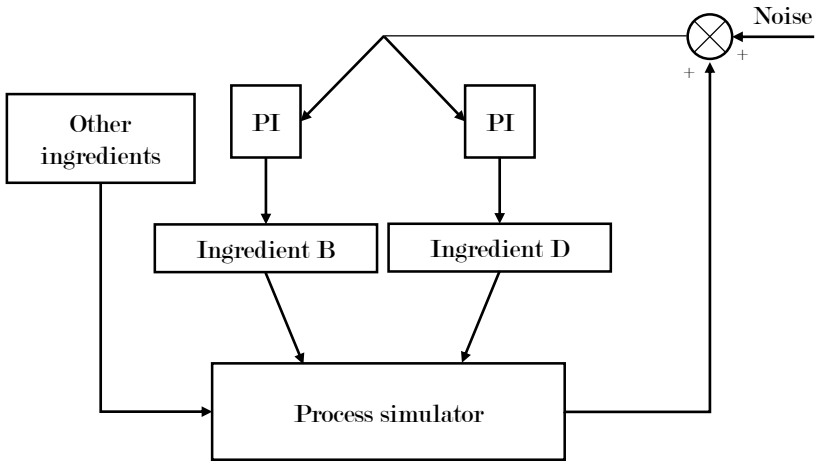

Figure 5.7: Schematic representation of the control loop with two feedback controllers

Time intervals for control action and sampling, time constants and time delays for simulator and tuning parameters for the two PI controllers are reported in Table 5.3. The measurements noise was applied as random noise of about ±2% of the nominal viscosities values, in more detail: -0.2 Pa·s<random noise<+0.2 Pa·s for $\mu_{0.1s^{-1}}$ and -0.003 Pa·s<random noise<+0.003 Pa·s for $\mu_{1100s^{-1}}$.

Parameter	Value
Time interval for control action	10 s
Measurement delay	30 s
Time constants for simulator[1]	20 s, 20 s
Time delays for simulator[1]	8 s, 8 s
K_C[1]	0.006, -2
τ_I[1]	40, 8

[1]values for each controlled viscosity, respectively $\mu_{0.1s^{-1}}$, $\mu_{1100s^{-1}}$

Table 5.3: Simulation parameters for the double feedback control system

Despite the two controllers work as two separate SISO and

the variables are decoupled, it is important to underline the fact that, in the real process, variations of ingredient D have an effect, even if minimal, also on high shear-rates. Analogously, variations on ingredient B affect viscosity at low shear-rates. The process simulator correctly describes this aspect.

In Figure 5.8 the response of the system to a step variation of the target is reported, confirming the goodness of the controller. In this case the goal of the controlling action was a decrease of the rheological response at any shear rate, in order to obtain a product with a lower viscosity for both high shear rate and low shear rate values.

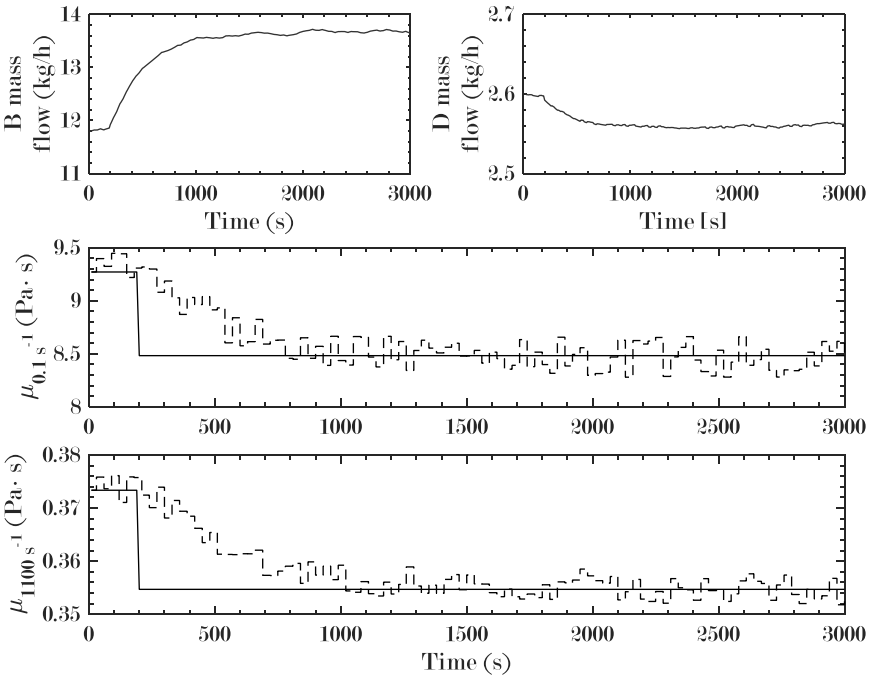

Figure 5.8: Behaviour of the system for set-point tracking

Nevertheless, the tested control system showed clearly two main issues. The first one is that the responses are slow in terms of dynamics. In fact, more than ten minutes are necessary to bring the two controlled variables to the new set-point values. The second problem is that there is no control at all for viscosities at intermediate shear rate values. This means that target values could not be guaranteed for the entire rheological curve.

For these reasons, a control system capable of faster responses and able to control a wider range of viscosities is necessary. A Model Predictive control was then chosen.

5.4 Model Predictive Control

A Model Predictive Control was designed and tested in its Dynamic Matrix Control (DMC) formulation. In this type of controllers, models of the process are used to predict the future responses of the system. New control actions are then calculated with the goal to satisfy a given objective function (for example the minimization of the distance between a target value and a measured value for a variable) (Ogunnaike and Ray [21]).

The configuration of the developed controller was the following: the process simulator provided the chosen points of the rheological curve corresponding to the actual situation of the process. Random noise was then added to these values in order to simulate the measurement noise. The MPC algorithm used the differences with targets and modelling errors to calculate the future control actions needed to minimize the distances between the targets and the future predicted evolution of the system. New control actions were then sent to the simulated process and the control loop started again. A schematic representation of the control loop is reported in Figure 5.9.

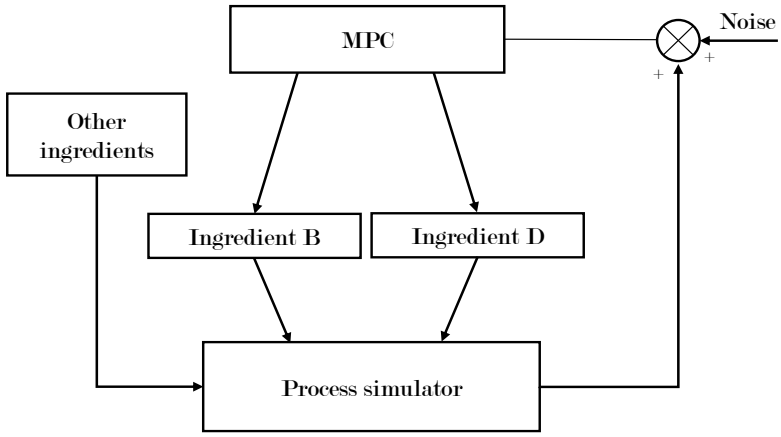

Figure 5.9: Schematic representation of the control loop for the MPC

Mass flow rates of ingredient B and D have been chosen as manipulated inputs. Because small variations that occured at $\dot{\gamma} = 1100s^{-1}$ may create problems regarding the robustness of the controller (Cogoni et al. [37]), only the other three viscosities (at $\dot{\gamma} = 0.1$ s^{-1}, 1 s^{-1} and 10 s^{-1}) have been chosen as controlled outputs.

Equation 5.7 reports the objective function O used by the MPC algorithm to calculate control actions. $\boldsymbol{F}$ represents the dynamic matrix, $\boldsymbol{W}$ is a weighting matrix whose elements are used as tuning parameters, $\boldsymbol{K}$ is a diagonal matrix used for penalizations of control actions, $e_P(k+1)$ represents the difference between current outputs, predicted as no further control actions were applied, and wanted outputs, $\Delta\boldsymbol{u}$ represents the future variations of control actions, H_p is the prediction horizon and H_u is the control horizon.

$$O = [(e_P(k+1) - \boldsymbol{F}\Delta\boldsymbol{u})^T \boldsymbol{W}(e_P(k+1) - \boldsymbol{F}\Delta u)] + [\Delta\boldsymbol{u}]^T \boldsymbol{K}[\Delta\boldsymbol{u}] \quad (5.7)$$

The weighting matrix $\boldsymbol{W}$ is a $(3\times\mathrm{H_p})\times(3\times\mathrm{H_p})$ diagonal matrix, composed of three diagonal matrices, one for each output, which have dimension $\mathrm{H_p x H_p}$. The elements on the diagonals of these matrices are positive weights for each specific output. The structure is reported in Equation 5.8.

$$\boldsymbol{W} = \begin{bmatrix} diag(w_1) & 0 & 0 \\ 0 & diag(w_2) & 0 \\ 0 & 0 & diag(w_3) \end{bmatrix} \quad (5.8)$$

The matrix $\boldsymbol{S}$ is a $(2\times\mathrm{H_u})\times(3\times\mathrm{H_u})$ diagonal matrix, composed of two diagonal matrices, one for each input, which have dimension $\mathrm{H_u x H_u}$. The elements on the diagonals of these matrices are penalizations for each specific input. The structure is reported in Equation 5.9.

$$\boldsymbol{S} = \begin{bmatrix} diag(s_1) & 0 \\ 0 & diag(s_2) \end{bmatrix} \quad (5.9)$$

To implement the DMC, a linear predictive model is required. In order to obtain this model, the simulator was stressed with step inputs variations and the recorded responses were used to build the $\boldsymbol{F}$ matrix ([21]). Starting from reference conditions, step changes of different amplitude were applied to manipulated

inputs (Foscoliano et al. [22], Mulas et al. [38]), and then the coefficients for the dynamic matrix were calculated by averaging the obtained results.

To assess the performance of this control strategy, various tests were carried out. The main objective of the work is to understand how some aspects of on-line measurements, like sampling delay and noise, can affect the control of the viscosity curve of the product, in view of future implementations of continuous monitoring and control of rheological properties. With this regard, ultrasound sensors are the most promising technologies in terms of future implementations. But information like reliability, repeatability and measurements noise are not available at this day. It may be useful for the future to know and understand, for example, what occurs if the time delay between the moment of the measurements and the moment in which the measurement is deployed is greater than the characteristic time of the process.

5.4.1 Set-point tracking

In the development of the MPC, parameters like control and prediction horizons, simulation time and weights, were found by tuning after various analysis of dynamic responses. The following parameters were chosen: the control action was applied every 10 seconds, the prediction horizon H_p was set equal to 16, the control horizon H_u was set equal to 4, and only the first control action was applied at each control loop. In Table 5.4 are reported other simulations parameters for a reference case. The measurements noise was applied as random noise of about ±2% of the nominal viscosities values, in more detail: -0.2 Pa·s<random noise<+0.2 Pa·s for $\mu_{0.1s^{-1}}$, -0.05 Pa·s<random noise<+0.05 Pa·s for $\mu_{1s^{-1}}$ and -0.02 Pa·s<random noise<+0.02 Pa·s for $\mu_{10s^{-1}}$.

Figure 5.10 shows the dynamic behaviour of the system in response to step variations of set-points for the three controlled viscosities. In this case a simulated sampling time of 30 seconds was chosen. As can be seen, the controller is capable to bring the controlled viscosities to desired value in short time. To avoid excessive overshoots, the action on the manipulated inputs were penalized.

Parameter	Value
Time interval for control action	10 s
Measurement delay	30 s
Time constants for simulator[1]	20 s, 20 s, 20 s
Time delays for simulator[1]	8 s, 8 s, 8 s
Weights[1]	w_1=1, w_2=12, w_3=40
Penalization[2]	s_1=3.5 x10^4, s_2=3.0 x10^2

[1]values for each controlled viscosity, respectively $\mu_{0.1s^{-1}}$, $\mu_{1s^{-1}}$, $\mu_{10s^{-1}}$

[2]values for each manipulated input, respectively ingredient D and B

Table 5.4: Simulation parameters for the reference case

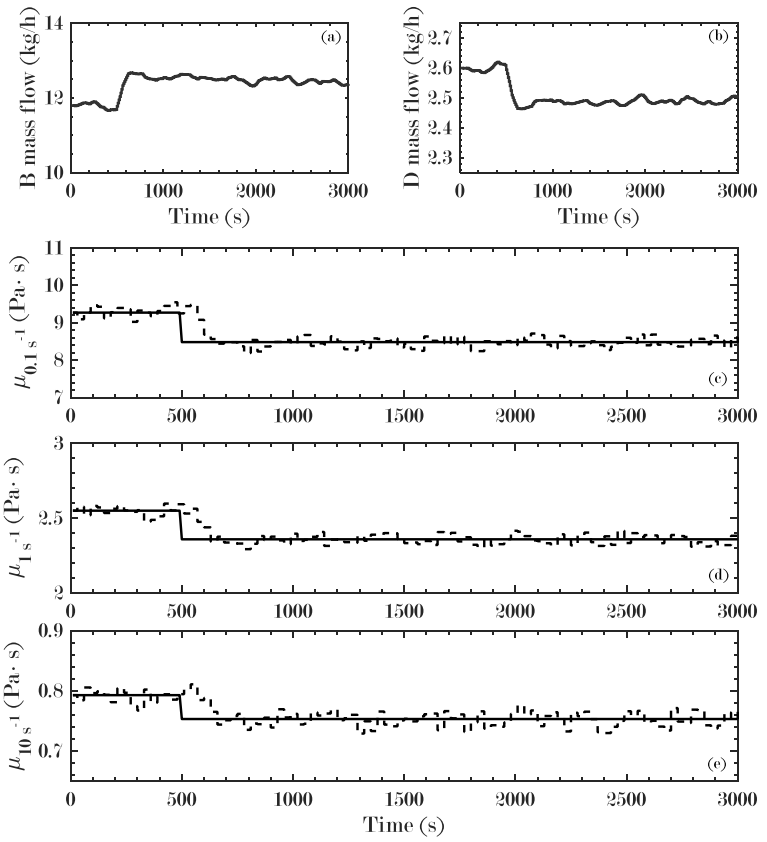

Figure 5.10: Behaviour of the system for set-point tracking with a simulated sampling time of 30 s

In Figure 5.11 and in Figure 5.12 the behaviour of the same

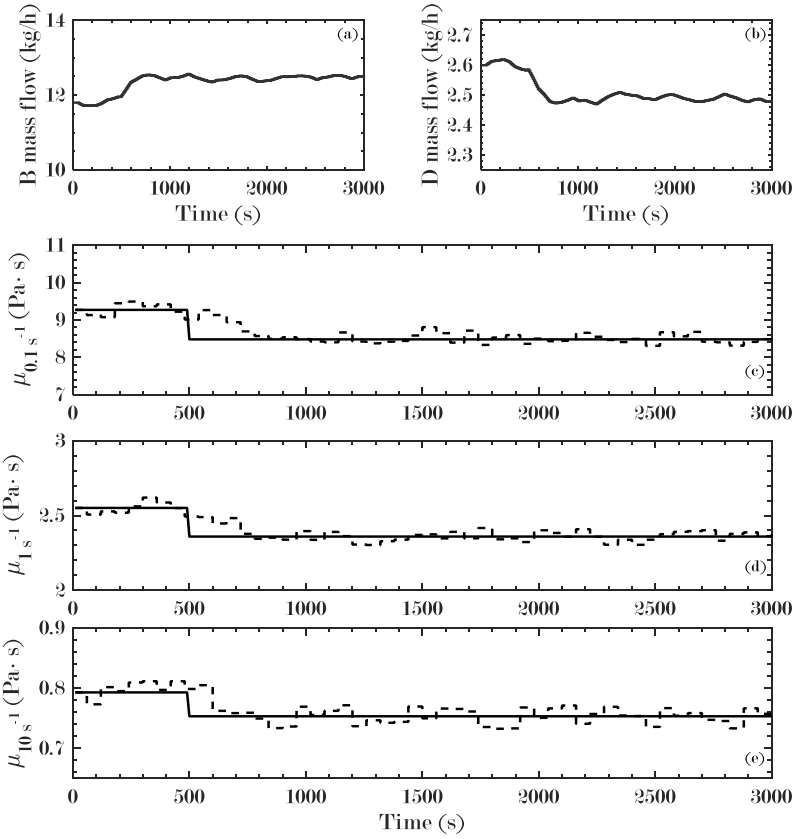

Figure 5.11: Behaviour of the system for set-point tracking with a simulated sampling time of 60 s

system in cases of measurements available, respectively, every 60 seconds (H_p=19) and 180 seconds (H_p=31) are reported. As can be seen, also in these cases the controller was capable to bring the system to desired values but slower responses with respect to the previous case were obtained. This was due to the fact that during the interval of time necessary between two consecutive samplings, the evolution of the system was unknown and this forced to tune the controller in a very conservative way. Because of that, high penalizations were applied to control actions, causing slow responses.

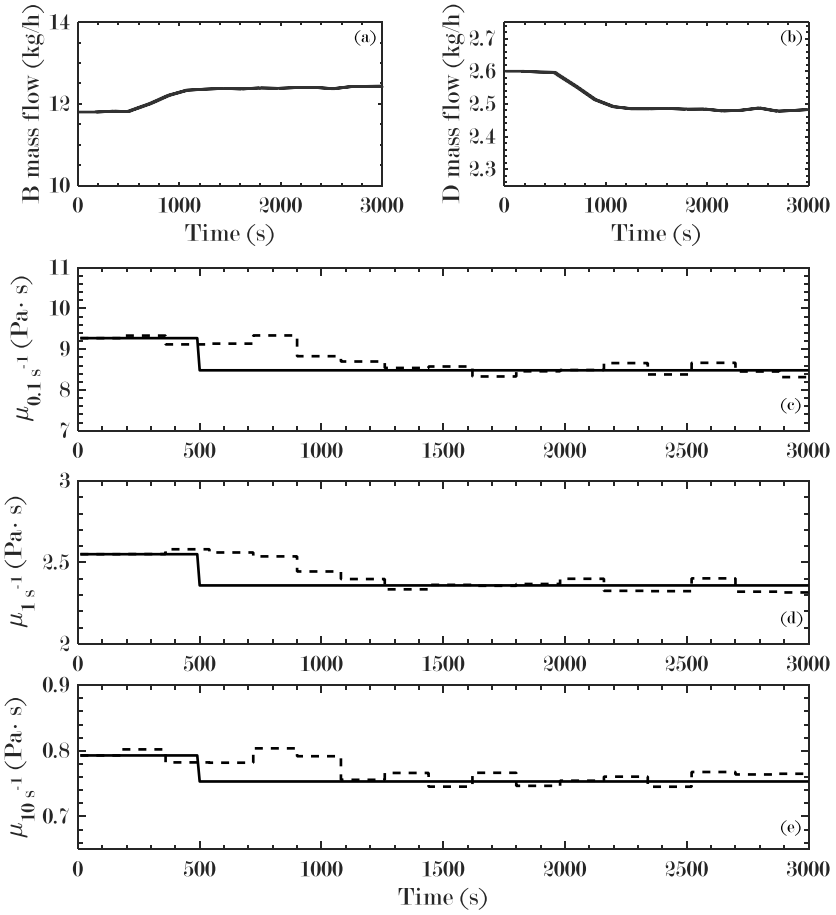

Figure 5.12: Behaviour of the system for set-point tracking with a simulated sampling time of 180 s

5.4.2 Disturbance rejection

To study the performances of the controller when various batches of ingredients are used for the production, a test with a different type of ingredient B has been designed. A second neural network with the same structure of the previous one has been trained with data collected when a different type of ingredient B was used in the production. This new model was used to simulate a disturbance entering the process. In fact, at a certain point of this simulation (t=500 s), the neural network used for the process simulator was replaced by the new model. It is important to underline that only the simulator was affected by this change.

The dynamic matrix $\boldsymbol{F}$ of the control algorithm did not change. In this way, a sudden change of a batch of ingredient, which has different rheological properties, was simulated. The simulation was carried out with the same parameters reported in Table 5.4.

Figure 5.13 reports the response of the system to this simulated sudden change of ingredient. As shown by the figure, the controller was capable to bring back the controlled viscosities (dashed lines) to target values (solid lines) after the perturbation of the system. In the figure also the responses in an open loop configuration are reported (dotted lines). The viscosity at 1100 s^{-1} was not

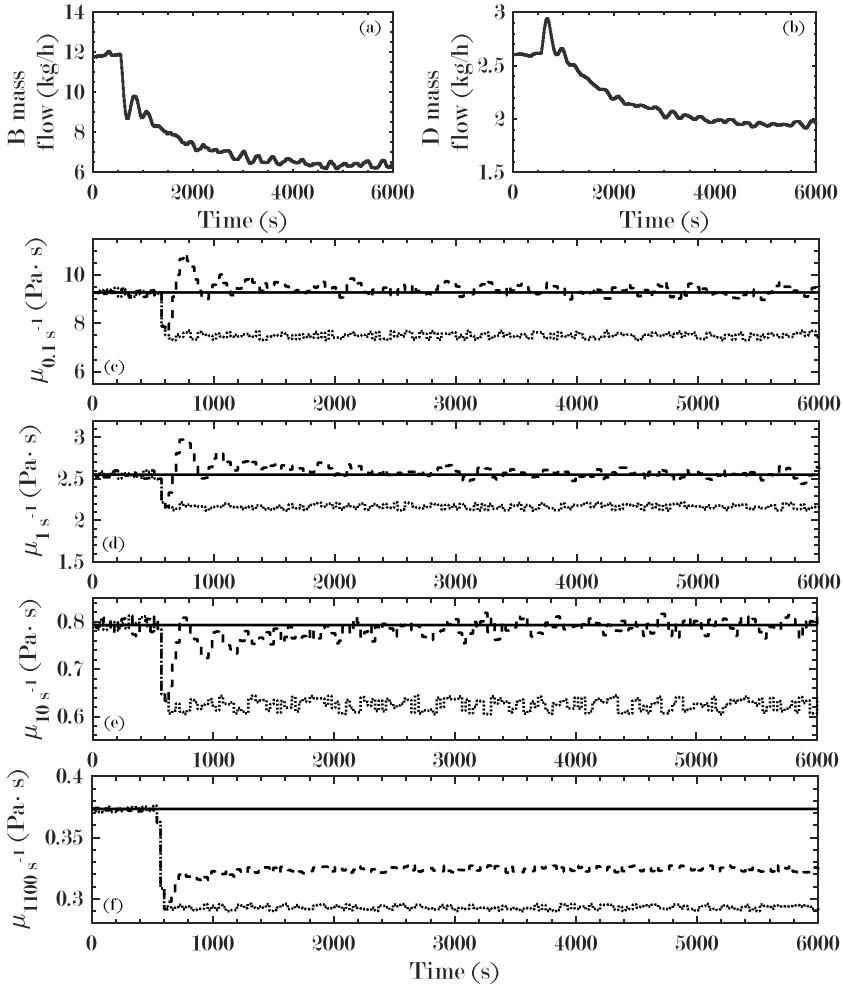

Figure 5.13: Behaviour of the system when subjected to a disturbance

controlled, but the difference between target and actual value was

reducing nevertheless.

5.5 Conclusions

In this Chapter multivariable control strategies were investigated in order to control multiple points on the viscosity curve of a non-Newtonian product.

A process simulator, based on a non-linear neural network, was built in order to provide dynamic responses of viscosities. The neural network relates viscosities at different values of shear rate to the amount of ingredients. A dynamic characterization was included in the model.

A double feedback controller was implemented with the goal to control, separately, two different point of the viscosity curve using two manipulated variables. The obtained outcomes showed that a double feedback control system was capable to control two points on the viscosity curve of the investigated product. However responses are relatively slow and with only two manipulated variables at disposal there is no way to control viscosities at intermediate values of shear rate.

Then, a model predictive control algorithm was applied with the purpose to control more than two points on the viscosity curve using the same manipulated variables. The obtained results showed that a model predictive control is capable to control various point of the viscosity curve both for set-point tracking and disturbance rejection. For the same sampling frequency, the MPC controller is faster than the two PI controllers. This is due to the control algorithm used by the MPC, which foreseeing future responses of the system, it is able to calculate proper control actions. The investigation regarding the sampling time led to the conclusion that high sampling time had the consequence to slow the response of the controller. It was evaluated that, for this industrial application, a proper sampling time should not be greater than about 60 seconds.

CHAPTER 6

Implementation of an on-line ultrasound rheological sensor for process control

In this Chapter, a brief summary on the previously designed and tested control systems is reported. An on-line ultrasound rheological sensor is then introduced. Data-driven models needed for the on-line based controller are developed. Finally, a control system which exploits the raw signals provided by the ultrasound rheological sensor is designed and tested.

6.1 Summary on designed and tested control systems

As discussed in Chapter 1, the development of an on-line rheological sensor proceeded in parallel with the modelling of the process and the analysis of control systems applicable to the continuous production of non-Newtonian fluids.

Because of the temporary unavailability of the rheological sensors, controllers have been studied and designed throughout simulations in which the sensor was replaced by a process simulator. Such simulator was designed to give as outputs viscosity values, taking as inputs ingredients amounts. The developed control systems had the goal to control different points in viscosity curves by acting on flow rates of ingredients.

All the discussed control systems revealed to be capable to control viscosity curves. In more detail, results obtained with the

double feedback controller implemented with PI actions (presented in Paragraph 5.3) were satisfactory and the design phase was simple but system responses obtained with such control system were relatively slow in terms of dynamics. The Model Predictive Control, presented in Paragraph 5.4, was able to control the viscosity curve ensuring faster dynamic responses than the two feedback controllers. Furthermore, it was capable of control more than two outputs using only two manipulated inputs. However, the design phase revealed to be definitely more complex.

Another important outcome obtained by these simulations was that, for both control systems, high sampling time and high measurement noise may cause control issues in terms of responses velocity and stability.

6.2 On-line ultrasound rheological sensor

6.2.1 Working principle of the sensor

In Paragraph 1.3.2, the motivations behind the need of on-line rheological sensors for monitoring and control industrial processes were explained and the most promising technologies were presented. One of these technologies consists of non-invasive measurements of rheological properties by means of ultrasound signals. This technique is the one of interest for the following discussion.

In fact, the on-line rheological sensor developed by CONSENS project partner TNO, is based on tomographic ultrasonic velocity technology. The measurement system is basically composed of a number of piezoelectric transducers positioned on the external side of a pipe, around the circumference. Inside the pipe, fluid flows without obstacles with a fully developed laminar flow. Each piezoelectric transducer is capable to transmit and receive ultrasound signals. A total of 36 transmission-reception pairs are possible. Each transducer emits, one at the time, an ultrasound signal which is received by the other transducers and then recorded. This cycle is repeated multiple times for each sample.

From the analysis of the raw ultrasound signals recorded, it is possible to extract some meaningful variables. The most im-

portant variables are the upstream-downstream time delays $\Delta\Gamma_{ij}$ and the average arrival times $\overline{\Gamma}_{ij}$. $\Delta\Gamma_{ij}$ represent the differences between the time that the signal, emitted by the i-th transducer, spends to travel to the j-th transducer ($\Gamma_{i\to j}$) and the time that the signal, emitted by the j-th transducer, spends to travel to the i-th transducer ($\Gamma_{j\to i}$). Upstream-downstream time delays are function of the velocity flow field and they are calculated as reported in Equation 6.1.

$$\Delta\Gamma_{ij} = \Gamma_{i\to j} - \Gamma_{j\to i} \tag{6.1}$$

$\overline{\Gamma}_{ij}$, calculated as reported in Equation 6.2, are a function of the medium stiffness.

$$\overline{\Gamma}_{ij} = \frac{\Gamma_{i\to j} + \Gamma_{j\to i}}{2} \tag{6.2}$$

From these measurements (36 values of $\Delta\Gamma_{ij}$ and 36 values of $\overline{\Gamma}_{ij}$, two values for each transmission-reception pair) and from values of pressure drop (ΔP) measured by a differential pressure sensor provided by Krohne, it is theoretically possible to infer rheological properties. In fact, the concept behind the discussed ultrasound sensor is to estimate the velocity profile of the fluid inside the pipe and then the viscosity curve of the product by exploiting $\Delta\Gamma_{ij}$ and ΔP values through the resolution of an inverse problem. With such sensor, it is not necessary to work with opaque fluids. Figure 6.1 shows a simplified scheme of the functioning of the sensor.

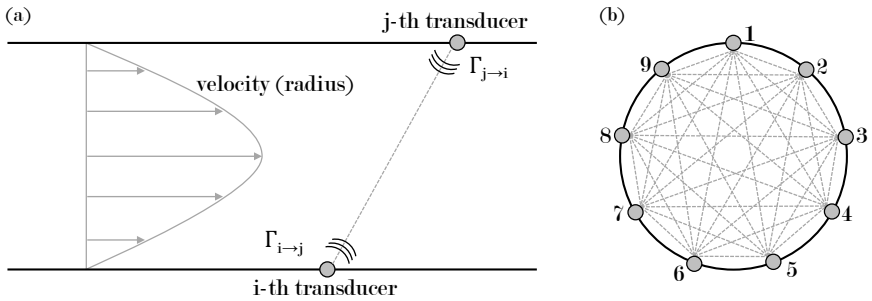

Figure 6.1: Simplified scheme of the function of the ultrasound sensor: (a) side view, (b) front view

More details regarding the geometry and the functioning of the sensor can not be disclosed for confidentiality reasons.

6.2.2 Test of the prototype

During the last phase of the project, on-line rheological measurements were finally performed in the pilot plant by means of the prototype of the sensor with the purpose to assess its performances. Unfortunately, the time required for the sampling and the resolution of the inverse problem, necessary to obtain the viscosity curve of the tested fluid, was too high to address a prompt control action.

This motivated a different strategy, based on an alternative data-driven approach, in order to exploit data coming from the sensor and use them together with black-box models, built with off-line rheological measurements, to perform the controlling of the system. The basic idea was to relate raw variables coming from the sensor, such as $\Delta\Gamma_{ij}$ and $\overline{\Gamma}_{ij}$, to off-line rheological measurements of viscosity performed on selected samples. This strategy is presented in the following paragraphs.

6.3 Data driven models

6.3.1 Design of experiments

The data-based approach consisted of relating ultrasound signals with rheological properties of the product. More in details, the objective was to find data-driven relationships between off-line viscosities measured in correspondence of shear rate values equal to 0.1, 1, 10, 100 and 1000 s^{-1}, and both upstream-downstream time delays and arrival times. In this way, viscosity measurements issues of the prototype may be partially reduced because the resolution of the inverse problem was replaced by the data-driven modelling. Nevertheless, real on-line data coming from the sensor were used.

The model was calibrated using data of experimental campaigns already discussed in the previous sections. Different experimental conditions, with changes in ingredients B and D amounts,

were considered. Figure 6.2 shows a summary of the explored ingredients combinations.

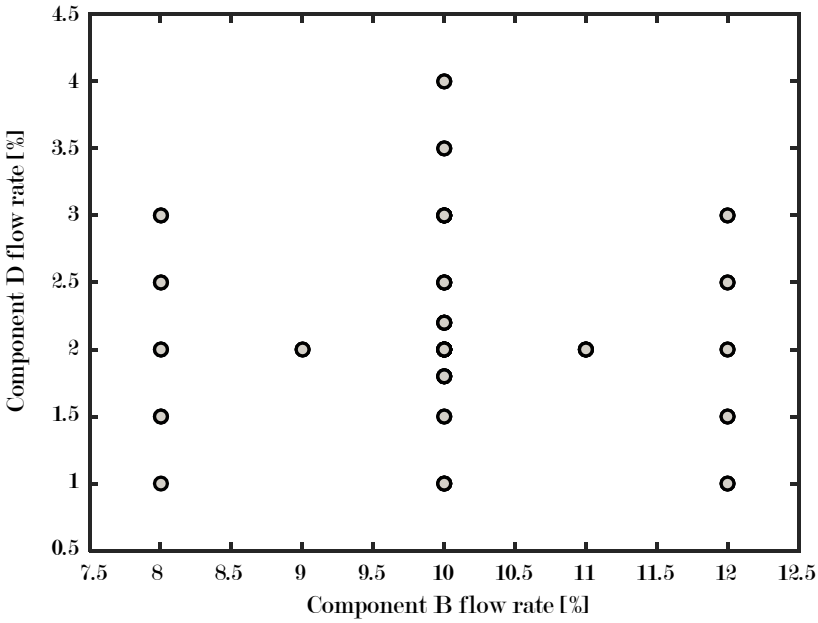

Figure 6.2: Summary of the explored ingredients combinations

6.3.2 Partial Least Squares regression

Introduction to Partial Least Squares regression technique

The Partial Least Squares regression (PLS-R) is a multiple linear regression technique which allows to find a correlation between process variables (inputs) and quality variables (outputs). Variables are projected into a lower dimensional sub-space, thus the amount of data considered is reduced. It is a very useful technique, especially for all those cases in which the amount of measurements available to predict quality variables is large (Wold, Sjöström, and Eriksson [39], Meng, Pan, and Jiang [40] and Godoy, Vega, and Marchetti [41]). However, one should remark that , when regressor variables are irrelevant, large variations on the prediction may occur and the regression algorithm may not find the correct subspace (Helland [42]). The proper selection of regressor variables

may improve the model performance and find a more suitable relationship between a reduced number of regressor variables and quality variables. To this purpose, a popular filtration method is represented by the Variable Importance in Projections (VIP) (Wold, Johansson, and Cocchi [43], Andersen and Bro [44], Wang, He, and Wang [45], Song et al. [46] and Liu [47]).

PLS-R algorithm

Assuming $\boldsymbol{X_P}$ (with dimension $I \times J$, where I represents the number of experimental points and J represents the number of regressor variables) as the predictions matrix containing, in this case, ultrasound data and assuming $\boldsymbol{Y_P}$ (with dimension $I \times M$, where M represents the number of quality variables) as the responses matrix containing rheological data, PLS-R projects $\boldsymbol{X_P}$ and $\boldsymbol{Y_P}$ into a low-dimensional sub-space, decomposing the matrices in scores and loadings variables. This sub-space is defined by a smaller number of latent variables A (Li, Qin, and Zhou [48]), with $A < J$. The choice of the number of latent variables A is a crucial aspect in order to describe data adequately. Assuming $\boldsymbol{T_A}$ as the orthonormal score matrix, $\boldsymbol{P_A}$ as the loading matrix for $\boldsymbol{X_P}$, $\boldsymbol{Q_A}$ as the loading matrix for $\boldsymbol{Y_P}$, $\boldsymbol{E_X}$ and $\boldsymbol{E_Y}$ as the residuals matrices, $\boldsymbol{X_P}$ and $\boldsymbol{Y_P}$ are decomposed as reported in Equations 6.3 and 6.4

$$\underset{I\times J}{\boldsymbol{X_P}} = \underset{I\times A}{\boldsymbol{T_A}} \cdot \underset{A\times J}{\boldsymbol{P_A^T}} + \underset{I\times J}{\boldsymbol{E_X}} \tag{6.3}$$

$$\underset{I\times M}{\boldsymbol{Y_P}} = \underset{I\times A}{\boldsymbol{T_A}} \cdot \underset{A\times M}{\boldsymbol{Q_A^T}} + \underset{I\times M}{\boldsymbol{E_Y}} \tag{6.4}$$

The PLS factors are generally found solving a maximization problem. To this purpose, the SIMPLS algorithm (de Jong [49]) was used in this case.

When the decomposition is completed, the obtained PLS-R model can predict the k-th quality variable $\hat{y}_k$ from the corresponding regressor vector x_k as expressed in Equation 6.5. In this equation, $\boldsymbol{B}$ is the regression coefficients matrix and it is estimated through Equation 6.6 where $\boldsymbol{R}$ is the pseudo-inverse matrix of the $\boldsymbol{P_A}$ matrix.

$$\underset{1\times M}{\hat{y}_k} = \underset{1\times J}{x_k} \cdot \underset{J\times M}{\boldsymbol{B}} \tag{6.5}$$

$$\underset{J\times M}{\boldsymbol{B}} = \underset{J\times A}{\boldsymbol{R}} \cdot \underset{A\times M}{\boldsymbol{Q}^{\boldsymbol{T}}_{\boldsymbol{A}}} \tag{6.6}$$

Prediction abilities for PLS-R can be evaluated through the Root Mean Square Error of Calibration (RMSEC) and through the Root Mean Square Error of Prediction (RMSEP) for the training set and the prediction set, respectively. RMSEC and RMSEP are calculated as reported in Equations 6.7 and 6.8, where N_T and N_P are the number of samples in the training set and in the prediction set, respectively, v_i is the observed value and $\hat{v}_i$ is the predicted value.

$$RMSEC = \sqrt{\frac{\sum_{i=1}^{N_T}(v_i - \hat{v}_i)^2}{N_T}} \tag{6.7}$$

$$RMSEP = \sqrt{\frac{\sum_{i=1}^{N_P}(v_i - \hat{v}_i)^2}{N_P}} \tag{6.8}$$

Finally, a Variable Importance in Projection (VIP) analysis was addressed. This is a useful technique to evaluate which variables in the $\boldsymbol{X_P}$ matrix mostly contribute to quality variables variations (Geladi and Kowalski [50] and Mehmood et al. [51]). VIP is applied after that loadings, weights and scores of the PLS-R have been determined. The VIP for the j-th variable is defined, in the form developed by Wold, Johansson, and Cocchi [43], in Equation 6.9. SSY_a is the sum of squares explained by the a-th component of the PLS and it is calculated as reported in Equation 6.10, where q_A and t_A are vectors of $\boldsymbol{Q_A}$ and $\boldsymbol{T_A}$ matrices. The term $(\frac{w_{a,j}}{||w_a||})^2$ measures the importance of the j-th variable, where w_a is the loading vector for the a-th component and $w_{a,j}$ is the loading for the a-th component relative to the j-th variable. Thus, the VIP analysis determines the contribution of each variable according to the variance explained by each PLS component. The j-th variable is considered significant if its VIP value exceeds a threshold. The selection criterion generally used is $VIP_j > 1$ (Chong and Jun [52] and Gosselin, Rodrigue, and Duchesne [53]).

$$VIP_j = \sqrt{J \frac{\sum_{a=1}^{A} \left(\frac{w_{a,j}}{||w_a||}\right)^2 SSY_a}{\sum_{a=1}^{A} SSY_a}} \tag{6.9}$$

$$SSY_a = q_A^2 t_A^T t_A \tag{6.10}$$

To perform the PLS regressions and analyses, the *libPLS* library was used (Li, Xu, and Liang [54]).

Model calibration

A model calibration was addressed exploiting PLS-R and correlating output variables, which were viscosities for shear rate values equal to 0.1, 1, 10, 100 and 1000 s^{-1}, with upstream and downstream time delays, arrival times, temperature and pressure drop. Assuming N as the number of experimental points, the final matrix of the outputs $\boldsymbol{X_P}$ had dimension $N \times 74$ (36 values of upstream and downstream time delays, 36 values of arrival times, 1 value for temperature and 1 value for pressure drop) and the quality matrix $\boldsymbol{Y_P}$ had dimension $N \times 5$ (one value for each viscosity).

Each column of the quality matrix $\boldsymbol{Y_P}$ was modelled separately. Before implementing the algorithm, both matrices were pre-processed to have zero mean and unity variance. The logarithm of $\boldsymbol{Y_P}$ was also considered. The number of latent variables A was chosen, for each column of the $\boldsymbol{Y_P}$ matrix, in order to minimize the Mean Square Error of Cross Validation (MSECV). Then, a leave-one-out procedure was implemented with the purpose to assess the capabilities of the PLS-R model to predict the viscosity of the observations left out.

The goodness of the fit was evaluated by means of the correlation coefficient $R^2_{pred,m}$, calculated as reported in Equation 6.11. In this equation, $PRESS_{i,m}$ is the Predicted Residual Error Sum of Squares, while $SS_{tot,m}$ is the total Sum of Squares. They are determined as reported in Equations 6.12 and 6.13, where $\mu_{i,m}$ is the viscosity of the i-th sample measured in correspondence of the m-th shear rate, with m=1, 2, 3, 4 and 5 that correspond to 0.1, 1, 10, 100 and 1000 s^{-1}, $\hat{\mu}_{i,m}$ is the predicted value of the same variable and $\bar{\mu}_m$ is the mean value of viscosity for the m-th shear rate.

$$R^2_{pred,m} = 1 - \frac{\sum_{i=1}^{N} PRESS_{i,m}}{SS_{tot,m}} \tag{6.11}$$

$$PRESS_{i,m} = (\mu_{i,m} - \hat{\mu}_{i,m})^2 \tag{6.12}$$

$$SS_{tot,m} = \sum_{i=1}^{N} (\mu_{i,m} - \bar{\mu}_m)^2 \tag{6.13}$$

Then, VIP analysis was performed in order to investigate and select the most significant regressor variables. Results are shown from Figure 6.3 to Figure 6.7. In these Figures, darker bars indicate VIP values larger than 1. As can be seen, VIP evaluation for upstream-downstream time delays is generally lower than 1, meaning that these variables have less influence than arrival times (for which most of the VIP values are larger than 1), in particular for viscosities at high shear rate values. This result means that even average arrival times, and not only upstream and downstream time delays, are informative about rheological properties of the fluid. The pressure drop was significant for all the shear rates. The VIP evaluation for temperature was never greater than 1. Thus, $\overline{\Gamma}_{ij}$ and pressure drop can be consider important variables.

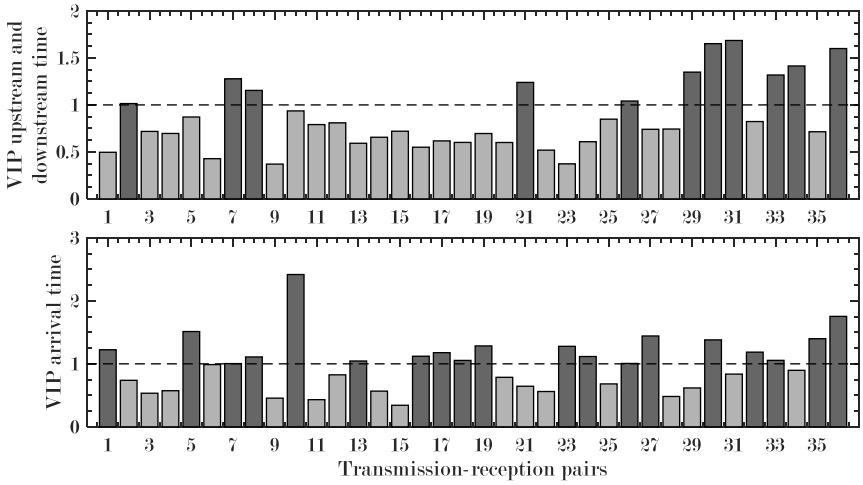

Figure 6.3: VIP analysis for viscosity at 0.1 s^{-1}

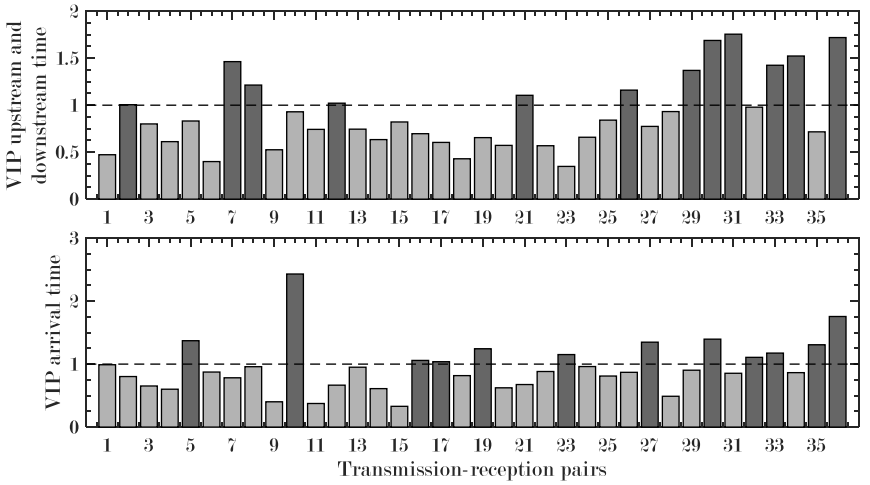

Figure 6.4: VIP analysis for viscosity at 1 s^{-1}

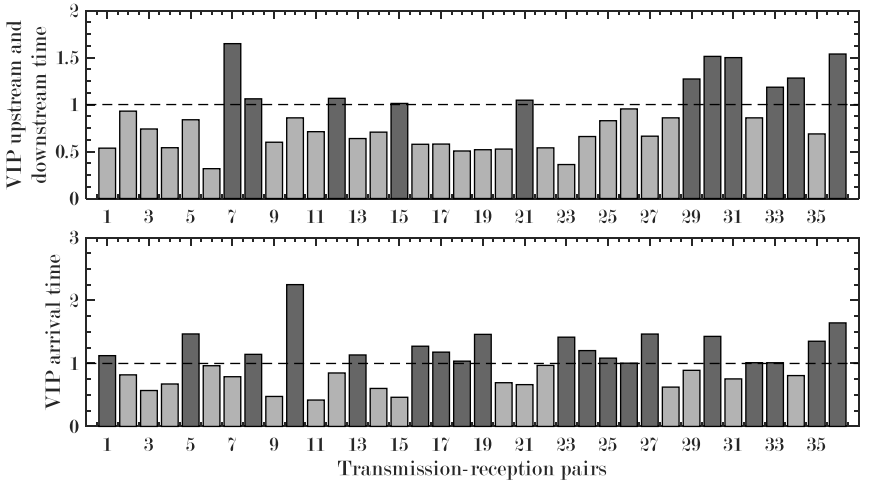

Figure 6.5: VIP analysis for viscosity at 10 s^{-1}

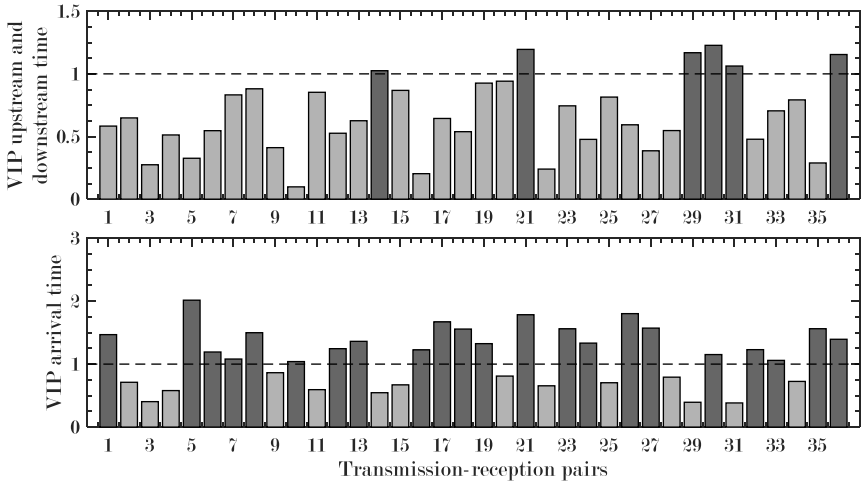

Figure 6.6: VIP analysis for viscosity at 100 s^{-1}

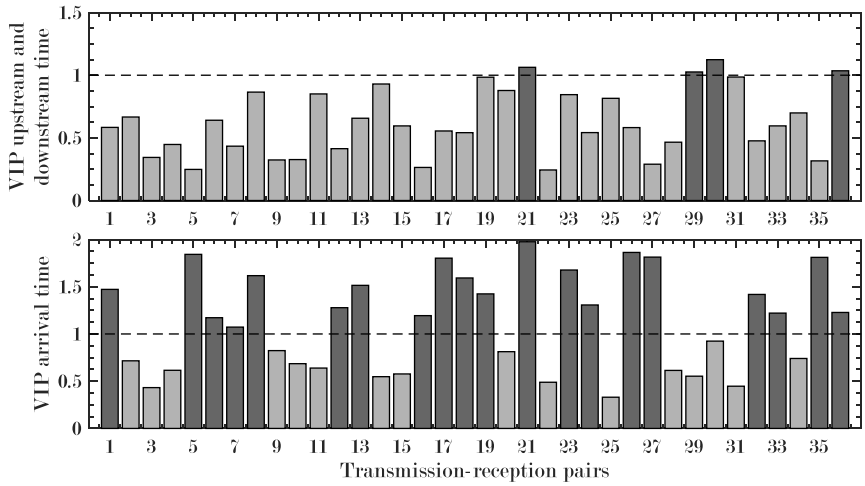

Figure 6.7: VIP analysis for viscosity at 1000 s^{-1}

The model was then updated by considering only the pressure drop and only ultrasound variables corresponding to transmission-receptions pairs with VIP values greater than 1. The number of variables in the $\boldsymbol{X_P}$ matrix was then reduced from 74 to 31 for viscosities at a shear rate values equal to 0.1 s^{-1} and 10 s^{-1}, to 25 for viscosities at 1 s^{-1} and 1000 s^{-1} and to 29 for viscosities at 100 s^{-1}. The matrices were, again, pre-processed and the number of latent variables A was chosen according to the MSECV criterion.

The leave-one-out procedure was implemented. Predicted values versus experimental viscosities at 0.1, 1, 10, 100 and 1000 s^{-1} are reported in Figure 6.8.

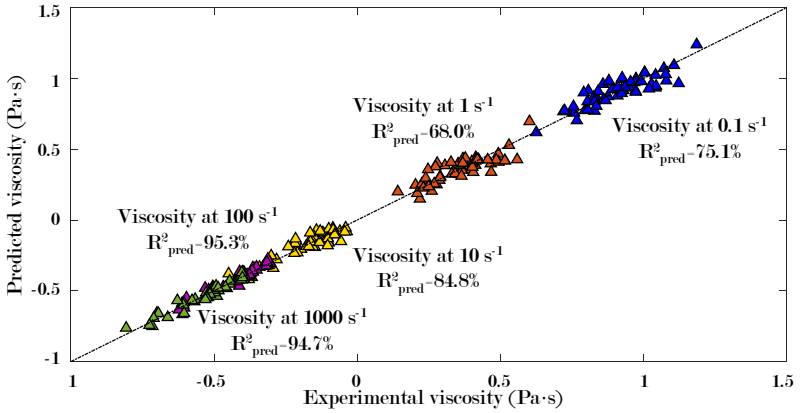

Figure 6.8: PLS-R: predicted viscosities vs experimental viscosities

As shown in Figure 6.8, there was a good agreement between predicted values and experimental data. Table 6.1 reports a summary of the performances obtained before and after the VIP procedure in terms of r, together with the number of latent variables A used.

Shear rate s^{-1}	$\boldsymbol{A}$ **(no VIP)**	$\boldsymbol{R^2_{pred}}$ **(no VIP)**	$\boldsymbol{A}$ **(VIP)**	$\boldsymbol{R^2_{pred}}$ **(VIP)**
0.1	8	70.7	5	75.1
1	8	62.1	4	68.0
10	8	84.1	5	84.8
100	4	89.4	6	95.3
1000	4	87.8	5	94.7

Table 6.1: PLS-R: summary of the performances of the model

Despite the fact that PLS-R gave good results in terms of prediction of experimental data, it was chosen to improve the modelling by means of non-linear models. To this purpose, non-linear neural network models were chosen.

6.3.3 Neural network modelling

A non-linear neural network was designed with the purpose to relate the same input-output variables chosen for the PLS regression. Output variables consisted of viscosities for shear rate values equal to 0.1, 1, 10, 100 and 1000 s^{-1}. Input variables consisted of average arrival times (provided by the ultrasound sensor) and pressure drop values.

The vector containing arrival times values calculated by the sensor was a 36-dimensional vector. It was decided to rely on a neural network with 3 layers. Assuming n_1, n_2 and n_3 as the number of neurons in the input layer, hidden layer and output layer respectively, the total number of parameters of the model is equal to $(n_1 + 1) \cdot n_2 + (n_2 + 1) \cdot n_3$.

To avoid the use of correlated inputs variables, Principal Component Analysis (PCA) was used to reduce the vector dimensionality with a fixed 95% threshold value for describing the input variance.

Different models were investigated to describe the rheological behaviour, differing in terms of number of principal components and number of hidden neurons and output neurons for the neural network. The model finally selected exploited 7 latent variables of the arrival times and pressure difference measurements. The neural network is therefore constituted of 8 inputs, 3 hidden neurons and 5 output neurons corresponding to the 5 viscosities values. A scheme of the designed neural network is reported in Figure 6.9.

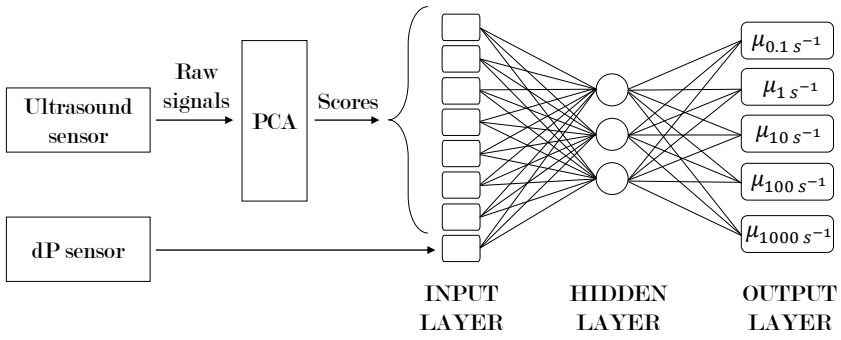

Figure 6.9: Scheme of the designed neural network

The model performances are reported in Table 6.2. It was found that the neural network model fitted experimental results better than the PLS model (see again Table 6.1 for a comparison).

	$\mu_{0.1s^{-1}}$	$\mu_{1s^{-1}}$	$\mu_{10s^{-1}}$	$\mu_{100s^{-1}}$	$\mu_{1000s^{-1}}$
R^2 (training set)	0.71	0.73	0.83	0.96	0.94
Prediction confidence interval (training set)	0.268	0.081	0.056	0.023	0.009
R^2 (test set)	0.83	0.88	0.86	0.95	0.86
RMSE (test set)	3.8	0.79	0.22	0.096	0.11

Table 6.2: Neural network: summary of the performances of the model

6.4 Control system

Despite accuracy issues of the sensor in measuring viscosity curves, the alternative modelling strategy presented was capable to exploit on-line data provided by the sensor. Nevertheless, due to the large value of the sampling time of the ultrasound sensor, transient behaviours were most likely missed by the sensor. It is highly likely that the information on the system are sampled only when new steady state conditions are reached. In these conditions, traditional control systems like feedback controllers and Model Predictive Controllers are not capable to control the system properly. This is due to the fact that, as showed in previous chapters, in these situations controllers actions need to be heavily penalized to guarantee the stability of the system. Because of this, controllers may need even a couple of hours to bring the system to set-points.

In order to address this issue, a control algorithm which mimics a "smart operator" action was implemented. In fact, experienced operator interventions are often required in plants to compensate the differences between targets values and measured variables when operating in open-loop mode. In this case this action is implemented by means of a neural network model. This model is

capable to provide ingredient B and ingredient D mass flow rates when a viscosity profile is given.

This neural network model is used together with the neural network described in Paragraph 6.3.3. Therefore, two data-driven models based on neural networks are implemented: one model relates the ultrasound signals to the off-line rheological measurements, providing on-line information on the rheology of the product, and the other model relates the viscosity curve at a given shear rate to the percentage of ingredient B and D flow rates. The control loop functioning is the following. A target viscosity value is assumed as set-point. Mass flow rate of ingredients B and D are calculated by the novel neural network model. Then, the viscosity is measured by exploiting ultrasound signals and the first neural network model. If the error between the target and the measured viscosities is greater than 0, a new set-point viscosity value is computed and the loop starts again. The control loop is also reported in Figure 6.10.

The control algorithm was tested on synthetic data, assuming target viscosities equal to 7.29, 2.59, 0.943, 0.537 and 0.431 Pa·s in correspondence of shear rate values equal to 0.1, 1, 10, 100 and 1000 s^{-1} respectively. A perturbation from the nominal conditions has been simulated leading to a measured viscosity respectively equal to 2.771, 1.358, 0.741, 0.504 and 0.427 Pa·s. The controller constants K_C were set equal to 0, 0.1, 0.1, 0 and 0.1 respectively. They were not consider for shear rate values of 0.1 s^{-1} and 100 s^{-1} because the corresponding neural network estimations demonstrated to be quite noisy. The first two iterations of the control algorithm are reported in Table 6.3.

	Target	**Init. condition**	**1st iteration**	**2nd iteration**
% B		9	10.2764	10.27
% D		2.5	2.7227	2.7118
$\mu_{0.1s^{-1}}$	7.29	2.7708	6.6341	6.5607
$\mu_{1s^{-1}}$	2.59	1.3578	2.5332	2.5133
$\mu_{10s^{-1}}$	0.943	0.7407	0.991	0.9874
$\mu_{100s^{-1}}$	0.537	0.5041	0.5721	0.5712
$\mu_{1000s^{-1}}$	0.431	0.4269	0.4572	0.4568

Table 6.3: Results of the control algorithm

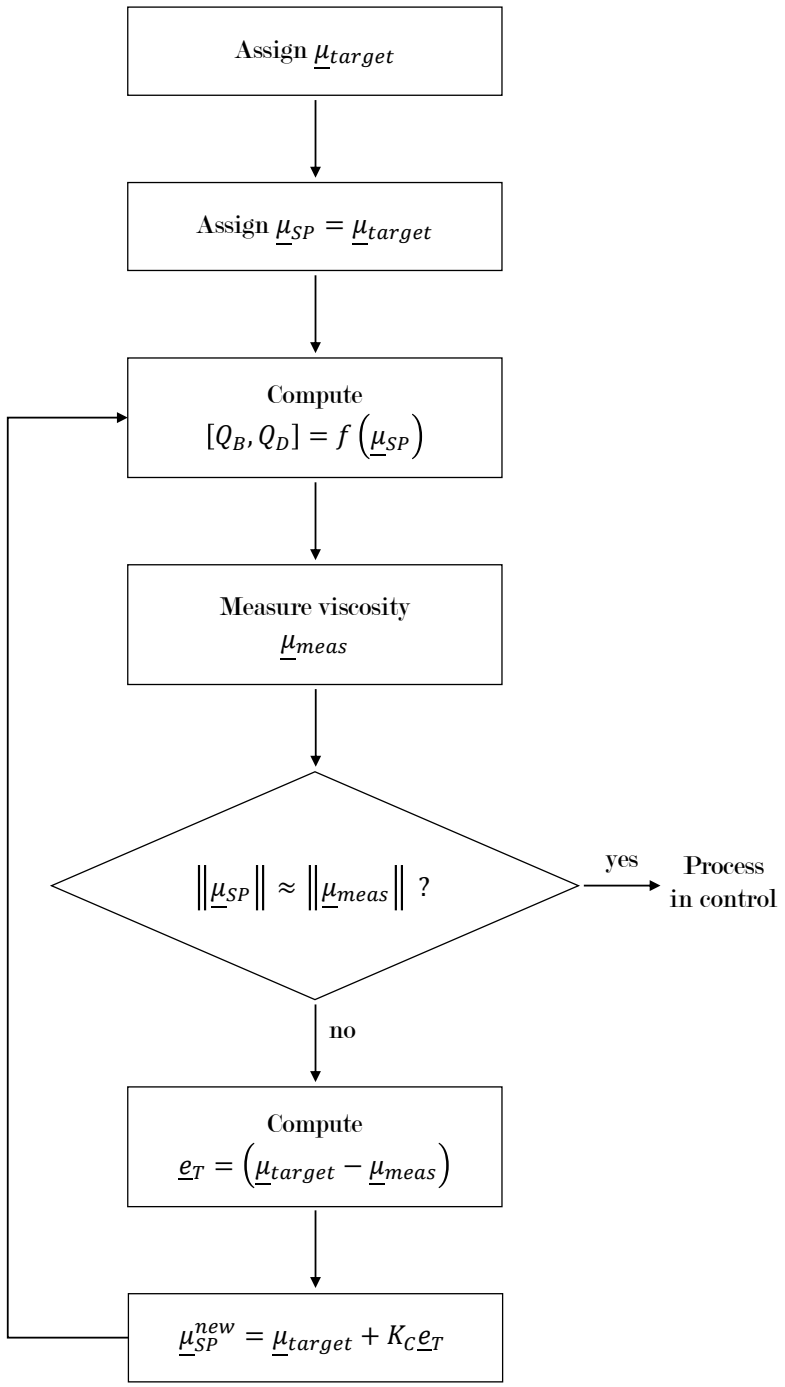

Figure 6.10: Scheme of the implemented control loop

In Figure 6.11, viscosity values for initial conditions, target values and the two iterations are reported against shear rate. It is clear that, although the target values (triangles) are quite far from the initial conditions (diamonds), after few iterations the system almost reached target conditions (circles).

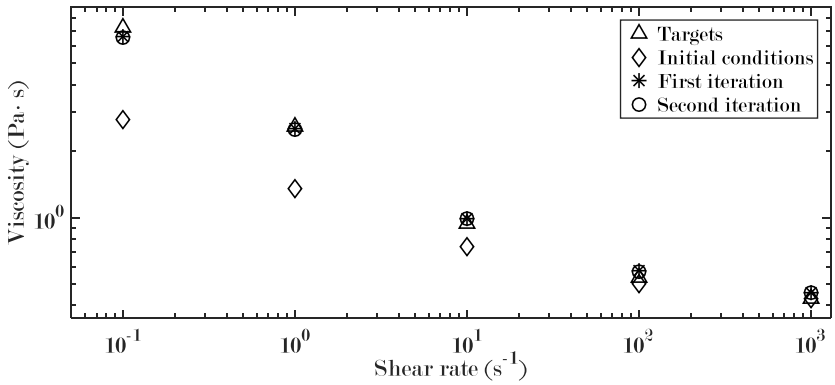

Figure 6.11: Results of the control algorithm

6.5 Conclusions

In this Chapter, the possibilities to control the detergent production process by using an on-line rheological sensor were explored. The sensor was developed by TNO and tested in its prototype stage. It consists of piezoelectric transducers placed around the external circumference of a pipe. These transducers emitted and received ultrasound signals which travelled through the flowing product. Raw ultrasound signals were exploited to calculate variables like upstream-downstream delays and arrival times. The concept behind the design of the ultrasound sensor was to resolve an inverse problem exploiting these variables and measurements of pressure drop. The goal was to obtain a velocity profile of the fluid flowing inside the pipe and then a viscosity curve of the product in real time. However, measurements performed by the prototype revealed to be not enough accurate and the sensor had a sampling time larger than three minutes. For these reasons, an alternative data-based approach was addressed with the purpose to control the process properly.

First, a data-driven modelling of the process by means of

Partial Least Squares technique was addressed in order to obtain a model capable to relate upstream-downstream delays and arrival times with off-line rheological measurements of viscosities of the product. The PLS modelling demonstrated that the idea to infer the rheology of the product by means of ultrasound data was valid. Furthermore, the PLS algorithm, coupled with the VIP technique, allowed the detection of the sensor combinations which appeared to be more informative for the rheological characterization. Nevertheless, it was chosen to resort to non-linear modelling to improve the performance of the black-box modelling. To this purpose, neural networks modelling was chosen. The trained neural network took as inputs the data coming from the ultrasound sensor and the pressure drop. It was found that the neural network model fitted experimental results better than the PLS model.

Finally, a control system was designed. Because of the large sampling time of the sensor, a "smart operator" action was implemented by means of a second neural network model. This neural network provided for ingredient B and D mass flow rates when a viscosity profile was given. This action had the goal to act like an experienced operator who compensates differences between targets values and measured variables operating in open-loop mode. Therefore, the control algorithm was based on two data-driven models, both of them based on neural networks: one model relating ultrasound signals to off-line rheological measurements and the other relating viscosity curve to the percentage of ingredient B and D.

Simulated tests of this control loop returned satisfactory results. Indeed, the novel control approach, based on data driven models, was capable to resolve the issues related to the prototype of the sensor and guarantee a proper control action. Therefore, the incorporation of this approach in the final control procedure is required.

Conclusions

This thesis dealt with the multivariable modelling and control of continuous industrial processes. Two main topics were analysed: the multivariable modelling, for control purpose, of a system subjected to persistent disturbances and the multivariable modelling and control of a continuous production process of complex fluids.

In the first part of the thesis, the multivariable system identification of a process subjected to disturbances was addressed exploiting wastewater treatment plants as case study. This type of plants need proper control systems to improve their efficiency and comply with the increasingly severe environmental regulations. The design of such controllers needs for process models, typically obtained through black box modelling. Therefore, dedicated experimental tests are needed. During these experiments, the normal functioning of the plant is suspended and this requires time and money. Furthermore, due to the persistent disturbances afflicting these plants, the system identification phase may last long and be quite problematic. In this work, a modelling strategy consisting of multivariable system identification was presented. The goal of the work was to develop a method to implement multivariable variations of manipulated inputs chosen for the identification phase, in order to obtain as much information as possible on the system in the shortest time. First, signals for manipulated inputs were randomly generated according to the Generalized Binary Noise approach with the purpose to generate a combination of input signals suited for identification. The generated combinations were selected on the basis of the D-Optimal Design criterion. The Benchmark Simulation Model No. 1 was used as process simulator for the wastewater treatment plant. It was configured as a plant operating with a series of activated sludge reactors and a settler. The system was then excited with the generated inputs and responses were analysed. In particular, the investigation was focused on the behaviour of two variables

chosen as outputs: nitrate nitrogen concentration in the second biological reactor of the plant and ammonia nitrogen concentration in the fifth biological reactor. A first attempt to model the input-output relationships of the system was made exploiting linear models. This attempt failed, probably due to the highly non-linear behaviour of the process. Thus, a non-linear modelling approach by means of neural networks was addressed. In particular, Non-linear Auto Regressive Neural Networks were used. Results were satisfactory, and all the input-output pairs were modelled correctly. Because the final goal of the work was to model the process for the application of linear control systems, a second modelling phase followed. Each neural network was excited with positive and negative variations of the corresponding inputs with the purpose to find linear, first order, transfer functions describing the input-output relationships. The procedure gave good results as regards the estimation of gain constants, but did not allow a reliable estimations of the time constants. The total simulated time needed for the experiments in the plant was estimated to be equal to 60 days. This value represents an improvement with respect to the results obtained in other studies where singular inputs variations were applied. This demonstrates that a multivariable identification approach, designed according to the D-Optimal Design criterion and applying the Generalized Binary Noise technique, can help to reduce the amount of time needed for system identifications and therefore reduce costs.

The second part of the thesis, concerned with the multivariable modelling and control of a continuous production process of a non-Newtonian fluid. In fact, during continuous production, the viscosity of the final product may go out of specifications for different reasons. Therefore, a precise control of the viscosity of the product during the manufacturing is necessary if a high degree compliance of specifications is required. In order to do that, on-line viscosity measuring instruments are required. Nowadays, there are no solutions in the market for on-line measurements of viscosity for non-Newtonian fluids. An ultrasound rheological sensor developed by a third party was used in its prototype stage. Water-free detergents production was considered as case study. They are composed of single concentrated doses of detergent, in form of pouches, which contain all the compounds needed for the

cleaning process but no water.

The study was conducted at pilot plant scale in Procter & Gamble research facilities in Belgium. The plant consisted of a main pipe in which ingredients, coming separately from a series of tanks, were mixed through static mixers. Off-line rheological characterization of the product was addressed exploiting off-line rheological measurements. In particular, measurements of viscosity curves (viscosity against shear rate) were investigated. The product was classified as a non-Newtonian shear-thinning fluid, with a viscosity that decreased with the shear rate. For the description of the rheological behaviour of the fluid, the Carreau model was chosen. Regarding the influence of ingredients on the viscosity, the focus went on the investigation of the effects of the solvent and of the rheological modifier. An on-line rheological characterization of the product was addressed by means of a Promass 83I viscometer positioned at the final part of the main pipe. This instrument was capable to return only a point viscosity of the fluid. Nevertheless, dynamic information obtained with this instrument, in terms of time constants and dead times, were considered reliable and were exploited for modelling the process. Retaining the rheological characterization of the fluid, a Carreau model was adopted to describe the off-line measurements. A first attempt to model the process was made relating the four parameters of the Carreau model, estimated by means of non-linear regressions on various experimental off-line rheological data, with the different amounts of rheological modifier used in the production of those samples. This model, consisting of stationary data, was completed with a dynamic part built with data obtained by the on-line viscometer and validated. This model was used also as a simulator of the process, in order to design the controller. Following, a single-input single-output feedback Proportional-Integral controller was designed with the purpose to control a point on the viscosity curve of the product, using the flow rate of the rheological modifier as manipulated variable. The correct selection of the point to control revealed to be a crucial aspect for the right working of the controller. With the purpose to analyse this, different configurations were simulated and tested, each of them with a different shear rate value in which control the corresponding viscosity. The main outcome was that the designed

controller was capable to control the viscosity curve and bring it close to a target curve, when the system was perturbed by a disturbance. This was true for cases in which the viscosity was controlled at low shear rate values. In fact, in configurations with viscosity controlled in correspondence of high shear rate values, the controller minimized the distance between actual and target viscosity in the controlled point but doing that, moved away most of the viscosity curve from the target. This demonstrated the importance of the selection of the point to control. Thus, a viscosity curve is controllable with a single-input single-output control configuration, but the design of the control system and the selection of the right controlled variable needs particular care.

A second attempt to model and control the process was made exploiting a multi-input multi-output control configuration. First, a process simulator, based on non-linear neural networks, was built to provide dynamic responses of viscosities. This neural network related off-line measured viscosities, at different values of shear rate, to the amount of ingredients used during manufacturing. The model was completed with a dynamic characterization that exploited data collected with the on-line Promass viscometer. Then, a double feedback controller was implemented with the objective to control two separate points of the viscosity curve using two manipulated variables. Results showed that such control system was capable to control two points on the viscosity curve. However, responses were relatively slow in terms of dynamics. Furthermore, only two controlled variables at disposal did not guarantee the control of the viscosity at intermediate values of shear rate. Thus, to improve the controllability of the process, a Model Predictive Control was designed with the purpose to control more than two points on the viscosity curve using the same manipulated variables. Results showed that such controller was capable to control various points of the viscosity curve, both for set-point tracking and disturbance rejection. Moreover, the Model Predictive Control returned faster responses in terms of dynamics with respect to the double feedback controller.

Finally, the possibility to control the detergent production process by using an on-line ultrasound rheological sensor developed by TNO was explored. The sensor consisted of piezoelectric transducers, placed around the external circumference of a pipe,

capable to emit and receive ultrasound signals. Variables like upstream-downstream delays and arrival times were calculated from raw ultrasound signals. The sensor resolved an inverse problem, calculating the velocity profile of the fluid in real-time and then its viscosity curve, exploiting ultrasound variables and measurements of pressure drop. However, experimental tests performed with the prototype revealed that the time required for the sampling and the resolution of the inverse problem was too high in order to address a prompt control action. For these reasons, an alternative data-driven approach was applied. The process was modelled by means of Partial Least Squares technique, in order to obtain a model capable to relate upstream-downstream delays and arrival times with off-line rheological measurements of viscosities of the product. The Partial Least Squares algorithm was coupled with the Variable Importance in Projection technique to detect the more informative variables. Despite the good results obtained, it was chosen to resort to non-linear neural networks modelling to improve the performance of the data-driven modelling. The trained neural network received, as inputs, data coming from the ultrasound sensor and values of pressure drop. Fittings of experimental data by the neural network were better than those obtained with the Partial Least Squares model. A "smart operator" action was implemented as a control system, by means of a second neural network model. This network provided for ingredient B and D mass flow rates for a given viscosity profile, acting like an experienced operator operating in open-loop mode. Thus, the control system was based on two data-driven models based on neural networks. Simulated tests of this control algorithm returned satisfactory results, proving the possibility of a real-time control of the viscosity curve of a complex fluid during its continuous production.

Nomenclature

Roman symbols

Symbol	Description
A	Number of latent variables
A_M	Constant matrix of the MPC algorithm
B	Regression coefficients matrix
C_m	Covariance matrix
d_1	Parameter for viscosity dependence on temperature
d_2	Parameter of function for viscosity dependence on temperature
e_N	Measurements noise vector
e_P	Difference between predicted and wanted outputs in the MPC algorithm
e_T	Difference between μ_{target} and μ_{meas}
E_X	Residuals matrix for X matrix
E_Y	Residuals matrix for Y matrix
f_{NN}	Memoryless model
F	Dynamic matrix of the MPC algorithm
g	Number of output variables
G	Shear modulus
h	Number of input variables
H_p	Prediction horizon of the MPC algorithm
H_u	Control horizon of the MPC algorithm
I	Number of experimental points
J	Number of regressor variables
k_p	Constant gain of the process
K	Matrix of gains
$\hat{K}$	Estimator of the matrix of gains
K_C	Proportional gain of the PI controller
l	Initial length of the solid
L	Longitudinal length of the deformation
M	Number of quality variables

continued on next page

continued from previous page

Symbol	Description
n_1	Number of elements in the input layer of the neural network
n_2	Number of elements in the hidden layer of the neural network
n_3	Number of elements in the output layer of the neural network
n_d	Number of points for viscosity curves discretization
N	Number of samples
N_P	Number of samples in prediction set
N_T	Number of samples in training set
o	Inputs vector
O	Objective function of the MPC algorithm
P	Pressure
P_A	Loading matrix for X matrix
q_A	Vector of Q matrix
Q_A	Loading matrix for Y matrix
Q_B	Mass flow rate of ingredient B
Q_D	Mass flow rate of ingredient D
r	Residuals
r^{std}	Standard residuals
R	Pseudo-inverse matrix of the P_A matrix
s_1, s_2	Penalization values of the MPC algorithm for ingredient D and B respectively
S	Penalization matrix of the MPC algorithm
t	Time
t_A	Vector of T_A matrix
t_d	Dead time of the process
T	Temperature
T_A	Orthonormal score matrix of the PLS-R
u	Manipulated inputs vector
U	Manipulated inputs matrix
v	Observed/measured value
$\hat{v}$	Predicted value
w_1, w_2, w_3	Weights of the MPC algorithm for $\mu_{0.1s^{-1}}$, $\mu_{1s^{-1}}$ and $\mu_{10s^{-1}}$ respectively
w_a	Loading vector for the a-th component
$w_{a,j}$	Loading for the a-th component relative to the j-th variable

continued on next page

continued from previous page

Symbol	Description
W	Weighting matrix of the MPC algorithm
x	State vector
$\dot{x}$	State vector rate
x_k	k-th regressor vector
X	Information matrix
X_P	Predictions matrix of the PLS-R
y	Outputs vector
$\hat{y}_k$	Predicted k-th quality variable
Y	Outputs matrix
Y_P	Response matrix of the PLS-R
z	Output of the first block

Greek symbols

Symbol	Description
α	Slope of the power law in the Carreau model
$\dot{\gamma}$	Shear rate
$\Gamma_{i \to j}$	Average arrival times between i-th and j-th transducers
$\Gamma_{j \to i}$	Average arrival times between j-th and i-th transducers
ΔP	Pressure drop
Δu	Control actions of the MPC algorithm
$\Delta\Gamma_{ij}$	Upstream-downstream time delays
λ	Parameter of the Carreau model
μ	Viscosity
$\overline{\mu}$	Average viscosity
$\hat{\mu}$	Estimated viscosity
μ_0	Viscosity at shear rate 0
μ_∞	Viscosity at shear rate ∞
μ_a	Apparent viscosity
μ_{meas}	Measured viscosity
μ^{NN}	Viscosity calculated with neural network
μ^P	Viscosity calculated with neural network at the previous control loop
μ_{SP}	Set-point viscosity

continued on next page

continued from previous page

Symbol	Description
μ_{target}	Target viscosity
ν	Parameter of the Carreau model
ρ	Perpendicular direction with respect to the flow
τ	Shear stress
$\dot{\tau}$	Shear stress rate
τ_I	Integral time of the PI controller
τ_p	Time constant of the process
φ	Velocity profile

List of Figures

List of Tables

Bibliography

[1] Rainier Hreiz, M.A. Latifi, and Nicolas Roche. "Optimal design and operation of activated sludge processes: State-of-the-art". In: *Chemical Engineering Journal* 281 (2015), pp. 900–920. ISSN: 1385-8947. DOI: 10.1016/j.cej.2015.06.125.

[2] *The CONSENS project official website*. URL: http://www.consens-spire.eu/.

[3] *The CONSENS project on the SPIRE official website*. URL: https://www.spire2030.eu/news/new/consens-project.

[4] *The CONSENS project on the CORDIS official website*. URL: https://cordis.europa.eu/project/rcn/193445_en.html.

[5] Mark L. Darby and Michael Nikolaou. "Identification test design for multivariabl emodel-based control: An industrial perspective". In: *Control Engineering Practice* 22 (2014), pp. 165–180. DOI: 10.1016/j.conengprac.2013.06.018.

[6] Christopher W. Macosko. *Rheology: Principles, Measurements, and Applications*. Ed. by Vch Pub. First Edition. 1994. ISBN: 978-0471185758.

[7] Gebhard Schramm. *A Practical Approach to Rheology and Rheometry*. Ed. by Gebrueder Haake. 1994.

[8] Reinhardt Kotzé, Johan Wiklund, and Rainer Haldenwang. "Optimisation of Pulsed Ultrasonic Velocimetry system and transducer technology for industrial applications". In: *Ultrasonics* 53 (2 2013), pp. 459–469. DOI: 10.1016/j.ultras.2012.08.014.

[9] Reinhardt Kotzé et al. "In-line rheological characterisation of wastewater sludges using non-invasive ultrasound sensor technology". In: *Water SA* 41.5 (2015), pp. 683–690. ISSN: 1816-7950. DOI: 10.4314/wsa.v41i5.11.

[10] Reinhardt Kotzé, Johan Wiklund, and Rainer Haldenwang. "Application of ultrasound Doppler technique for in-line rheological characterization and flow visualization of concentrated suspensions". In: *The Canadian Journal of Chemical Engineering* 94 (6 2016), pp. 1066–1075. DOI: 10.1002/cjce.22486.

[11] Valentino Meacci et al. "Flow-Viz - An integrated digital in-line fluid characterization system for industrial applications". In: *2016 IEEE Sensors Applications Symposium (SAS)*. 2016, pp. 1–6. DOI: 10.1109/SAS.2016.7479832.

[12] Taiki Yoshida, Yuji Tasaka, and Yuichi Murai. "Rheological evaluation of complex fluids using ultrasonic spinning rheometry in an open container". In: *Journal of Rheology* 61 (3 2017), pp. 537–549. DOI: 10.1122/1.4980852.

[13] George Tchobanoglous et al. *Wastewater Engineering: Treatment and Resource Recovery*. Ed. by McGraw-Hill Education. Fifth Edition - Metcalf & Eddy | AECOM. 2013. ISBN: 978-0073401188.

[14] Renato Vismara and Paola Butelli. *La gestione degli impianti a fanghi attivi*. Italian. Ed. by C.I.P.A. 1999. ISBN: 1126-1129.

[15] IWA Taskgroup on Benchmarking of Control Stategies for WWTPs. *Benchmark Simulation Model no. 1 (BSM1)*. 2008.

[16] Jens Alex et al. "Benchmark for evaluating control strategies in wastewater treatment plants". In: *1999 European Control Conference (ECC)*. IEEE, 1999. DOI: 10.23919/ECC.1999.7099914.

[17] Mogens Henze et al. *Activated Sludge Models ASM1, ASM2, ASM2D, ASM3*. IAWPRC scientific and technical reports no. 9, IAWPRC. 2000. ISBN: 9781780402369. DOI: 10.2166/9781780402369.

[18] Imre Takács, Gilles G. Patry, and Daniel Nolasco. "A dynamic model of the clarification-thickening process". In: *Water Research* 25 (10 1991), pp. 1263–1271. DOI: 10.1016/0043-1354(91)90066-Y.

[19] *IWA Task Group on Benchmarking of Control Strategies for WWTPs website*. URL: http://apps.ensic.inpl-nancy.fr/benchmarkWWTP/.

[20] Henk Vanhooren et al. *Development of a simulation protocol for evaluation of respirometry-based control strategies*. Tech. rep. 1996.

[21] Babatunde A. Ogunnaike and W. Harmon Ray. *Process Dynamics, Modeling, and Control*. Ed. by Oxford University Press. 1994. ISBN: 9780195091199.

[22] Chiara Foscoliano et al. "Predictive control of an activated sludge process for long term operation". In: *Chemical Engineering Journal* 304 (2016), pp. 1031–1044. DOI: 10.1016/j.cej.2016.07.018.

[23] Graham C. Goodwin and Robert L. Payne. *Dynamic System Identifications: Experiment Design and Data Analysis*. Ed. by Academic Press. 1977. ISBN: 9780080956459.

[24] *NIST/SEMATECH e-Handbook of Statistical Methods*. 2012. URL: http://www.itl.nist.gov/div898/handbook/.

[25] Herbert J. A. F. Tulleken. "Generalized binary noise test-signal concept for improved identification-experiment design". In: *Automatica* 26 (1 1990), pp. 37–49. DOI: 10.1016/0005-1098(90)90156-C.

[26] Francesc Corominas, Laurens Beelen, and Mohamed Akalay. "Methods for producing liquid detergent products". US 2013/0225468 A1. Feb. 27, 2012.

[27] *Web page of the AR 2000 rheometer*. URL: www.tainstruments.com/pdf/literature/ar2000.pdf.

[28] *Web page of the HTR 301 rheometer*. URL: https://www.it.endress.com/en/Field-instruments-overview/Flow-measurement-product-overview/Product-Coriolis-flowmeter-Proline-Promass-83I.

[29] *Web page of the MCR 102 rheometer*. URL: https://www.anton-paar.com/corp-en/products/details/rheometer-mcr-102-302-502/.

[30] *Web page of the Proline Promass 83I Coriolis flowmeter*. URL: https://www.it.endress.com/en/Field-instruments-overview/Flow-measurement-product-overview/Product-Coriolis-flowmeter-Proline-Promass-83I.

[31] R. Byron Bird and Pierre J. Carreau. "A nonlinear viscoelastic model for polymer solutions and melts - I". In: *Chemical Engineering Science* 23 (5 1968), pp. 427–434. DOI: 10.1016/0009-2509(68)87018-6.

[32] Pierre J. Carreau, Ian F. MacDonald, and R. Byron Bird. "A nonlinear viscoelastic model for polymer solutions and melts - II". In: *Chemical Engineering Science* 23 (8 1968), pp. 901–911. DOI: 10.1016/0009-2509(68)80024-7.

[33] Sequare Daniel-Berhe and Heinz Unbehauen. "Identification of nonlinear continuous-time Hammerstein model via HMF-method". In: *36th IEEE Conference on Decision and Control*. IEEE, 1997, pp. 2990–2995. DOI: 10.1109/CDC.1997.657906.

[34] Stefania Tronci et al. "Flow instabilities in rheotens experiments: Analysis of the impacts of the process conditions through neural network modeling". In: *Polymer Engineering and Science* 53 (6 2012), pp. 1241–1252. DOI: 10.1002/pen.23387.

[35] Stefania Tronci and Roberto Baratti. "A Gain-Scheduling PI Control Based on Neural Networks". In: *Complexity* 2017 (2017). DOI: 10.1155/2017/9241254.

[36] E. Bristol. "On a new measure of interaction for multivariable process control". In: *IEEE Transactions on Automatic Control* 11.1 (Jan. 1966), pp. 133–134. DOI: 10.1109/TAC.1966.1098266.

[37] Giuseppe Cogoni et al. "Controllability of Semibatch Nonisothermal Antisolvent Crystallization Processes". In: *Industrial & Engineering Chemistry Research* 53.17 (2014), pp. 7056–7065. DOI: 10.1021/ie404003j.

[38] Michela Mulas et al. “Predictive control of an activated sludge process: An application to the Viikinmäki wastewater treatment plant”. In: *Journal of Process Control* 35 (2015), pp. 89–100. DOI: 10.1016/j.jprocont.2015.08.005.

[39] Svante Wold, Michael Sjöström, and Lennart Eriksson. “PLS-regression: a basic tool of chemometrics”. In: *Chemometrics and Intelligent Laboratory Systems* 58 (2 2001), pp. 109–130. DOI: 10.1016/S0169-7439(01)00155-1.

[40] Xianghe Meng, Qiuyue Pan, and Lianzhou Jiang. “Rapid determination of phospholipid content of vegetable oils by FTIR spectroscopy combined with partial least-square regression”. In: *LianzhouJiang* 147 (2014), pp. 272–278. DOI: 10.1016/j.foodchem.2013.09.143.

[41] José L. Godoy, Jorge R. Vega, and Jacinto L. Marchetti. “Relationships between PCA and PLS-regression”. In: *Chemometrics and Intelligent Laboratory Systems* 130 (2014), pp. 182–191. DOI: 10.1016/j.chemolab.2013.11.008.

[42] Inge S. Helland. “Some theoretical aspects of partial least squares regression”. In: *Chemometrics and Intelligent Laboratory Systems* 58 (2 2001), pp. 97–107. DOI: 10.1016/S0169-7439(01)00154-X.

[43] Svante Wold, Erik Johansson, and Marina Cocchi. “PLS - Partial Least Squares Projections to Latent Structures”. In: *3D QSAR in Drug Design: Theory Methods and Applications*. 1993, pp. 523–550. ISBN: 9789072199140.

[44] Charlotte Møller Andersen and Rasmus Bro. “Variable selection in regression - a tutorial”. In: *Journal of Chemometrics* 24 (11-12 2010), pp. 728–737. DOI: 10.1002/cem.1360.

[45] Zi Xiu Wang, Q. Peter He, and Jin Wang. “Comparison of variable selection methods for PLS-based soft sensor modeling”. In: *Journal of Process Control* 26 (2015), pp. 56–72. DOI: 10.1016/j.jprocont.2015.01.003.

[46] Kai Song et al. “Quality Based Prioritized Sensor Fault Monitoring Methodology”. In: *Chinese Journal of Chemical Engineering* 16 (4 2008), pp. 584–589. DOI: 10.1016/S1004-9541(08)60125-1.

[47] Jialin Liu. "Developing a soft sensor based on sparse partial least squares with variable selection". In: *Journal of Process Control* 24 (7 2014), pp. 1046–1056. DOI: 10.1016/j.jprocont.2014.05.014.

[48] Gang Li, S. Joe Qin, and Donghua Zhou. "Geometric properties of partial least squares for process monitoring". In: *Automatica* 46 (1 2010), pp. 204–210. DOI: 10.1016/j.automatica.2009.10.030.

[49] Sijmen de Jong. "SIMPLS: An alternative approach to partial least squares regression". In: *Chemometrics and Intelligent Laboratory Systems* 18 (3 1993), pp. 251–263. DOI: 10.1016/0169-7439(93)85002-X.

[50] Paul Geladi and Bruce R. Kowalski. "Partial least-squares regression: a tutorial". In: *Analytica Chimica Acta* 185 (1986), pp. 1–17. DOI: 10.1016/0003-2670(86)80028-9.

[51] Tahir Mehmood et al. "A review of variable selection methods in Partial Least Squares Regression". In: *Chemometrics and Intelligent Laboratory Systems* 118 (2012), pp. 62–69. DOI: 10.1016/j.chemolab.2012.07.010.

[52] Il-Gyo Chong and Chi-Hyuck Jun. "Performance of some variable selection methods when multicollinearity is present". In: *Chemometrics and Intelligent Laboratory Systems* 78 (1-2 2005), pp. 103–112. DOI: 10.1016/j.chemolab.2004.12.011.

[53] Ryan Gosselin, Denis Rodrigue, and Carl Duchesne. "A Bootstrap-VIP approach for selecting wavelength intervals in spectral imaging applications". In: *Chemometrics and Intelligent Laboratory Systems* 100 (1 2010), pp. 12–21. DOI: 10.1016/j.chemolab.2009.09.005.

[54] Hong-Dong Li, Qing-Song Xu, and Yi-Zeng Liang. "libPLS: An integrated library for partial least squares regression and linear discriminant analysis". In: *Chemometrics and Intelligent Laboratory Systems* 176 (2018), pp. 34–43. DOI: 10.1016/j.chemolab.2018.03.003.

[55] Jan Mewis and Norman J. Wagner. *Colloidal Suspension Rheology*. Ed. by Cambridge University Press. 2011. ISBN: 9780521515993.

[56] Kathrin Reinheimer et al. “Fourier Transform Rheology as an innovative morphological characterization technique for the emulsion volume average radius and its distribution”. In: *Journal of Colloid and Interface Science* 380 (1 2012), pp. 201–212. DOI: 10.1016/j.jcis.2012.03.079.

[57] Thomas Wunderlich and Peter O. Brunn. “Ultrasound pulse Doppler method as a viscometer for process monitoring”. In: *Flow Measurement and Instrumentation* 10 (4 1999), pp. 201–205. DOI: 10.1016/S0955-5986(99)00016-3.

[58] Navid Ghadipasha et al. “On-line control of crystal properties in nonisothermal antisolvent crystallization”. In: *AIChE Journal* 61 (7 2015), pp. 2188–2201. DOI: 10.1002/aic.14815.

[59] Mark L. Darby and Michael Nikolaou. “MPC: Current practice and challenges”. In: *Control Engineering Practice* 20 (4 2012), pp. 328–342. DOI: 10.1016/j.conengprac.2011.12.004.